Gene Cloning and Characterization of Enzymes From Marine Extremophiles

INAUGURALDISSERTATION

zur
Erlangung des akademischen Grades eines
Doktors der Naturwissenschaften

doctor rerum naturalium (Dr. rer. nat.)

an der Mathematisch-Naturwissenschaftlichen Fakultät
der
Ernst-Moritz-Arndt-Universität Greifswald

vorgelegt von

Le Huu Cuong

in Hanoi, Vietnam

Greifswald, Oktober 2013

Dekan: Prof. Dr. Klaus Fesser

1. Gutachter: Prof. Dr. Thomas Schweder

2. Gutachter: Prof. Dr. Peter Neubauer

Tag der Promotion: 29.01.2014

SUMMARY

Microorganisms requiring extreme environments for their growth are called extremophiles. Extreme environment is a relative term which may refer to physical extremes (e.g. temperature, pressure or radiation), but also to geochemical extremes such as salinity and pH. The variety of microbes inhabiting in such environments is a valuable source of proteins and enzymes with extreme stability, novel activities and applications.

Deep subsurface petroleum reservoir, the unique extreme environment is usually characterized by high temperatures (up to 180°C), high pressures (up to 40 Mpa) and high salinity. This wide variety of geochemical conditions is typically associated with the depositional environment, source rock and oil maturity. Life in such extreme conditions has been studied intensively with focus on the diversity of organisms including their molecular and regulatory mechanisms.

The investigated bacterial strain 64G3 was isolated from an offshore oil well in Vung Tau, Vietnam. By means of 16S rDNA sequence alignment and DNA-DNA hybridization with *Petrotoga mexicana* DSM 14811, the isolate was identified as *Petrotoga mexicana* species. Morphologically, the 64G3 cells were rod-shaped and cell sizes varied widely from 1.0 µm up to 60 µm in length and from 0.6 to 1.2 µm in width. The cells appeared single, pairwise or in chains within a sheath-like structure (a typical characteristic of the order *Thermotogales*) that ballooned over the cell ends. Cells were immobile and no flagella were observed. Strain 64G3 grew anaerobically at temperatures ranging from 30 to 65°C and within the pH range of 5.0 to 8.5 with optimum growth at 55°C and the pH 7.0. The isolate 64G3 utilized various substrates including glucose, galactose, ribose, xylose, maltose, starch and xylan as sole carbon source. Elemental sulfur and thiosulfate served as alternative electron acceptors whereas sulfate did not. The growth of strain 64G3 was completely inhibited by penicillin, ampicillin and chloramphenicol at concentration of 10 µg mL^{-1}, whereas rifampicin and steptomycin at concentration of 100 µg mL^{-1} slightly decreased cell growth.

Cellular extract of strain 64G3 grown in a basal medium containing soluble starch displayed hydrolytic activity towards soluble starch. The amylase system includes at least two individual enzymes. Amylase activity of the cell extract was detected in a wide temperature range (30-80°C), with optimum enzyme activity at 75°C. By using degenerate primer for PCR amplification of GH13 enzyme coding regions in combination with other molecular methods, one full amylase coding gene containing four conserved regions of α-amylase was obtained. The deduced sequence showed low identities (up to 40%) to other known amylases. This 1992

bp coding gene was expressed in *E. coli* and its product (amylase) was characterized. Under common expression conditions, the 77 kDa amylase (rAmyA) was predominantly produced as inclusion bodies (insoluble form). The minor amount of soluble active amylase was used for enzyme purification and characterization. rAmyA was active on starch at temperatures between 30-55^{o}C, with an optimum at 45^{o}C. It was not thermostable because it was completely inactivated after incubation at 65^{o}C for 15 min. The enzyme was active over a pH range from 4.5-8.0, with an optimum at pH 6.5. Beside starch, rAmyA also hydrolysed glycogen, amylose, amylopectin and other oligosaccharides. Pullulan and cyclodextrins were not the substrates for this amylase. The enzyme hydrolyzed starch in an endo-acting manner, releasing maltose and maltotriose as major products and a lesser amount of glucose. In comparison with other α-amylases, the enzyme possesses a rare hydolysis pattern on starch.

On the basis of the primary structure, the substrate specificities and the hydrolysis pattern, rAmyA was classified as an endo-acting α-amylase (EC. 3.2.1.1).

Psychrophilic (or cold adapted) microorganisms inhabit low temperature environments (-2–15°C), such as polar regions or ocean deeps. Their abilities to grow at low temperatures could serve as an excellent model system to understand the molecular basis of cold temperature adaptation and to optimize the biological processes required for cell growth and survival. Production of recombinant protein using mesophilic hosts (or expression systems) often results in un-desirable products due to formation of inclusion bodies caused by incorrect folding of the nascent polypeptide chains. To some extent, this problem can be avoided when the production of “difficult” proteins is conducted at low temparatures that destabilize hydrophobic interactions needed for intermediate aggregation. A rational alternative to mesophilic expression system is the use of cold adapted bacteria as host for protein production at low temperatures (even at arround 0°C).

Another part of this thesis focused on cloning and expression of the psychrophilic chaperonin (Cpn) operon consisting of *cpn10* and *cpn60* genes from *Oleispira antarctica*. The impact of the recombinant chaperonin on cold-adaptation of *Bacillus subtilis* and the co-production of active yeast α-glucosidase was also studied.

Chaperones are involved in a multitude of cellular functions, including de *novo* folding, refolding of stress-denatured proteins, oligomeric assembly, intracellular protein transport and assistance in proteolytic degradation. Bacterial Cpn60 and its co-chaperonin Cpn10 function in oligomeric assembly and protein folding in cytosol. It is known that expression of *O. antarctica cpn* operon or *Pseudoalteromonas haloplanktis cpn60* gene in *E. coli* facilitates adaptation of the host to low temperature conditions (≤10°C). Furthermore, in *E. coli* co-

expression of psychrophilic *cpn10/60* operon also promoted correct folding of other proteins into their active form, avoiding inclusion body aggregation.

B. subtilis is a significant bacterium in scientific research field as well as in biotechnology and industry. The development of a cold-adapted expression systems using *B. subtilis* as host is of importance because the recombinant production of several proteins such as thermolabile proteins, "difficult" proteins and toxic proteins require low temperature conditions. Recently, a cold inducible expression system for *B. subtilis* based on the *des* promoter of Δ5 desaturase gene was constructed and the use of this system at 25°C showed promising results with regards to quantity and quality of recombinant proteins. The cold shock protein (CspB) of *B. subtilis* is also involved in the tolerance of cells to low temperatures and the use of *cspB* promoter enhances the yield of *E. coli* active galactosidase produced in *B. subtilis* at 10°C. However, CspB does not support the cold adaptation of *B. subtilis*. So far, expression systems working at ≤ 20°C for *B. subtilis* have not been investigated or discussed.

In the second part of this study, the *cpn10/60* operon from *O. antarctica* was cloned and expressed in *B. subtilis*. The amounts of soluble Cpn60 and Cpn10 produced at temperature ranging from 10-30°C were high and stable during cell growth. To investigate the impact of psychrophilic chaperonin on cold adaptation, cells with (*cpn+*) and without (*cpn–*) *cpn10/60* operon were grown at 10 and 15°C. Growth comparison revealed that psychrophilic chaperon did not support cold adaptation of *B. subtilis* as explained by the similar growth profiles between *cpn+* and *cpn–* cells at low temperatures.

A single copy of *O. antarctica cpn10/60* operon was integrated into the *amyE* locus of the *B. subtilis* chromosome. Yeast α-glucosidase, a theoretic protein substrate for this chaperonin was heterologously produced in *B. subtilis* at temperatures ranging from 15-30°C, with highest activity at 25°C but the insoluble enzyme was still found upon production at low temperature (15°C). Co-expression of *O. antarctica cpn10/60* operon at 15°C, however, did not result in a higher activity of glucosidase in comparison to *cpn–* cells which served as the control. Moreover, the amount of insoluble enzyme produced in *cpn+* cells did not decrease in comparion to that produced in *cpn–* cells, indicating that the heterologous chaperonin had no impact on recovery of active α-glucosidase from the inclusion bodies

CONTENT

Page

SUMMARY ii

CONTENT v

I. INTRODUCTION ……..... 1

1.1. Starch degrading enzymes and the genus *Petrotoga*..... 1

1.1.1. Starch properties and amylolytic enzymes ……..... 1

1.1.1.1. Starch properties…….…… 1

1.1.1.2. Enzymatic hydrolysis of starch…….. 2

1.1.1.2.1. α-Amylase family (glycoside hydrolase family 13, GH13)……..... 5

1.1.1.2.2. Starch hydrolysis mechanism……. 9

1.1.1.3. Application of amylolytic enzyme……. 10

1.1.2. Oil reservoir, a habitat for various groups of microorganisms……. 11

1.1.2.1. Oil reservoir properties…….. 11

1.1.2.2. The genus *Petrotoga* and their starch degrading enzymes…… 12

1.2. The protein folding and chaperonin activity……... 14

1.2.1. Protein structure and its folding problems…… 14

1.2.1.1. Structure of proteins…….….. 14

1.2.1.2. Protein folding problems …….. 14

1.2.1.3. Dominant force in protein folding ……. 16

1.2.2. The protein folding *in vivo*…… 17

1.2.3. Hsp60 proteins ……. 20

1.2.3.1. The expression of bacterial *cpn* operon …….. 20

1.2.3. 2. Architecture and functions of GroEL and GroES …… 21

1.2.3. 3. The functional cycle of GroE ……... 22

1.2.4. Chaperonin from psychrophilic *Oleispira antartica*……. 24

1.2.4.1. The characterization of *O. antartica* RB-8……. 24

1.2.4.2. *O. antarctica* chaperonins (Cpn60 and Cpn10) ……. 25

1.2.4.3. Potential applications of psychrophilic bacteria ……..... 25

II. AIMS OF THIS STUDY …….……... 27

(continued)

III. RESULTS ……..…… 29
3.1. Taxonomic characterization of the isolate 64G3 and the expression of amylase gene …… 29
3.1.1. Molecular identification of the strain ……..…… 29
3.1.2. Morphological and phenotypic properties ……..... 29
3.1.3. Amylolytic enzymes from strain 64G3…… 31
3.1.4. Cloning and sequence analysis of *amyA* gene…….. 32
3.1.5. Construction of genomic library of the strain 64G3 ……..…… 33
3.1.6. Southern hybridization ……..…… 34
3.1.7. The expression of *amyA* gene in *E. coli* ……38
3.1.7.1. Construction of an expression vector in *E. coli*…….……38
3.1.7.2. Expression of *amyA* gene…….…….. 38
3.1.7.3. Optimization of production of AmyA in soluble form …….……40
3.1.8. Characterization of enzymes ……..……44
3.1.8.1. Effect of temperature on enzyme activity…….….. 44
3.1.8.2. Effect of pH on enzymatic activity …… 45
3.1.8.3. Effect of different divalent ions on rAmyA activity …….. 46
3.1.8.4. Substrate specificity and mode of starch degradation …….……... 46
3.2. Cloning and expression of a chaperonin (*cpn*) operon in *B. subtilis*…….…..... 48
3.2.1. Subcloning of *cpn10/60* operon into *E. coli* using pJET1 …….... 48
3.2.2. Sub-cloning of the two *cpn* operons in pKTH290 and transformation in *B. subtilis* …… 50
3.2.3. Expression of *cpn* operons in *B. subtilis* …….. 52
3.2.4. Growth of *B. subtilis* carrying pKTH/changedRBS at low temperature and impact of psychrophilic chaperonin on cold-adaptation of the host 53
3.2.5. Construction of *B. subtilis* carrying a single chromosomal copy of the *cpn* operon …… 55
3.2.5.1. Subcloning of changedRBS operon in pAC5 …… 55
3.2.5.2. Integration of a single copy of the *cpn* operon into *B. subtilis* chromosome ……. …… 56
3.2.6. Expression of yeast α-glucosidase gene in *B. subtilis*……... 58
3.2.7. Impact of co-expression of *cpn* operon on PI activity ……. 61

(continued)

IV. DISCUSSION …… 63

4.1. Taxonomy of the strain 64G3 ……..…. 63
4.2. Bio-physical characteristics of the strain ……..…… 63
4.3. Amylase and the cloning of amylase coding gene …….. 66
4.4. The expression of *amyA* gene and the enzyme characteristics …… 67
4.4.1. Expression of *amyA* gene…….…… 67
4.4.2. Bio-characteristics of rAmyA ……..…..67
4.5. Cloning and expression of *cpn* operon in *B. subtilis* and impact of *O. antarctica* chaperonin in cold adaptation of the host. ……70
4.6. The heterologous production of yeast α -glucosidase (PI) in *B. subtilis* ... 72
4.7. Integration of *O. antarctica cpn* operon in the *B. subtilis* chromosome …. 72
4.8 Co-expression of α-glucosidase gene and *O. antarctica cpn* operon and the impact of psychrophilic chaperonin on enzyme activity …… 73

V. MATERIALS AND METHODS ……... 76
5.1. Materials ……...…….. 76
5.1.1. Bacteria ……. 76
5.1.2. Plasmids ……..... 76
5.1.3. Oligonucleotides ……... 77
5.1.4. Chemicals and buffers …….. 78
5.1.4.1. Chemicals and buffers for isolation of plasmids …… 78
5.1.4.2. Chemicals for gel electrophoresis of DNA …… 78
5.1.4.3. Chemicals and buffers for *B. subtilis* protoplast transformation …... 79
5.1.4.4. Chemicals and buffers for SDS-PAGE …….. 79
5.1.4.5. Chemicals and buffers for immunochemiluminescent detection ….. 80
5.1.4.6. Chemical components in protein refolding kit ……80
5.1.4.7. Chemical components in His bind purification kit ……. 81
5.1.5. Media …….……..…….. 81
5.1.5.1. Luria-Bertani (LB) broth ……..….. 81
5.1.5.2. SOC (super optimal broth with catabolic repression) …….81
5.1.5.3. Media for protoplast transformation of *B. subtilis* ……. 81
5.2. Methods ……... 82
5.2.1. Microbiological methods …….…… 82
5.2.1.1. Enrichment and isolation of strain 64G3…… 82

(continued)

5.2.1.2. Cultivation conditions 82
5.2.1.3. Scanning electron microscopy 82
5.2.2. Molecular methods 83
5.2.2.1. Isolation of bacterial chromosomal DNA 83
5.2.2.2. Isolation of plasmid DNA 83
5.2.2.3. Polymerase chain reaction (PCR) 84
5.2.2.4. Restriction endonuclease digestion 84
5.2.2.5. Dephosphorylation of linearized DNA fragments 85
5.2.2.6. DNA ligation 85
5.2.2.7. Agarose gel electrophoresis of DNA 86
5.2.2.8. Purification of DNA fragment from agarose gels and from solution . 86
5.2.2.9. Transformation 86
5.2.2.9.1. Electrotransformation 87
5.2.2.9.2. *B. subtilis* protoplast transformation 87
5.2.2.10. Construction of *P. mexicana* 64G3 genomic DNA library 88
5.2.2.11. DNA base composition analysis 88
5.2.2.12. PCR DIG probe synthesis 89
5.2.3. Protein and biochemical methods 89
5.2.3.1. Determination of protein concentration 89
5.2.3.2. Polyacrylamide gel electrophoresis (PAGE) 90
5.2.3.3. Activity staining – native PAGE 91
5.2.3.4. Southern blotting 91
5.2.3.5. Southern hybridization 92
5.2.3.6. Immunochemiluminescent detection 92
5.2.3.7. Overexpression of *amyA* and purification of rAmyA 92
5.2.3.8. Refolding of cellular inclusion bodies 93
5.2.3.9. Preparation of cellular fractions of *B. subtilis* 94
5.2.3.10. Amylase activity assay 94
5.2.3.11. α- Glucosidase activity assay 96
5.2.3.12. The effect of divalent metal ions on rAmyA activity 97
5.2.3.13. Substrate specificity of rAmyA 97
5.2.3.14. Analysis of hydrolysis products by TLC 97
5.2.4. Computational analysis 97
5.2.5. Nucleotide sequence accession number 98

(continued)

VI. REFERENCES ……..…. 99

Addendum ……..….113
Lists of figures and tables…….…..... 113
Appendix …….…...115
Abbreviation ……..…. 120
Publication …… 123

I- INTRODUCTION

1.1. Starch degrading enzymes and the genus *Petrotoga*

1.1.1. Starch properties and amylolytic enzymes

1.1.1.1. Starch properties

Starch is the major storage carbohydrate in many plants. It consists of two high molecular weight components, the linear amylose and branched amylopectin (Fig. 1.1). These two polymers differ in molecular size, their solubility in water and their susceptibility to enzymatic hydrolysis. Amylose is a polymer approximately consisting of 500–1,000 glucose units with α-1,4 glycosidic bonds and few α-1,6 branching points. The amylose content varies between almost 0 and 75%, with a common value of 15–25%. Amylopectin is a major fraction of starch (75–85%) and is more complex than amylose because of its highly branched structure (Leveque et al. 2000b; Bertoldo and Antranikian 2002). Amylose consists of short α-1,4 linked linear chains of 10–60 glucose units and α-1,6 linked side chains composed of 15–45 glucose units. Average number of branching points (α-1,6 linkage) in amylopectin is about 5%, and branches occur every 12 to 23 glucose units on the linear chain, depending on the botanical origin (Tester et al. 2004). One amylopectin molecule can contain more than 2,000,000 glucose units, thereby representing the largest molecules in nature. Amylose is hardly dissolved in water, whereas amylopectin is reasonably water- soluble.

Native starch is roughly spherical and partially crystalline where amylopectin forms the crystalline component and amylose exists mainly in the amorphous form. In grain, amylopectin represents the most important component of the crystalline regions whereas the amylose component is combined with lipids to form a weak crystalline structure that reinforce the granule (Maarel et al. 2002)

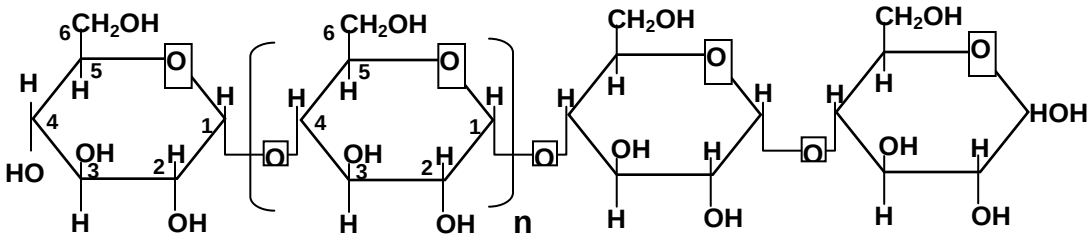

Amylose: α–1,4 glucan; average n= ca. 1000

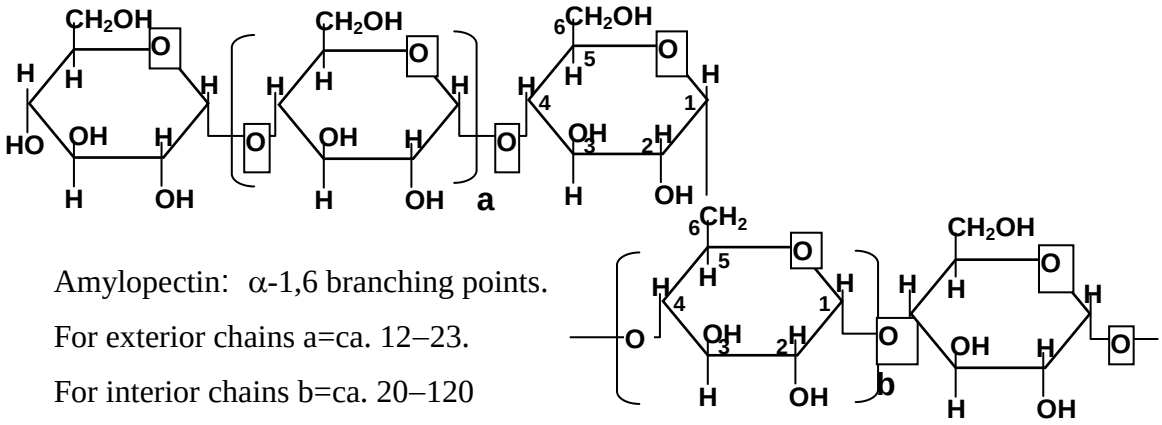

Amylopectin: α-1,6 branching points.

For exterior chains a=ca. 12–23.

For interior chains b=ca. 20–120

Figure 1.1. Structures of amylose and amylopectin with α-1,4 and α-1,6 glucosidic linkages

1.1.1.2. Enzymatic hydrolysis of starch

Starch degrading enzymes are widely distributed in the microbial, plant and animal kingdoms. Because of the complex structure of starch, cells usually require a combination of various types of hydrolyzing enzymes for the depolymerization of starch and related polysaccharides to diverse products including dextrin, smaller polymers or oligosaccharides (Windish and Mhatre 1965). The process of enzymatic starch conversion is displayed in Fig.1.2. In general, these enzymes are called amylases or amylolytic enzymes and belong to the glycoside hydrolase groups (GHs). Amylolytic enzymes catalyze the hydrolysis or transfer of glycosidic bonds between two carbohydrate monomers or between a carbohydrate monomer and a non-carbohydrate moiety in the starch or related polysaccharides.

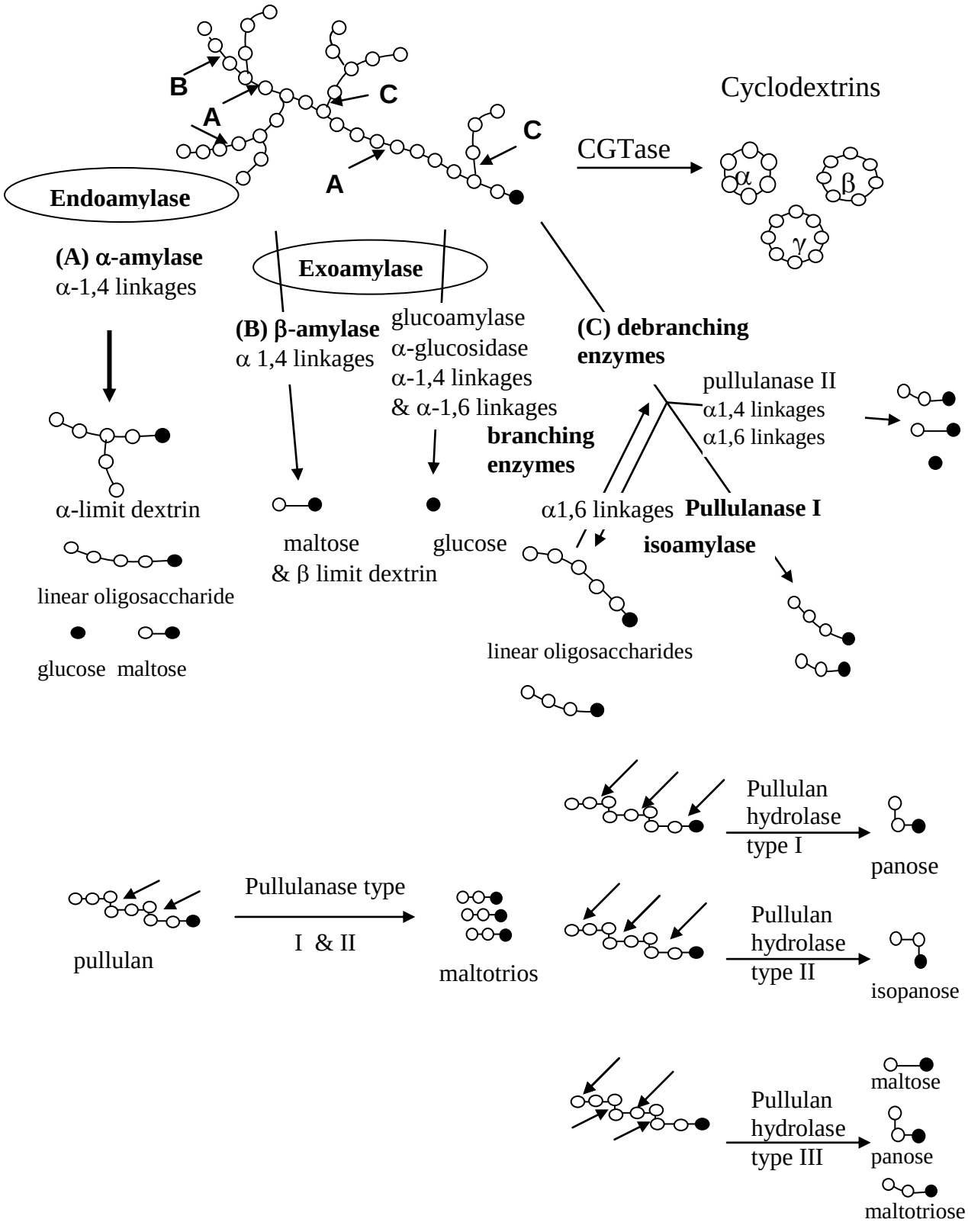

Figure 1.2. Schematic demonstration of the action of amylolytic and pullulytic enzymes. Adapted from Bertoldo & Antranikia (2002). Black circles refer to reducing sugars.

Traditional division of amylases, expressed in different EC numbers, is based on the type of enzymatic activity, i.e. modes of action, substrates used and hydrolytic products. There are basically four groups of the enzymes: (i) endoamylases; (ii) exoamylases; (iii) debranching enzymes; and (iv) transferases (Maarel et al. 2002).

a- Endo-amylases

Endo-amylases or endo acting amylases hydrolyze α-1,4 glycosidic linkages in the inner part of the amylose or amylopectin chain in a random manner. The end products of endo-amylase action on starch are oligosaccharides of varying length with an α-configuration and α-limit dextrins, which constitute branched oligosaccharides.

b- Exo-amylases

Exo-amylases include β-amylase, glucoamylase and α-glucosidase. These enzymes either exclusively cleave α-1,4 glycosidic bonds such as β-amylase (EC 3.2.1.2) and α-glucosidase (EC 3.2.1.20) or cleave both α-1,4 and α-1,6 glycosidic bonds like glucoamylase (or amyloglucosidase) (EC 3.2.1.3). Exo-amylases act on the external glucose residues of amylose or amylopectin from the non-reducing end, producing defined oligosaccharides, i.e. glucose (glucoamylase and α-glucosidase), or maltose and β-limit dextrin (β-amylase). β-Amylase and glucoamylase also convert the anomeric configuration of the liberated sugars from α to β. Glucoamylase and α-glucosidase differ in substrate preference: α-glucosidase hydrolyses short maltooligosaccharides and liberates glucose with an α-configuration while glucoamylase acts best on long-chain polysaccharides. Other exo-acting amylases are for instance cyclodextrin glycosyltransferase (EC 2.4.1.19), an enzyme that has both hydrolysis and transglycosylation activity and maltogenic α-amylase (glucan 1,4-α-glucanhydrolase, EC 3.2.1.133), that releases α-maltose from the hydrolysis of starch (Diderichsen and Christiansen 1988).

c- Debranching enzymes

Debranching enzymes hydrolyze α-1,6 glycosidic bonds in amylopectin and related polymers. This group includes isoamylases (EC 3.2.1.68) and pullanases type I (EC 3.2.1.41). Pullulanases hydrolyze α-1,6 glycosidic bond in pullulan and amylopectin, while isoamylases can only hydrolyze the α-1,6 bond in amylopectin. Pullulanases type II that hydrolyse both α-1,4 and α-1,6 glycosidic bonds and they could be referred to as α-amylase–pullulanase or amylopullulanase. Pullulanases type I debranch pullulan to maltotriose as final product, but they also weakly attack the α-1,4 bonds in starch. A special enzyme of the pullulanase group is

neopullulanase, which can additionally have transglycosylation activity with the formation of a new α-1,4 or α-1,6 glycosidic bond (Takata et al. 1992).

d- Transferases

The fourth group of amylases are transferases that cleave an α-1,4 glycosidic bond of the donor molecule and transfer one part of the donor to a glycosidic acceptor with the formation of a new glycosidic bond. In this group, amylomaltase (EC 2.4.1.25) and cyclodextrin glycosyltransferase (CGTase) (EC 2.4.1.19) form a new α-1,4 glycosidic bond (Bonilha et al. 2006) while branching enzymes (EC 2.4.1.18) form a new α-1,6 glycosidic bond (Palomo et al. 2011). CGTase has a very low hydrolysis activity but catalyzes the formation of circular α-1,4-linked oligosaccharides (cyclodextrins) from starch. Amylomaltase or 4-α-glucanotransferases is very similar to CGTase in formation of new α-1,4 bonds, but they yield linear products instead of circular products.

1.1.1.2.1. α-Amylase family (glycoside hydrolase family 13, GH13)

Henrissat (1991) proposed a scheme for classification of glycoside hydrolases, based on protein sequence rather than their specificity of action. All the enzymes showing well defined sequence similarities are grouped in one family, a basic unit of the classification. According to this classification, nearly one hundred families of glycosidases and transglycosidases have been identified.

Most of the enzymes acting on starch belong to one major family: the α-amylase family or glycosyl hydrolases family 13 (GH13 enzyme), including α-amylase, pullulanase, α-glucosidase, cyclodextrin glucosyl transferase, etc. (Table 1.1).

GH13 enzyme displays about 30 different reaction and product specificities, including exo/endo specificity, preference for hydrolysis or transglycosylation, α-1,1, α-1,4 or α-1,6-glycosidic bond specificity and glucan synthesizing activity. Maarel et al. (2002) listed their major features as follows:

(i) They act and hydrolyze α-glycosidic bonds to form α-anomeric mono- or oligosaccharides (hydrolysis), or form new α-1,4 or α-1,6 glycosidic linkages (transglycosylation), or a combination of both activities;

(ii) They possess a $(\alpha/\beta)_8$ (or TIM barrel) structure and three catalytic residues (Asp, Glu and Asp) located in conserved regions;

(iii) They have four highly conserved regions in the primary sequence and some amino acids that are essential for the stability of the conserved TIM barrel topology.

Table 1.1. Reaction specificities of starch degrading α-amylases of GH13 family (Leemhuis et al. 2003)

Enzyme	EC number	H or T [a]	Bonds processed	Preferred substrate
α-Amylase	3.2.1.1	H	α-1,4	Starch
Maltotetraose forming amylase	3.2.1.60	H	α-1,4	Starch
Maltopentaose forming amylase	3.2.1.-	H	α-1,4	Starch
Maltohexaose forming amylase	3.2.1.98	H	α-1,4	Starch
α-Glucosidase	3.2.1.20	H	α-1,4	Terminal non-reducing glucose residues
Cyclodextrin glycosyltransferase	2.4.1.19	T	α-1,4	Starch
4-α-glucanotransferase	2.4.1.25	T	α-1,4	Starch
Cyclomalto-dextrinase	2.4.1.54	H&T	α-1,4 and α-1,6	CDs[b], pullulan, starch
Neopullulanase	3.2.1.135	H&T	α-1,4 and α-1,6	CDs[b]. Pullulan, starch
Maltogenic amylase	3.2.1.133	H&T	α-1,4 and α-1,6	CDs[b], pullulan, starch
Oligo-1,6-glucosidase	3.2.1.10	H	α-1,6	Terminal non-reducing glucose residues
Pullulanase type I	3.2.1.41	H	α-1,6	Pullulan, starch
Isoamylase	3.2.1.68	H	α-1,6	Starch
Branching enzyme	2.4.1.18	T	α-1,4→1,6	Starch
Glucodextranase	3.2.1.70	H	α-1,6	α-1,6 glucan
Pullulanase type II[c]	3.2.1.41	H	α-1,4	Starch
Pullulanase type II[c]	3.2.1.41	H	α-1,6	Pullulan

[a] Main activity, H is hydrolysis and T is transglycosylation
[b] CDs, cyclodextrins
[c] These enzymes have two distinct active sites that are responsible for the two separate activities.

The most common amylases are α-amylase (EC 3.2.1.1), β-amylase (EC3.2.1.2) and glucoamylase (EC 3.2.1.3). They differ in their primary and tertiary structures as well as in their catalytic machineries and reaction mechanisms. They are classified into different GH families: GH13-α-amylases, GH14-β-amylases, and GH15-glucoamylases (Henrissat 1991). Some amylases with sequence specific and structural differences from the main GH13 α-amylases have been placed into different families such as GH31, GH57, GH70 and GH77. For instance, two "unusual" α-amylases, a AmyA from *Dictyoglomus thermophilum* and one enzyme from *Pyrococcus furious* act on starch but lack the typical conserved sequences of the

GH13 family and thus are classified into GH57 family. The above mentioned GHs form the α-superfamily, also known as GH-H clan. Some heteromeric amino acid transporter proteins with sequence similarities may be considered to be the non-amylolytic members of the clan GH-H (Janecek et al. 1997).

The three – dimensional (3D) structure of GH13 protein

Over six thousands of known primary sequences of the α-amylase family enzymes were deposited in sequence databases and 3-D structures of 35 α-amylase family enzymes from various sources have been determined (MacGregor 2005). The GH13 enzymes are multi domain proteins with a common $(\beta/\alpha)_8$ or TIM-barrel catalytic domain, known as domain A.

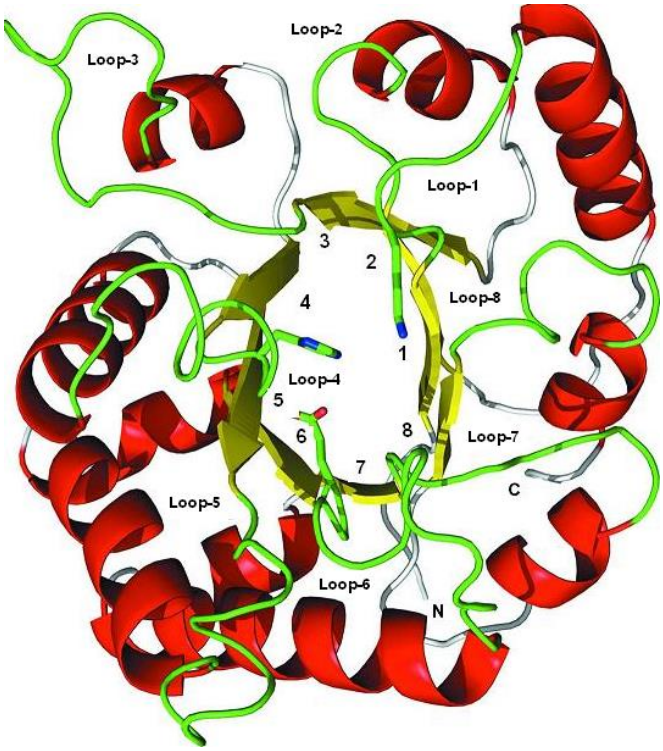

Figure 1.3. Parallel $(\beta/\alpha)_8$ barrel of triosephosphate isomerase (TIM). Adapted from Salin et al. (2010). The classical TIM-barrel motif composes of eight parallel β-strands (numbers 1-8) forming the inner β-barrel sheet which surrounded by eight α-helices. Thus, a common $(\beta/\alpha)_8$ barrel contains eight repeated $(\beta/\alpha)_8$ units. The N-terminus and C-terminus are labelled N and C, respectively.

Domain A folds symmetrically with eight inner, parallel β-strands surrounded by eight helices (Fig.1.3). The TIM barrel structure was first determined for the structure of chicken muscle triosephosphate isomerase (TIM) in 1975 (Banner et al. 1975) and afterwards for many other enzymes catalyzing distinct reactions. In this structure, the β-strands lie approximately parallel to one another, as if on the surface of a cylinder, with the helices locating outside the β-strands.

The C-terminal ends of β-strands are joined to the N-terminal ends of the following helices by irregular loops, and the loops link the C-terminal ends of helices to the N-terminal ends of adjacent β-strands. Strands β2, β3, β4, β5, β7 and β8 contain the best conserved regions found in GH13 enzymes. The three catalytic residues, Asp, Glu and Asp occur in the strand β4, β5 and β7 respectively. The β strands are better conserved than the corresponding α-helix. In most cases, the long loop 3 connecting strand β3 to helix 3 folds as an independent unit, and sometime belongs to domain B which is considered to evolve from a common ancestor (Janecek 1997).

Domain B shows the highest variations within the amino acid sequence and contains about 44–133 residues. A short conserved sequence locating near the C-terminus of domain B (e.g. 173 LPDLD in Taka-amylase A) is involved in the binding of a calcium ion (Boel et al. 1990), or in substrate binding. Noticeably, the differences in the length, sequence and secondary structure of domain B may be directly related to functional diversity and enzyme specificity (Janecek 1997).

Domain C, just after the catalytic TIM $(\beta/\alpha)_8$-barrel (Fig. 1.4), contains the antiparallel β-sheet domain. Domain C could stabilize the catalytic domain (domain A) by protecting the hydrophobic residues of the $(\beta/\alpha)_8$ -barrel from solvent (Katsuya et al. 1998). Domain C shows the characteristic β-sandwich structure of GH13 proteins which is missing in GH77 and GH70 family.

Typical α-amylases (EC.3.2.1.1) harboring the domains A, B and C are monomeric, calcium-containing enzymes. However, some α-amylases may have additional domains such as domain D (just after the TIM-barrel), and E (contain additional β-strand) following the C domain (Janecek et al. 2003) (Fig 1.4). The enzymes possessing the catalytic $(\beta/\alpha)_8$ barrel (domain A) and four domains B, C, D and E are thus five-domain proteins. C domain is however not present in amylase of the GH77. D and E domains are typical for cyclodextrin glycosyltransferase (CGTases). Domain E functions as a raw starch binding domain and may be present in certain β-amylase (GH14), and glucoamylase (GH15). The role of D-domain remains unclear. N domain are found in cyclomaltodextrinase, neopullulanase and maltogenic-amylase and it functions in dimerization and oligomerization of enzyme monomers. However, a few domains have been identified in α-amylase family enzymes, but their functions remain to be elucidated.

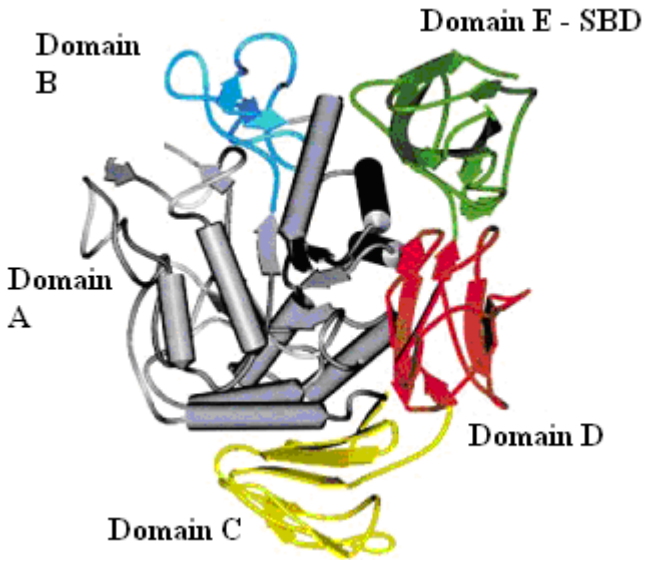

Figure 1.4. Stereo structure of the GH13 α amylases. Adapted from Janecek et al. (2003). A typical α-amylase contains domain A, B and C, while a CGTase containing 5 domains (additional E and D domains)

1.1.1.2.2. Starch Hydrolysis mechanism

A general acid catalysis participating in enzymatic hydrolysis of starch requires two components: a proton donor (an acid) and a nucleophile (a base). For GH13 enzymes, the catalytic mechanism can be divided into two steps. First, the anomeric configuration of the processed O-glycosidic bond (α→β or β→α) is inverted. Second, the anomeric configuration of the processed glycosidic bond (α→α or β→β) is retained, generating a product with the same anomeric configuration as substrate (McCarter and Withers 1994). α-Amylase requires a double displacement mechanism and a covalent glycosyl-enzyme intermediate is formed (Fig. 1.5). In contrast, β-amylase (GH14) and glucoamylase (GH15) are inverting hydrolases, indicating that the direct displacement mechanism generates a product with opposite anomeric configuration to the substrate.

In the retaining mechanism, the two catalytic residues in the active site of domain A are glutamic (Glu) acid and aspartate (Asp), serving as the acid/base catalyst and nucleophile, respectively. After the binding of substrate in active site, Glu (acid form) donates a proton to the glycosidic oxygen between two glucose molecules. Then, the nucleophilic Asp attacks the C1 atom of glucose molecule (glucose 1) (Fig. 1.5 A). An oxocarbonium ion – like transition state is formed and a covalent intermediate is produced. The protonated glucose molecule (glucose 2) leaves the active site, followed by the movement of a water molecule (hydrolysis)

or a new sugar molecule (transglycosylation) into the active site and that attack the covalent bond between the glucose molecule (glucose 1)- the Asp and an oxocarbonium ion like transition state is formed again (Fig. 1.5 B). A hydrogen from an incoming water (hydrolysis) or the newly entered sugar molecule (transglycosylation) was transferred to the catalyst glutamate. The oxygen of the incoming water or the newly entered sugar replaces the oxocarbonium bond between the glucose molecule (glucose 1) and the aspartate. Thus, a new hydroxyl group at C1 position of the glucose molecule (glucose 1) or a new glycosidic bond between the glucose molecule (glucose 1) and new enterred glucose (transglycosylation) is formed (Fig. 1.5 C)

Besides the two residues which play a direct role, a third residue, the second Asp, binds to the OH-2 and OH-3 groups of the substrate, changing the substrate shape.

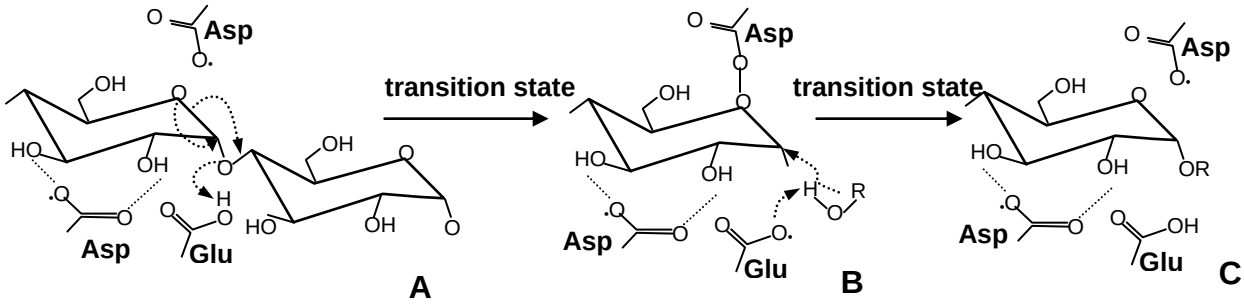

Figure 1.5. The α-retaining double displacement bond mechanism possessed by the α- amylase of GH13. Adapted from van der Maarel et al. (2002). H-O-R: indicate water (in hydrolysis) or another sugar (in transglycosylation)

1.1.1.3. Application of amylolytic enzymes

Amylases are among the most important enzymes and are of great significance for biotechnology and industrial applications. They are used in industrial scales for a variety of different applications like starch liquefaction, textile desizing, bread improvement, alcohol production, and as an additive to detergent formulations (Table 1.2). Minor applications of these enzymes are found in the pulp and paper industry (Sauza and Magalhaes 2010). Commercially, the heat stable α-amylase from *B. licheniformis* or *B. stearothermophilus* are currently used in hydrolyzing processes of starch (Maarel et al. 2002). In detergent application, the demand for these enzymes is growing, both for laundering and dish washing. α-Amylases with high activity and stability under alkaline and oxidizing conditions (pH as high as 10.5) are of choice. Most of liquid detergents (account for 90%) contain amylase.

Table 1.2. Uses of amylases in various sectors of industry (Sivaramakrishnan et al. 2006)

Sector	Uses
Food industry	Production of glucose syrups, maltose syrups crystalline glucose and high fructose corn syrups Reduction of viscosity of sugar syrups Reduction of haze formation in juices Solubilization and saccharification of starch for alcohol fermentation in brewing industry Retardation of staling in baking industry
Detergent industry	Used as an additive to remove starch based dirts
Paper industry	Reduction of viscosity of starch for appropriate coating of paper
Textile industry	Warp sizing of textile fibers
Pharmaceutical industry	Used as a digestive aid

1.1.2. Oil reservoir, a habitat for various groups of microorganisms

1.1.2.1. Oil reservoir properties

Petroleum reservoirs are considered as habitats for a large diversity of microorganisms. An unusual combination of extreme environmental conditions, including temperature (up to 180°C), pressure (up to 40 Mpa) and salinity (20 g/L) is found in most deep petroleum reservoirs. They contain a layer of water known as connate water or formation water which is trapped beneath the gases and the oil. The water layer is rich in dissolved gases such as CO_2, CO, CH_4, H_2 and H_2S (Orphan et al. 2003).

Microorganism in oil reservoir.

Different types of data suggest a threshold temperature between 80 and 90°C as the upper limit for growth of indigenous bacteria in oil fields (Philippi 1977; Fisher 1987; Barth 1991). Besides extreme physical properties, the nutrient content also limits microbial life, for instance the phosphorous compounds. Due to the lack of dissolved oxygen, only strict anaerobes can exist and are truly indigenous to oil reservoirs. They are actually those more frequently isolated and can be divided into several major microbial groups, including sulfate reducing, methanogenic archaea and fermentative bacteria (Magot et al. 2000).

Sulfate reducing bacteria (SRB) have been studied most commonly. They are mesophilic or thermophilic bacteria and hypethermophilic archaea, depending on the *in situ* temperature (ranging from 18 to 90°C). Certain representatives of the mesophilic SRBs for instance *Desulfovibrio longgus* (Magot et al. 1992) or *D. vietnamensis* (Nga et al. 1996), are halotolerant. From hot oil reservoirs, members of genera like *Desulfotomaculum*,

Desulfacinum, *Thermodesulforhabdus* and *Thermodesulfobacterium* were isolated. SRB can use hydrogen, lactate and pyruvat as electron donor to reduce sulfate to sulfite (Ruwisch et al.1987).

The second group present in oil reservoirs are members of methanogeni bacteria. They are classified as archaea and reduce CO_2 or organic acids such as acetate, formate and butyrate by using hydrogen as electron donor to produce methane. Thermophilic species of the genera *Methanobacterium*, *Methanoculleus* and *Methanococcus* were observed in continental Californian oil reservoirs (Orphan et al. 2000).

The third bacterial group are fermentative bacteria, including mesophilic, thermophilic and hyperthermophilic species. They represent an important microbial community of oil reservoirs. These bacteria use sugar, peptides, amino acids, or organic acids as energy source. Some of them may use inorganic sulfur compounds, ferric iron and nitrate as electron acceptors to oxidize substrates. Thermophilic, fermentative bacteria are much greater frequently isolated from hot oil reservoirs. Most of them belong to the order *Thermotogales* (Osmolovskaya et al. 2003). Noticeably, within this order, the genus *Petrotoga* and *Geotoga* have been isolated only from oil reservoirs, indicating their indigenous origin. The genus *Thermotoga* comprises mostly thermophilic bacteria with *T. maritime* as representative which grows at an optimum temperature of 80°C (Huber et al. 1986). Besides *Thermotogales*, the genera *Thermoanaerobacter* and *Thermoanaerobacterium* were also frequently isolated from hot and slightly saline reservoirs (Grassia et al. 1996). Hyperthermophilic fermentative archaea are also present in hot oil reservoirs. Most of them belong to the order *Thermococcales*, including members of the genera *Thermococcus* and *Pyrococcus*.

1.1.2.2. The genus *Petrotoga* and their starch degrading enzymes

Genus *Petrotoga* belongs to the order *Thermotogales* which represents the second deepest branch in the bacterial line. *Petrotoga* comprises six species, including *P. miotherma, P. mobilis, P. mexicana, P. olearia, P. sibirica* and *P. halophila* (Miranda-Tello et al. 2007). They are fermentative, anarobic, thermophilic, rod-shaped eubacteria and were only isolated from oil reservoirs. Among them, *P. halophila* was the last one isolated from an offshore producing well in 2007 (Miranda-Tello et al. 2007). *Petrotoga* members have an outer sheath like structure, called “toga”, which balloons over the cell ends. The toga is a typical characteristic of the *Thermotogales*, and is not found in other bacteria.

Petrotoga species can ferment a wide range of carbohydrates including starch and xylan as an energy source, to produce organic acids such as lactate or acetate (Lien et al. 1998; Miranda-Tello et al. 2004, 2007; Davey et al. 1993). Cellulose is not the substrate for the

growth of *P. olearia* and *P. sibirica* (L'Haridon et al. 2002), *P. mobilis* (Lien et al. 1998). *Petrotoga* reduce either thiosulfate or elementary sulfur to sulfite. L-alanine is one of the products of glucose metabolism by *Petrotoga* species, which is interpreted as a remnant of an ancestral metabolism. (Miranda-Tello et al. 2007)

The occurrence of *Petrotoga* species only in oil reservoirs so far raises questions about (i) their survival in this deep subsurface environment and (ii) their possible indigenicity to this peculiar ecosystem.

Amylolytic enzymes from *Petrotoga*

Davey et al. (1993) first reported the presence of *Petrotoga* in the petroleum reservoirs located in Oklahoma and Texas. Polysaccharides degrading activities have been reported for several *Petrotoga* members, including xylanase activity of *P. mobilis* (Lien et al. 1998) and *P. mexicana* (Miranda-Tello et al. 2004) or amylase activity of *P. miotherma* (Davey et al. 1993). All *Petrotoga* species were able to ferment starch as a sole carbon source, indicating their amylase activities. However, their enzyme information still remains unclear. Only a few amylolytic enzymes from the *Thermotogales* have been characterized at the biochemical and genetic level; and all of the studied enzymes originate from the species *T. maritima* (Ballschmiter et al. 2006; Bibel et al. 1998; Lim et al. 2003; Liebl et al. 1997), *Fervidobacterium pennavorans* (Koch et al. 1997) and *T. neapolitana* (Park et al. 2010). The investigated enzymes exhibited high thermoactivity: *T. maritima* amylases A and C showed a temperature optimum (Topt) between 85 – 90°C (Ballschmiter et al. 2006; (Liebl et al. 1997); *T. maritima* pullulanase with Topt of 90^{o}C (Bibel et al. 1998); *F. pennavorans* pullulanase with Topt of 85°C (Bertoldo et al. 1999) and *T. neapolitana* amylase with Topt of 75°C (Park et al. 2010). Apart from their thermostability, a few enzymatic properties which are applicable in starch industry have been observed, such as α-1,6 glucosidic bond specificity of *F. pennavorans* pullulanase (Bertoldo et al. 1999) and the formation of maltose by *T. neapolitana* exo-type α-amylase (Park et al. 2010).

1.2. The protein folding and chaperonin activity

1.2.1. Protein structure and its folding problems

1.2.1.1. Structure of proteins

Proteins are polymers of amino acids that are covalently linked through peptide bonds into a chain. They are important cellular components and are involved in most biological functions, including structural roles (cytoskeleton), catalysts (enzymes), molecule transporters, antibodies and chaperones. To fulfill the biological roles, polypeptide chains must fold into specific three dimensional structure (3D or native state). The folding process includes a number of non-covalent interactions (hydrogen bonding, ionic interaction, van der vaals forces) and hydrophobic packing. Protein structures are described at four levels of complexity:

Primary structure is determined by the sequence of amino acids in polypeptides. The amino acids composition and their sequence of a chain is coded by the gene corresponding to the protein.

Secondary structure is formed by folding or coiling of different regions within the sequence. Two types of secondary structure are α-helices and β-pleated sheet (Pauling and Corey 1951).

Tertiary structure refers to the 3D structure of a protein. In a polypeptide chain, a larger number of amino acids residues have non-covalent interactions which result in folding. Tertiary structure displays the relationship of different domains in a polypeptide.

Quaternary structure refers to a combination of two or more polypeptide chains (called subunits) to form a large and complete unit. In this structure, chains interact together via non-covalent and disulfide bonds.

1.2.1.2. Protein folding problems

Protein folding is a physical process by which a polypeptide chain folds into its characteristic and functional 3D structure. There exist three questions concerning the protein folding:

(1) The thermodynamic question of what balance of interatomic forces dictates the structure of the protein. This refers to the folding code;

(2) The question if a native protein structure be predicted from its amino acid sequence;

(3) The question of what routes or pathways protein use to fold so quickly into its native form.

Classical view of protein folding:

It was proposed that the protein folding was a spontaneous process (Anfinsen 1972, 1973; Haber and Anfinsen 1962). By studying on renaturation of fully denatured ribonuclease, Anfinsen propose a hypothesis, stating that "*3D structure of a native protein in its normal physiological millieu (solvent, pH, ionic strength, temperature, etc.) is the one of which Gibbs free energy of the whole system is lowest; that is, that the native conformation is determined by the totality of interatomic interactions and hence by the primary amino acid sequence, in a given environment*" (Anfinsen 1973). In the study, the author observed only two – state folding protein (unfolded and native states) of folding process. Thus, in this hypothesis, the folding route or intermediates during the folding process remained unclear.

The classical view of protein folding states that "*The search for the native state through the vastness of conformational space flows through predetermined pathways defined by discrete intermediates and barriers*".

New view of protein folding:

The general accepted model of protein folding is that proteins have funnel-shaped energy landscapes, i.e. many high-energy states and few low-energy states (Schultz 2000) (Fig. 1.6). Folding intermediates occur for larger proteins of > 100 residues (~90% of all cellular proteins) and they have a high tendency to collapse into compact non-native conformation. The folding process is better described by a multi-dimensional energy landscape. Each point on the energy surface refer to one conformation of the polypeptide and the corresponding free energy. The lowest point in the energy landscape, or the bottom of the funnel represents the native state of a protein. Denatured or non-native proteins with a higher energy usually resemble a random coil containing the dominating local interactions and this forms the top of the funnel. During folding, the protein follows a route from the top to the bottom of the funnel. When the intermediates are kinetically trapped and eventually misfold in an off-pathway reaction, molten globule (native like structure) or aggregation states will occur.

The funnel-shaped energy landscape clearly explains the process of reaching a global minimum in free energy and doing so quickly by multiple folding routes.

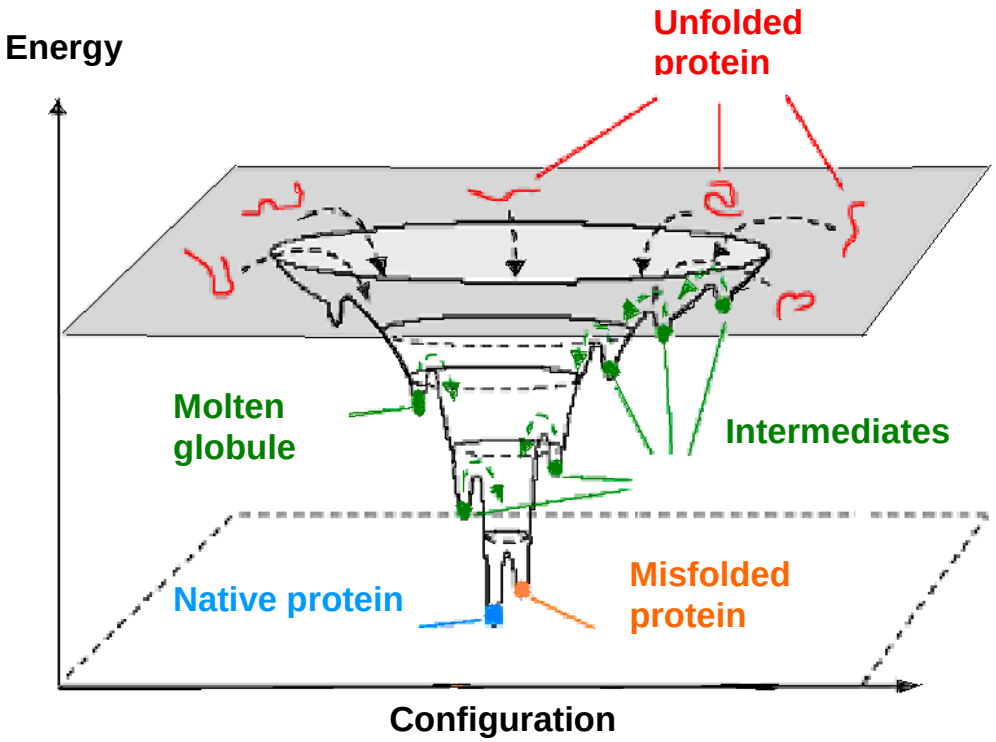

Figure 1.6. The folding funnel. Adapted from Schultz (2000)

A folding funnel represents the free energies of all potential protein structures. Denatured protein at the top of the funnel may fold into the native state via a myriad of different routes. Some local energy minima represent productive folding, transient intermediates which might possess a stable and native-like structure (molten globules), whereas others involve significant kinetic traps, resulting in a misfolded or nonnative state.

1.2.1.3. Dominant force in protein folding

Before the mid-1980s, most view proposed that protein folding code is the sum of many different small interactions (hydrogen bonds, ion pairs, van der Waals interactions, hydrophobic interactions), mainly expressed through secondary structures and mainly local in the sequence (Anfinsen and Scheraga 1975).

By statistical mechanical modeling, hydrophobic interactions is a dominant component, and the folding code is distributed both locally and non-locally in the sequence. Hydrogen-bonding interactions and van der Waals interactions are also important (Chen and Stites 2001).

Hydrophobic interactions in protein folding are the most important, explained by the following evidences: (a) Proteins have hydrophobic cores, implying that non-polar residues are sequestered from water. (b) 1–2 kcal/mol is needed to tranfer one hydrophobic side chain from water into oil-like media (Wolfenden 2007), and there are many of them. (c) Proteins are quickly denatured in non-polar solvents like chlorofom. (d) The correct hydrophobic cores are

retained and polar patterning folds to the native states without charges and hydrogen bondings (Cordes et al. 1996; Hecht et al. 2004; Kamtekar et al. 1993; Kim et al. 1998).

1.2.2. The protein folding *in vivo*

High cellular protein concentration, temperature and ionic strength are extremely unfavorable for correct protein folding because these conditions favor aggregation (Shortle 1996). It was estimated that 20–30% of the cellular volume is occupied by macromolecules, mainly protein, RNA and DNA with a concentration of at least 300 g/L (Zimmerman and Trach 1991). These concentrations cause an increase in the thermodynamic activity (effective concentration) of partially folded states (Minton 2000). Thus, the intermolecular binding constants between partially folded states are increased, resulting in a high probability of aggregation during folding (van den Berg et al. 1999).

The *in vivo* folding involves in biosynthesis process, which is vectorial, i.e. from the N-terminus to the C-terminus of the polypeptide. During protein synthesis, the folding information in terms of the amino acid sequence is not available all at once. After amino acids segment protrude from the ribosome, they fold to the lowest energy minimum for that length of chain and exist for prolonged periods of time. Their hydrophobic regions which are sensitive to aggregation states expose to the cellular environments (Agashe and Hartl 2000). The newly translated polypeptide chains attached on the ribosome will be in danger of misfolding and aggregating.

Cellular molecular chaperones participate in a multitude of cellular functions, including protein folding, refolding of denatured proteins, oligomeric assembly, intracellular protein transport and in proteolytic degradation. Chaperones usually accumulate at high concentrations in all cells, from bacteria to humans. A molecular chaperone is defined as '*a protein which transiently binds and stabilize an unstable conformer of another protein, facilitating its correct fate in vivo: be it folding (following de novo synthesis, transit across a membrane, or stress-induced denaturation), oligomeric assembly, interaction with other cellular components, switching between active and inactive conformations, intracellular transport, or proteolytic degradation, either singly or with the help of co-factors*' (Agashe and Hartl 2000).

Most chaperones are also heat shock proteins (Hsp) and their level of expression is greatly increased when cells encounter extreme environments. On the basis of molecular weights, amino acid sequences and functions, the hsp are classified into seven families: Hsp110/Hsp100, Hsp90, Hsp70, Hsp60, Hsp40, small Hsps (sHsp) and Hsp10 (Gething 1997). A cell can produce multiple members of the same chaperone family, e.g. the yeast *S. cerevisiae*

produces 14 different versions of Hsp70 (Craig et al. 1999). The common functional features of most molecular chaperones are shown in Table 1.3.

Table 1.3: **Reprentative folding chaperones**. Adapted from Bhutani and Udgaonkar (2002)

Class	Selected member	Function
CCT	TF55, TriC	Folding of nascent polypeptides and misfolded protein in eukaryotic cytosol
DnaJ	DnaJ, Dj1A, CbpA, HscB, Hsp40, Ydj1, Sec63, Auxilin, CSP's, Mdj1, Hdj1, Hdj2	Co-chaperone of Hsp70
GimC	Gim 1-6, Prefoldin	Folding of actin and tubulins
GrpE	GrpE, Mge1p	Co-chaperone of Hsp70 in bacteria, mitochondria and chloroplast
Hsp10	GroES, Gp31, Hsp10, Cpn10	Co-chaperonin of Hsp60
Hsp47	Hsp47	Folding and assembly of collagen
Hsp60	GroEL, Hsp60, Cpn60	Folding of nascent polypeptides and misfolded protein in bacteria mitochondria and plastids
Hsp70	DnaK, HscA (Hsc66), Hsc70, Hsp68, 70, 71 and 73, Bip, Grp75, 78 and 80, KAR2, SSA1-4, SSB1, SSC, SSH1, LHS1, KAR2	Protein assembly and translocation across membranes in prokaryotes and eukaryotes
Hsp90	HtpG, Hsp90, Grp84, Erp90, Endoplasmin, Hsp108, gp96, Hsp83, 87	Prevention of aggregation and regulations of activity of steroid receptors and kinase
Hsp100	ClpA, B, X and Y, Hsp104, Hsp78	Assist in proteolysis and disaggregation
Prosequ-ences	Pro-subtilisin, proα-lytic protease	Protease assembly and maturation
sHSP	IbpA, IbpB, Hsp16.5, Hsp12, Hsp42, $\alpha\beta$-crystallin	Prevention of aggregation
Triger factor	TF	Associated with ribosomers, chaperones nascent chains and catalyses prolyl isomerisation

The chaperone network in the cytosol. In all three domains of life, the chaperone pathways participating in protein folding frequently follow organizational principles (Frydman 2001; Hartl and Hayer-Hartl 2002). Generally, chaperone action was divided in two tiers as displayed in Fig.1.7.

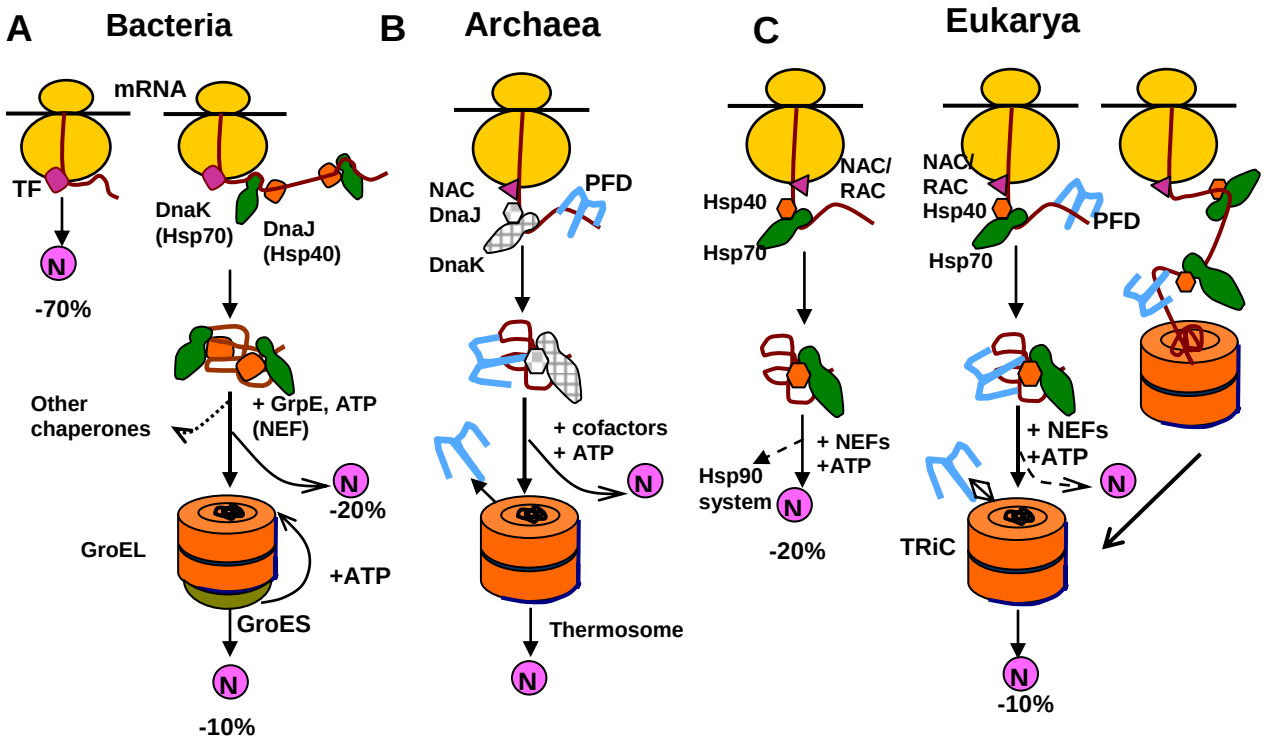

Figure 1.7. Models for the chaperone-assisted folding of newly synthesized polypeptides in the cytosol. Adapted from Vabulas et al (2009).

(i) The first tier: ribosome-associated chaperones are involved in binding and stabilization of newly synthesized polypeptides on the ribosome and initiate the local folding;

(ii) The second tier: downstream chaperones act in completing the folding process (Albanese, Yam et al. 2006) (Langer et al. 1992).

+ The first tier: There exist the ribosome – associated chaperones, including trigger factors (TF) in bacteria, specialized Hsp70 systems called RAC (ribosome associated complex) in eukaryotes and nascent chain associated complex (NAC) in eukaryota and archaea (Tang and Chang 2007; Kramer et al. 2009). TF bind to hydrophobic side chains of the nascent polypeptide, protecting them from wrong interactions and prevent premature folding until the domain has completely emerged from the ribosome (Fig 1.7A) (Bukau et al. 2000). Most small, single domain proteins (about 70% of total protein) can fold quickly into their native structures, without guidance of discrete chaperones. Like TF, NAC probably interact generally with nascent chains. RAC (ribosome-associated complex), Hsp70 and Hsp40 assist the folding of about 20% of chains into their native states (Fig. 1.7 B).

+ The second tier includes the two best studied chaperone systems, the Hsp70 family (DnaK in bacteria and Hsc70 in higher eukaryotes) and hsp60 family (Cpn in bacteria and

TriC/CTT in eukaryotes). A large, multi-domain proteins (>20 kDa) will need downstream chaperones such as Hsp70 or Hsp60 system for their correct folding. Hsp70 binds to nonnative substrate transiently, shielding exposed hydrophobic segments of protein, thereby prevent aggregation and arrests the folding process (so called 'holder' activity) (Flynn et al. 1991; Craig et al. 1999). Hsp70 also unfolds proteins locally but is not actively involved in the folding process. They alone assist the self-folding of 10–20% of all bacterial proteins (Bukau et al. 2000; Hartl and Hayer-Hartl 2002) (Fig. 1.7 A). Hsp60 receives unfolded protein delivered by Hsp70 and facilitates the protein folding inside this chaperone (so called 'folder' activity) (Fig. 1.7 A). Most of protein substrates of Hsp60 have molecular masses ranging from 20 to 50 kDa. Large proteins such as the 82 kDa yeast aconitase (Chaudhuri et al. 2001) and the 86 kDa fusion protein (Huang and Chuang 1999; Chuang et al. 1999) are also folded by Hsp60.

In eukaryotes, a fraction of protein substrates from the first tier is transferred to Hsp90. Another fraction (about 10%) is transfered by Hsp70 and PFD to the chaperones TRiC/CCT (Fig 1.7 C).

1.2.3. Hsp60 proteins

The Hsp60 proteins are found in all organisms from bacteria to human and are further subdivided into two classes: group I and group II (Horwich et al. 2007; Tang and Chang 2007). Members of group I occur in bacteria (called Cpn60), mitochondria and chloroplasts. They have seven-membered rings and functionally co-operate with Hsp10 proteins (bacterial Cpn10, eukaryotes Hsp10), which form the lid of the folding cage. The group II chaperonins in archaea (called thermosome) and in the eukaryotic cytosol (called TRiC/CCT) consist of eight- or nine-membered rings. They are independent of Hsp10 factors (Bhutani and Udgaonkar, 2002).

It was estimated that under cellular stress the folding of 30% newly synthesized polypeptides was dependent on the Hsp60 (Horwich et al. 1993).

1.2.3.1. The expression of bacterial *cpn10/60* operon

The chaperonin of *E. coli* represents the best studied system. It comprises two proteins: Cpn60 (a 57 kDa GroEL) and Cpn10 (a 10 kDa GroES). In chromosome, *groEL* and *groES* genes are organized in a single operon (*groE*) under the control of two promoters: a heat shock promoter, recognised by sigma factor σ32, and a constitutive promoter, active at normal growth temperature. GroEL and its co-chaperonin GroES are constitutively produced to a relatively high level (1-2% of total protein in *E. coli*). Elevated temperatures strongly induce the production of the chaperonins and thus their amounts can be increased up to 10-15% of the total cell protein (Neidhardt et al. 1984). In addition to temperature, the presence of damaged or aggregated proteins in the cytosol can induce the *groE* operon.

In *E. coli*, GroEL interacts with more than 250 different cytosolic proteins, of which about 85 are predicted to be obligate substrates for this chaperone (Kerner et al. 2005).

1.2.3. 2. Architecture and functions of GroEL and GroES

Architecture

The structure of the GroEL oligomer and its various complexes have been determined by X-ray crystallography (Braig et al. 1994; Boisvert et al. 1996) and by electron cryo-microscopy (Chen et al. 1994; Roseman et al. 1996). A 800 kDa-GroEL is a homo-oligomer of 14 subunits, each unit with a molecular mass of 57 kDa, arranged into two heptameric rings. The rings are stacked back-to-back, forming two discontinuous cavities in which unfolded polypeptides bind (Fig.1.8) (Chennubhotla and Bahar 2006). The unliganded GroEL complex is 151 Å in height and 140 Å in diameter with the 45 Å sized central cavity locating within each ring (Xu et al.1997).

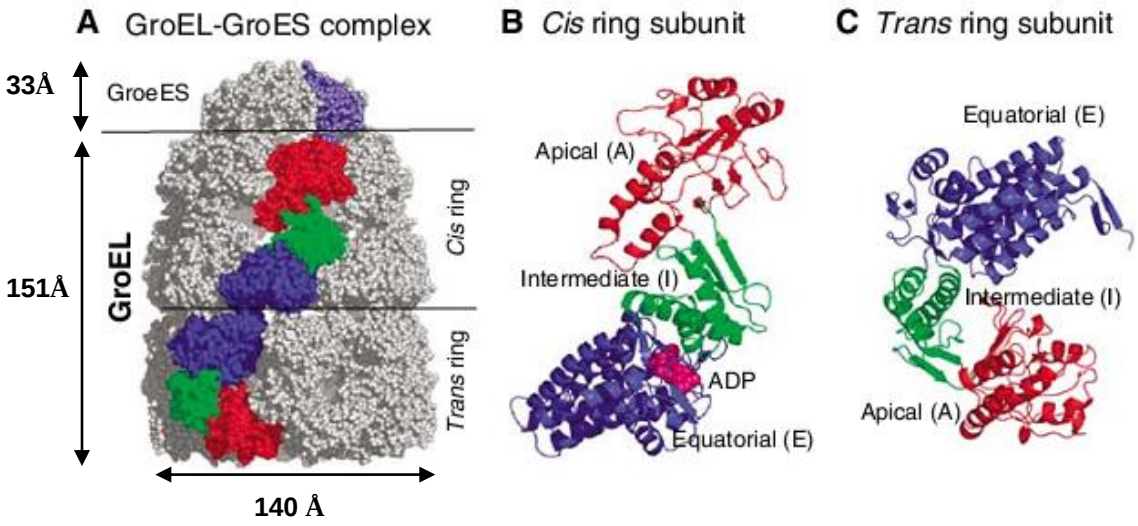

Figure 1.8. Structure of *E. coli* GroEL/GroES complex. Adapted from Chennubhotla and Bahar (2006)

(A) Space-filling model from the crystal structure. The two heptameric rings of GroEL are stacked back-to-back. GroES binds to one ring, forming *cis*-GroEL ring while leaving the other ring, the *trans*-ring, open. **(B)** and (**C**) display ribbon diagrams of these two subunits belonging the *cis* and *trans* ring respectively. The flexible hinge-like intermediate domain (green) link the equatorial ATPase domain (blue) to the substrate–binding apical domain (red).

Each monomeric subunit of GroEL consists of three following domains (Fig. 1.8): an apical, an intermediate, and an equatorial domain (Xu et al. 1997).

+ The equatorial domain (residues 6-133 and 409-523) is the largest domain and provides the majority of the subunit-subunit interactions within the heptameric rings. The ATP molecule is hydrolyzed by this domain.

+ The intermediate domain (residues 134-190) is the smallest domain and links the equatorial and the apical domains together. It plays a role as mobile hinge that permits structural re-arrangements during the functional cycle of GroE

+ The apical domain (residues 191–376) is located on the outer rims of the barrel. It is responsible for binding the protein substrates and GroES.

Functions of chaperonin system

GroEL isolates the misfolded or partially folded protein in a hydrophobic environment of GroEL and enables them to fold inside. The folding takes place in the GroEL central cavity, called as folding cage, which precludes aggregation.

GroES functions as a lid and has a dome-shaped ring-structure with a diameter of 75 Å and 30-33 Å in height, and consists of seven identical 10 kDa subunits (Hunt et al. 1996). Each GroES subunit has a core β-barrel structure consisting of two β-hairpin loops. These loops bind to the GroEL subunit at residues in the apical domain (Fenton et al. 1996). After GroES caps GroEL, the folding cavity increases in volume and the physical properties of the walls change from hydrophobic to hydrophilic.

1.2.3. 3. The functional cycle of GroE

The binding of ATP to GroEL and the subsequent hydrolysis of ATP regulate the reaction cycle of folding in the cavity. These serve as signals for protein substrate and GroES binding, followed by release of the substrate from GroE, as well as a clock for the time of packing the substrate inside the cavity.

GroE mediates protein folding through three phases: binding, folding, and release of the protein substrate (Thirumalai and Lorimer 2001).

a) The binding phase

GroEL recognizes the exposed hydrophobic surface area of a non-native protein. The binding of a substrate protein (red circles in Fig. 1.9) to a GroEL ring (*cis* ring, I) stimulates the binding of ATP and GroES (II). Binding of ATP induces movements of the apical domains which then initiate the oligomeric structure to elongate and twist the apical domains to different positions. This binding also causes the change in the *trans* ring conformation, resulting in a decrease in affinity of the *trans* ring for the substrate and GroES. The binding of

ATP and subsequent GroES to the *cis* ring enlarges the *cis* cavity volume, which provides sufficient space for the protein substrate to re-arrange its conformation. The *cis* cavity is enclosed by GroES, sequestering the protein substrate from crowded cellular environment (Bhutani and Udgaonkar 2002).

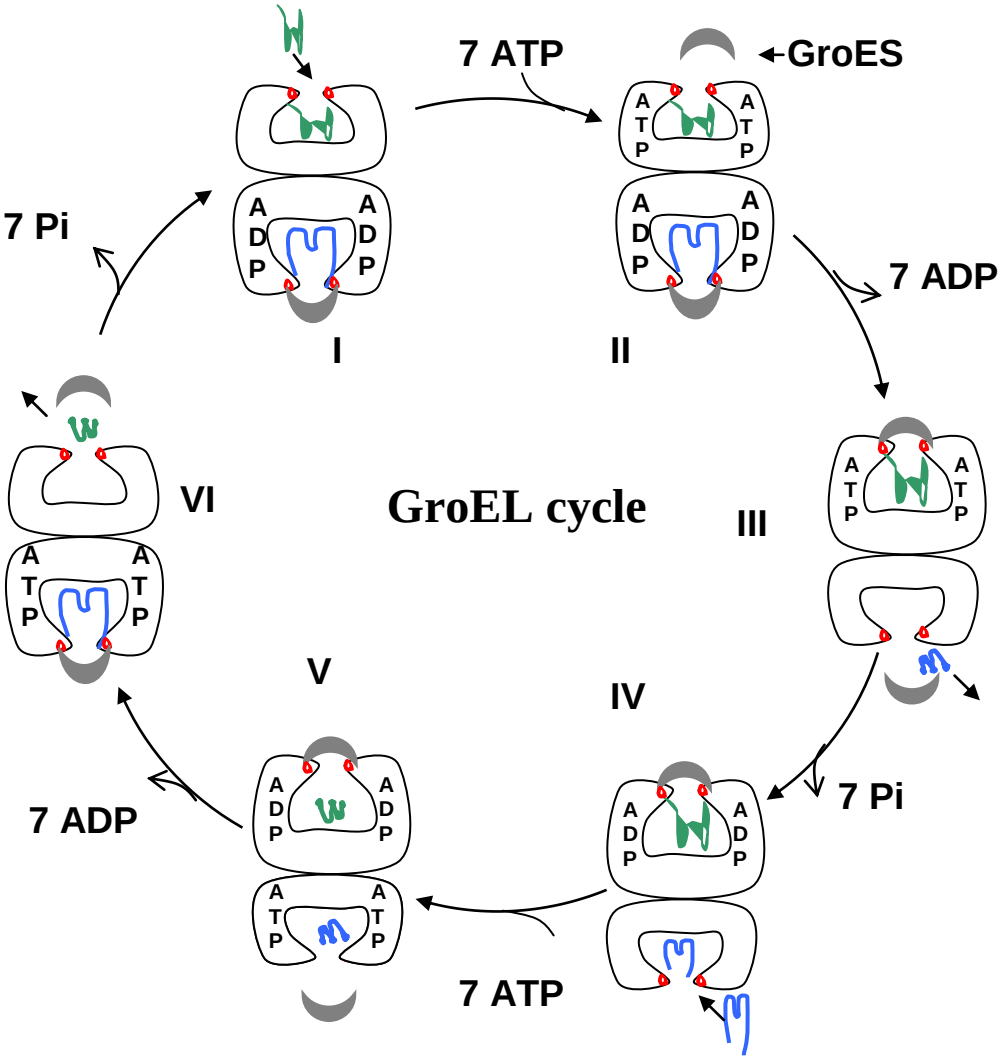

Figure 1.9. Cycle of protein folding by chaperonin system. Adapted from Mogk et al. (2002). Two misfolded proteins (green and blue) are simultaneously folded in a phase-shifted manner. The red circles symbolize the hydrophobic substrate binding sites of GroEL.

b) The folding phase

The movement of the apical domains changes the physical properties of the cavity. The hydrophobic patches in the apical domains which are responsible for polypeptide binding are replaced by largely polar residues. Concomitantly, the GroEL (*cis* ring) decreases the affinity for other protein substrates. The bound protein substrate moves into the closed cavity and

unproductive hydrophobic interactions are thereby broken and the protein has a new chance to fold.

Proteins up to approximately 60 kDa fold in the hydrophilic environment for 10–15 seconds, the time needed for ATP hydrolysis in *cis*-ring. It is noteworthy that some proteins fold in the GroEL folding chamber, others only after releasing from GroEL. Many proteins require several binding and release cycles for their complete folding. Large proteins (> 60 kDa), however, may use different mechanism of GroE-mediated folding (Mogk et al. 2002).

c) The release phase

After complete folding the protein substrate leaves the cavity. The hydrolysis of the 7 *cis*-ring ATP molecules to ADP results in conformational changes that are transmitted to the *trans* ring. The *trans* ring is then able to bind a non-native protein substrate as well as ATP and GroES (IV, V, VI). The *trans* ring containing the protein substrate, ATP and GroES initiates the dissociation of GroES from the *cis* ring.

There exists a concert event during the folding by GroEL. After hydrolysis of the ATP at the other ring (the *cis* ring), the *trans* ring first binds the protein substrate and ATP. Subsequently, the GroES binds to the *trans* ring and concomitantly other GroES dissociates from the *cis* ring, initiating the next reaction cycle.

Thus, the GroEL machinery works as a 'two-stroke' machine: release of GroES and protein substrate from *cis*-folding active ring is coupled to the conversion of the *trans* ring into the folding-active ring.

1.2.4. Chaperonin from psychrophilic *Oleispira antartica*

1.2.4.1. The characterization of *O. antartica* RB-8

The psychrophilic bacterium, *O. antartica* RB-8, was first isolated from superficial sea-water samples collected in the inlet Rod Bay (Ross Sea, Antarctica) (Giuliano et al. 2003). *O. antarctica* belongs to the c-Proteobacteria, genus *Oleispira*. This bacterium is an aerobic, gram-negative, non-spore-forming, catalase-and oxidase-positive organism. The phenotypic characteristics that differentiate this bacterium from other species of related genera is that *O. antarctica* optimally grows at 2–4^{o}C whereas others from related genera grow optimally at 20–37^{o}C (Giuliano et al. 2003). It is an oil degrading bacterium, with a narrow range of growth supporting substrates limited to aliphatic hydrocarbons, tweens and volatile fatty acids. The common carbohydrates such as glucose, fructose and mannose are not utilized by this bacterium. Cells appear characteristically vibrioid to spiral, with a cell length of 2–5 μm and a cell width of 400–800 nm. It is motile and possesses a single polar flagellum of about 5 mm in

length. At one or both ends of the cell, the drumstick-like thickening was observed and that is a distinguishing morphological feature (Yakimov et al. 2003).

Phylogenetically, *O. antarctica* showed the 16S rDNA similarity values lower than 90% with closest relatives within the bacteria. The G+C contents amounted to 41–42 mol% and the size of the genome was about 2.0 Mbp. Futhermore, the strain carried no detectable plasmids (Yakimov et al. 2003)

1.2.4.2. *O. antarctica* chaperonins (Cpn60 and Cpn10)

The chaperonins and their corresponding genes were characterized in details by Ferrer (2004b). The two genes are organized in a bicistronic operon and encode proteins of 548 amino acids (56872 Da) and 97 amino acids (10286 Da), respectively.

Within the cell, Cpn60 can exist in two states: as single rings (heptamers, 400 ± 14 kDa), and double rings (tetradecamer, 800 ± 37 kDa). At low growth temperatures between 4–8°C, single rings occurred abundantly. However, at elevated temperatures >10^{o}C, single- and double-ring species occur and the ratio of double rings versus single rings increases progressively with increasing temperature. At 25^{o}C, the double ring represents the predominant species.

The transition from single to double rings of Cpn60 is essential for the its activity both *in vitro* and *in vivo*. By in *vitro* folding of bovine rhodanese, the single rings retained intact function below 10^{o}C, with maximal refolding activity at 4^{o}C, four times higher than the double ring (Ferrer et al. 2004). In contrast, the double ring is a more efficient chaperone at temperatures >10^{o}C, with maximal activity at 30^{o}C, similar to *E. coli* GroEL and recovery of rhodanese activity is 40 times higher compared to the single rings. The two residues at the C-terminus (K468 and S471) may be responsible, at least for the interaction within the two rings in Cpn60 and thus for the alteration of chaperonin. Mutation of both residues to T and G (as observed in *E. coli* GroEL) resulted in a stable double-ring mutant of *Oleispira* Cpn60 (Ferrer et al. 2004b).

1.2.4.3. Potential applications of psychrophilic bacteria

So far, psychrophiles are well-known as the source of producing cold-adapted proteins. In some cases, the use of psychrophiles and their enzymes in biotechnological processes comprise several advantages, such as (i) saving energy, (ii) saving of labile or volatile compounds, (iii) prevention of microbial contamination, (iv) reduction of toxic effects of the products, and (v) in-activation of cell detrimental enzymes.

Several types of cold-adapted enzymes and their industrial applications were presented (Huston 2008). In fact, the preparation of proteins from their original psychrophilic producers is difficult due to their low content or limited cell growth. Many recombinant proteins have been actively produced by common hosts such as *E. coli, B. subtilis* and eukaryotic organisms like *S. cerevisiae*, *Pichia patoris.* However, these conventional systems are often unproductive for some types of "difficult" proteins which could be low stable or toxic to the host or occur as inclusion bodies. Low production temperatures have been shown to increase yields of active protein by minimizing undesired hydrophobic interactions during protein folding. However, cold environment leads to a slow growth and reduced synthesis rates, resulting in a lower protein production and increased production time (Ferrer et al. 2004a).

Thus, in some cases, the use of cold-adapted bacteria as hosts for protein production at low temperature (even at around 0°C) is a rational alteration to conventional mesophilic hosts (Ferrer et al, 2004a). The term "cold adapted host" includes both naturally psychrophilic hosts and mesophilic bacteria with recombinant psychrophilic chaperones which as a consequence, grow well at low temperatures. The use of naturally cold adapted organisms as host is still in a very early stage of development and further improvements of cold-adapted expression systems (e.g. modification of the host and vector) are required, to increase the yield of produced proteins. Myiake et al. (2007) used cold adapted S*hewanella* sp. as the host to produce a heat labile peptidase more efficiently than *E. coli*. Duilio et al. (2004) constructed a low temperature expression system with *Pseudoalteromonas haloplanktis* TAC125 as host to produce various recombinant proteins in active form, such as cold-active amylase from *P. haloplanktis* TAB23, two psychrophilic β-galactosidases and yeast α-glucosidase.

One new strategy to create a cold adapted expression system is to clone psychrophilic chaperonin genes into mesophilic hosts. Ferrer (2004a) demonstrated that *O. antartica* Cpn60 and Cpn10 supported the growth of *E. coli* K12 at temperatures of 4–8^{o}C, at which the parental cells did not grow. This cold-adapted *E. coli* strain was designated "Arcticexpress" and the use of this host has been widely applied to produce proteins that are poorly produced in their active or soluble form (Joseph and Andreotti 2008; Hartinger et al. 2010; Ferrer et al. 2004).

Moreover, usage of cold adapted mesophiles facilitates a better screening system to analyze (meta)genome expression libraries (e.g. bacteriophage lambda libraries) for thermo-sensitive enzymes that normally can not be assessed by using *E. coli* host. The use of cold-adapted mesophiles as a model system is useful in proteomic studies of cold shock responses, especially in understanding the roles of chaperone and protein folding mechanisms (Strocchi et al. 2006). The cold-induced systems failure in *E. coli* is due to the inactivation of GroESL which is known to fold four key proteins: Dps, ClpB, DnaK and RpsB (Strocchi et al. 2006).

II- AIMS OF THIS STUDY

Life in extreme environments has been studied intensively with focus on the diversity of organisms, molecular and regulatory mechanisms. Microbes inhabiting in such environments are the valuable source of proteins, enzymes with extreme stability, novel activities and application.

For the intended investigation, one bacterial strain, named 64G3 was isolated in a deep offshore oil reservoir in Vung Tau, a province of Vietnam. The strain was strictly anaerobic and thermophilic. In the field of molecular biology and technology, thermophilic bacteria are the source of thermostable proteins and novel enzymes. In the oil industry, the taxanomic information on this strain may be also applicable in oil recovery.

Thus, the first part of this study focused on investigation of strain 64G3 with respect to:

1) Identification and characterization of the strain 64G3 by means of molecular and classical microbiological techniques.

2) Cloning and characterization of an amylase from strain 64G3.

It has been demonstrated that chaperonins enable the host to adapt to stress by preventing proteins from aggregation and refolding them. So far, the impact of psychrophilic chaperonins on cold adaptation of the host as well as their folding activities have been studied only in *E. coli*. This organism, however, has some some disadvantages in recombinant protein production, such as lipopolysacharides production and its inability to secrete proteins. Thus, industrially important alternative expression hosts like *Bacillus* species are vastly applied in the production of biological products.

During production in *B. subtilis*, recombinant proteins can sometimes be deposited in insoluble form (Parente et al. 1991; Nurminen et al. 1992). For *B. subtilis*, more than 34 cold shock proteins were identified, and two out of them had chaperone activity. Thuy Le and Schumann (2007) developed a novel cold-inducible expression system for *B. subtilis*, based on the usage of the promoter from its own cold shock protein, Δ5 desaturase. The expression system worked properly at temperatures around 20^{o}C but inefficiently at 15^{o}C. Until now, a cold-active expression system for *B. subtilis* (working temperatures from 4–15^{o}C) has not been

established yet, although a similar one has been successfully established for *E. coli* (Ferrer et al. 2004b).

In order to possibly improve the production of active recombinant proteins at low temperatures in *B. subtilis*, the second part of this study focuses on the following targets:

3) Cloning and expression of a psychrophilic chaperonin operon from *O. antarctica* in *B. subtilis*.

4) Co-expression of psychrophilic chaperonins and yeast α-glucosidase in *B. subtilis*

The obtained results should answer the questions if

+ The psychrophilic chaperonins can support a cold adaptation of *B. subtilis* as shown for *E. coli* and if;

+ The cold expression of psychrophilic chaperonins at low temperatures can efficiently enhance the activity of yeast α-glucosidase which requires chaperonin to fold.

III- RESULTS

3.1. Taxonomic characterization of the isolate 64G3 and the expression of amylase gene

3.1.1. Molecular identification of the strain

A 1,429 bp-DNA fragment of the 16S rDNA gene of strain 64G3 was PCR amplified using the genomic DNA of the strain as the template and primers Cyaf, and Cyar (Fig. 3.1). A BLAST search of the nucleotide database in the GenBank with the sequence of this DNA fragment as the query (JQ417660) revealed six highly similar 16S rDNA sequences including *P. mexicana* (identity: 99.3%, NR029058), *P. halophila* (98.6%, AY800102) *P. olearia* (98.1%, NR028947), *P. sibirica* (97.8%, NR025466), *P. mobilis* (97.4 %, CP000879) and *P. miotherma* (96.6%, L10657). The sequence similarities indicated that strain 64G3 is closely related to the genus *Petrotoga.* The GC-content of the DNA was 33.4%, falling into the range of 31 - 36.1% for the six known members of the *Petrotoga* genus (Miranda-Tello et al. 2007). The genomic DNA-DNA relatedness of the strain 64G3 with *P. mexicana* (DSM 14811) (Miranda-Tello et al. 2004) yielded a value of 74.7%, which is above the threshold of 70% recommended for definition of bacterial species (Wayne et al. 1987). Therefore, strain 64G3 was identified as *P. mexicana* species.

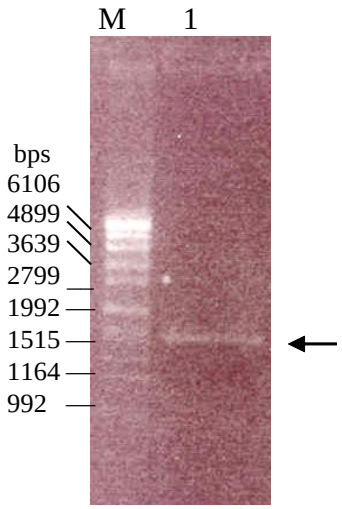

Figure 3.1. PCR amplification of partial 16S rDNA
Lane M: DNA marker VII; lane 1: PCR product, indicated by an arrow

3.1.2. Morphological and phenotypic properties

Morphologically, the 64G3 cells were rod-shaped and varied widely from 1.0 µm up to 60 µm in length and from 0.6 to 1.2 µm in width. The cells appeared singly, in pairs or in chains, within a sheath-like structure (a typical characteristic for members of *Thermotogales*)

that ballooned over the cell ends (Fig.3.2). The cells were immobile and no flagella were observed.

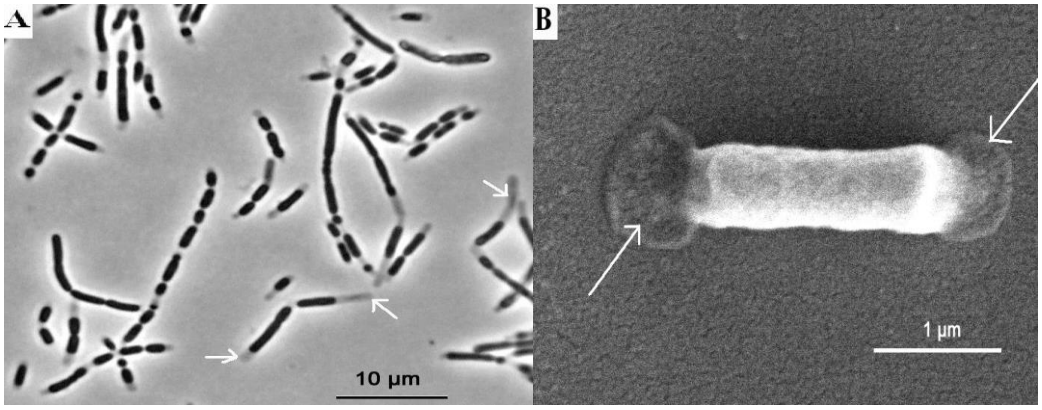

Figure 3.2. Cellular morphology of strain 64G3.
(**A**). Light micrograph of cells, bar 10 µm;
(**B**). Scanning electron micrograph of a cell with toga at each end indicated by white arrows. Bar 1 µm.

The bacterial growth was mesuared during 7 day incubation of the cells in the basal medium at various temperatures. Strain 64G3 grew anaerobically well at the temperatures ranging from 40 to 60°C, with an optimum at 55°C (Fig.3.3). The cell density reached highest value of 1.2 after 3 day incubation at 55°C and entered the stationary phase at day 5. A litte growth was observed after 3 days at 30 and 70°C, with the OD value of 0.3 and 0.11 respectively. The growth was obtained in the pH range of 5.0 to 8.5 with optimum growth at pH 7.0. Strain 64G3 utilized various substrates including glucose, galactose, ribose, xylose, maltose, starch and xylan as sole carbon source. Elemental sulfur and thiosulfate could served as alternative electron acceptors whereas sulfate did not. The growth of strain 64G3 was totally inhibited by penicillin, ampicillin and chloramphenicol at 10 µg mL^{-1}, whereas rifampicin and steptomycin at concentration of 100 µg mL^{-1} slightly decreased cell growth.

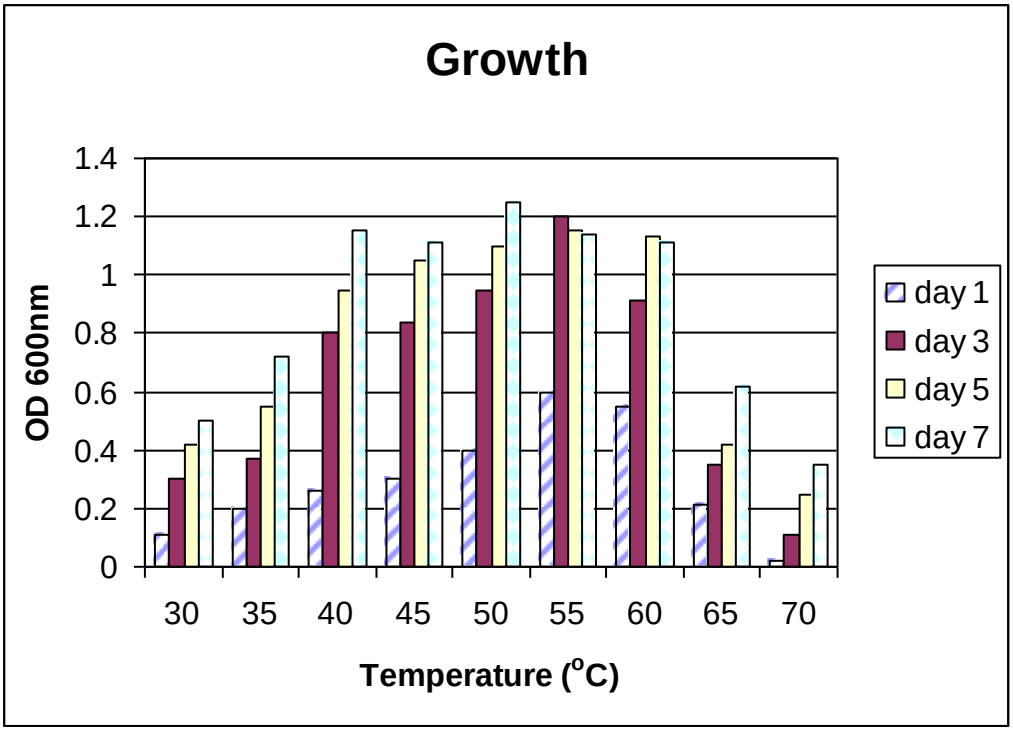

Figure 3.3. Effect of temperatures on cell growth
Cell densities were measured at A_{600nm} during 7 days incubation at various temperatures

3.1.3. Amylolytic enzymes from strain 64G3

Cell extract of strain 64G3 grown in a basal medium containing 0.5% soluble starch displayed hydrolytic activity towards soluble starch, three types of cyclodextrin and pullulan as measured by the release of reducing sugars. The highest starch degrading activity of the cell extract was determined at 75°C (Fig. 3.4 A). An activity staining of this extract revealed two active bands (Fig. 3.4 B), suggesting that strain 64G3 produced at least two amylases. In this study, most amylase activity was found intracellular or associated with the "toga", i.e. the outer sheath of the cell. In the culture medium, concentrated 20 fold by ultrafiltration (10,000 molecular weight cut-off Durapore membrane), no amylase activity was detected.

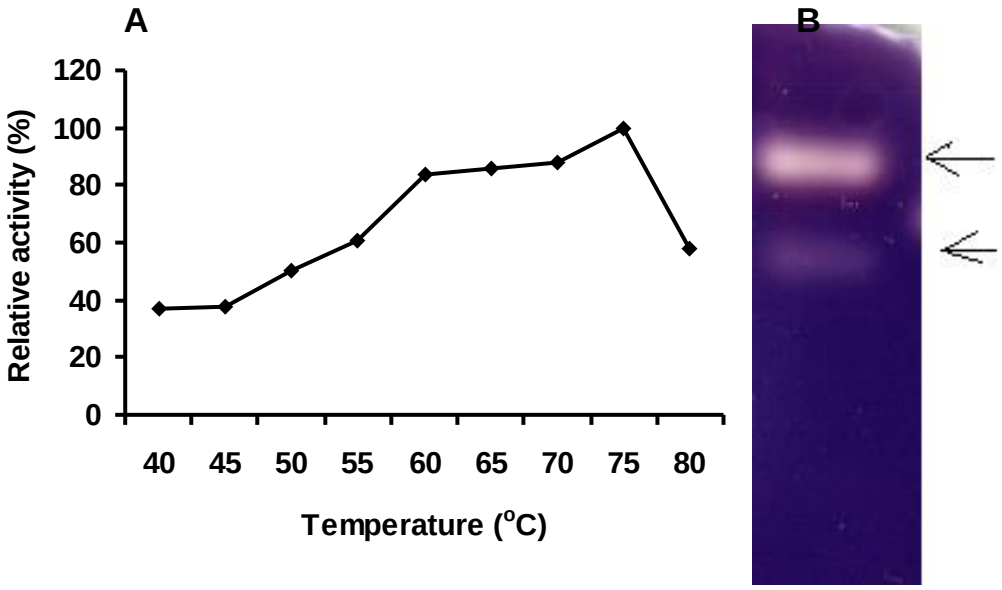

Figure 3.4. Effect of temperature on the starch degrading activity of cellular extract of strain 64G3
(A): The active staining of the extract
(B): Activity staining of enzyme showed two active bands (indicated by 2 arrows)

3.1.4. Cloning and sequence analysis of *amyA* gene

We used six alternative combinations of degenerate primers (see Table 5.3) for PCR amplification of a DNA fragment encoding GH13 enzymes. However, under the given PCR condition, only use of GA2f and GA5r as forward and reverse primer, respectively, resulted in amplification of a DNA band of about 420 bp (Fig 3.5). The length of the PCR product was consistent with the distance in bases from conserved region 2 to region 5 of GH13. Nucleotide sequence of this fragment coded for a single truncated open reading frame (ORF) of 125 residues containing the conserved region 3 and 4 of GH13 (Fig. 3.6).

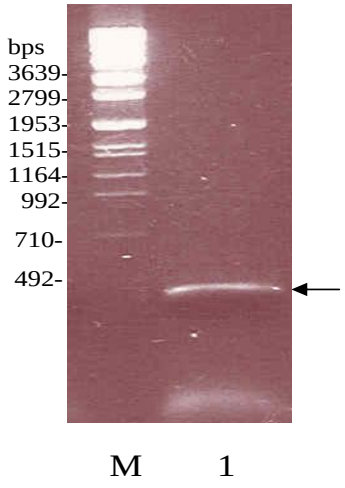

Figure 3.5. PCR amplification of a partial *amyA* gene (lane 1), indicated by an arrow.

A BLAST search revealed that the deduced protein showed highest homologies of 45%, 38% and 38% with a glycosidase from *Thermotogales* sp. (accession number CAJ75713), an amylase II from *Thermoactinomyces vulgaris* (accession number 1WZK_A) and a cyclomaltose dextrinase from *Laceyella sacchari* (accesion number AAX29990) respectively. It indicated that one fragment of *amyA* gene from strain 64G3 was amplified by PCR.

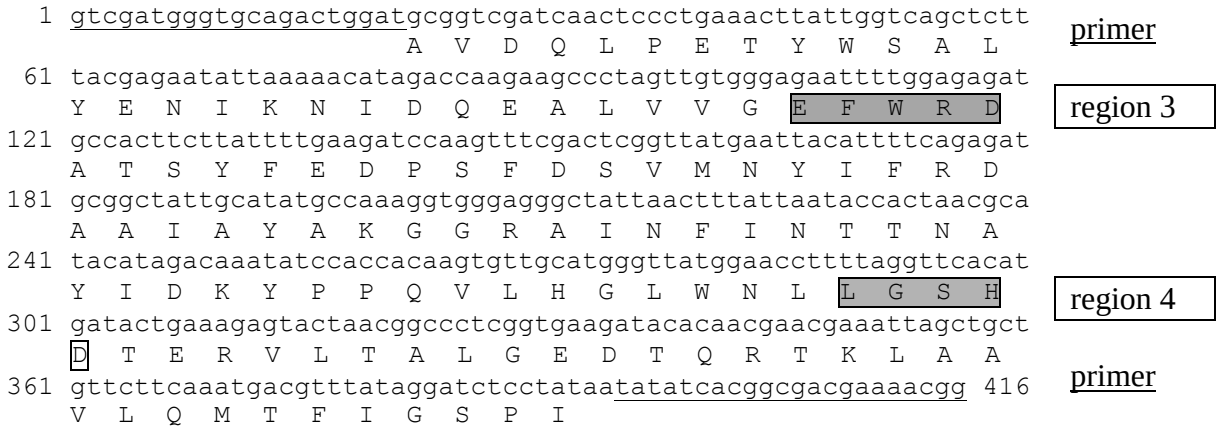

Figure 3.6. Incomplete ORF of *amyA* gene. Conserved regions 3 and 4 are shaded and boxed

The sequence of PCR product obtained was used to design a set of primers for PCR-based synthesis of a DNA probe to be used in Southern hybridization experiments. The probe, approximately 210 bp in length, was PCR labeled using the DIG-DNA labeling and detection kit (Boehringer Mannheim, Germany) with primers SgamylF and SgamylR (see Table 5.3) and genomic DNA of strain 64G3 as the template.

3.1.5. Construction of genomic library of the strain 64G3

A plasmid library was constructed in pUC18 using *E. coli* DH5α as the host (see 5.2.2.10). This library contained about 20,000 clones. 20 clones were randomly selected for plasmid isolation and restriction analysis with *Hind*III nuclease for evaluation of the genomic library. The results showed that 16 of 20 clones contained DNA inserts with different sizes, 4 clones (lane 3, 7, 9 and 20) seemed to contain no or short length inserts (Fig. 3.7). Thus, this genomic library was considered suitable for subsequent screening using the Sourthern hybridization technique.

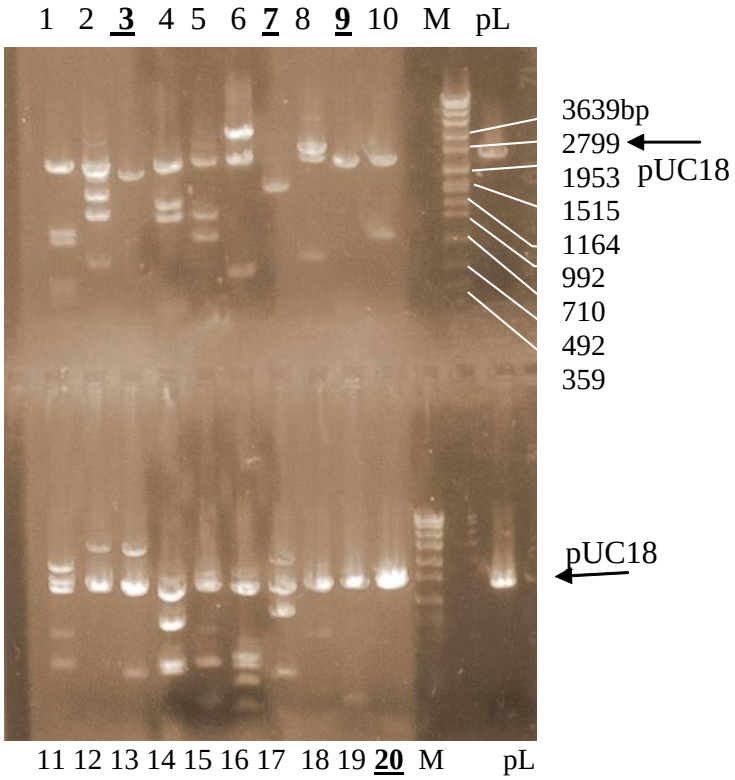

Figure 3.7. Digesion of 20 selected plasmids with *Hind*III.
Lane 3, 7, 9 and 20 contain plasmids with no or small inserts.
Lane M: marker DNA 1kb and lane pL: *Hind*III digested pUC18

3.1.6. Southern hybridization

A number of 2,500 clones were selected and their cell suspensions were divided in 50 tubes, each contained 50 individual cell suspensions. Plasmid mixtures from 50 tubes were isolated and used for the first screening using Southern hybridization technique (Fig. 3.8 A).

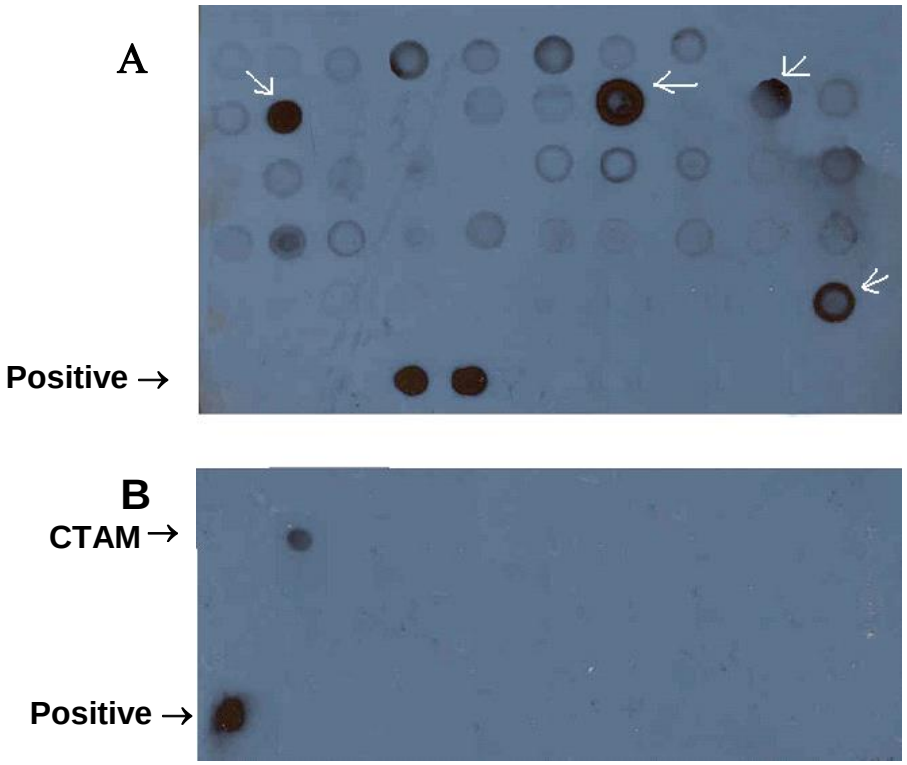

Figure 3.8. Screening of the genomic library using Southern hybridization technique
(A). Screening of 50 plasmid samples, each contained plasmid mixture of 50 individual clones
(B). Screening of 50 individual plasmids. CTAM, the label of a clone whose plasmid showed a positive signal. Dark dots indicate the presence of full or partial *amyA* gene.

Within the first screening, at least 4 positive signals indicated by white arrows (Fig. 3.8 A) were detected. In the next step, 50 individual clones distributed in one positive tube were cultured and their plasmids were separately isolated and used for the second screening. By this, one positive signal, named as CTAM, was detected (Fig. 3.8 B). Plasmid digestion with *Hind*III revealed a DNA insert of about 2,800 bp (consisting of two smaller fragments, approximately 2,300 and 500 bp). Partial sequencing of the insert revealed one complete ORF of 1,992 bp encoding a polypeptide of 663 amino acids (calculated molecular mass of 77,042 Da) flanked by two other incomplete ORFs. The deduced sequence was subjected to BLASTp analysis. The matches with the highest sequence identities were found to a glycosidase (45%) of an uncultured *Thermotogales* strain (GenBank accession number CAJ75719), a cyclomaltodextrinase (41%) of *Laceyella sacchari* (AAX29990) and an amylase (40%) of *Kosmotoga olearia* (ACR80687). The complete ORF also contained sequences coding for four conserved regions that are common in GH13 enzymes. The complete ORF and deduced amino acid sequence is presented in Fig. 3.9.

```
 1 cgttacttcaccttctgtcgtttcacaagacgacgtggaaagggctattaattttgtgaga
   V  T  S  P  S  V  V  S  Q  D  D  V  E  R  A  I  N  F  V  R
 62 aaaatggataagccgattatcgggatagttgaaaatatgtcttattttatctgtccaaat
   K  M  D  K  P  I  I  G  I  V  E  N  M  S  Y  F  I  C  P  N
122 tgtaaaactaaacactacatttttggtgaaaatggtggaaaatctttagcagaaaggtac
   C  K  T  K  H  Y  I  F  G  E  N  G  G  K  S  L  A  E  R  Y
182 aacttagaattacttgcacaaattccttttggattcaactgtcagagaaaacatggatgca
   N  L  E  L  L  A  Q  I  P  L  D  S  T  V  R  E  N  M  D  A
242 ggtaaacccgttgcttatttcggaactccagaagtaactaatgtctacgttaacttggca
   G  K  P  V  A  Y  F  G  T  P  E  V  T  N  V  Y  V  N  L  A
302 aagacggtaatagaaaaagtagaagccgttagttaataaggtattagatcactgtctcga361
   K  T  V  I  E  K  V  E  A  V  S  *  *
```

Incomplete ORF of nucleoside triphosphate hydrolases

Stop codon, uncoding sequence

```
362 atcagtaaacttttttcattgataggggggttactttc 399
400 atgaagaaagtattattcattgtaatgatacttatttttggtgtagtttctttttct
   M  K  K  V  L  F  I  V  M  I  L  I  F  G  V  V  S  F  S    19
457 gttagtactacgtttttatattcgaaagaagcgacttctgtttatttagttgccagtttt
   V  S  T  T  F  L↑ Y  S  K  E  A  T  S  V  Y  L  V  A  S  F 39
517 aacaactttgaacctatcgccatggaaaaaagcttcacgggactatggcgttacaatgtt
   N  N  F  E  P  I  A  M  E  K  S  F  T  G  L  W  R  Y  N  V 59
577 gatttagaacctggtgaatacctgtataaattcatcgtagatggaaaaagaacgatagat
   D  L  E  P  G  E  Y  L  Y  K  F  I  V  D  G  K  R  T  I  D 79
637 ttttcaaacgaggatgtacaagcctataacggtgaaatcttcaacgtacgcaccgttcaa
   F  S  N  E  D  V  Q  A  Y  N  G  E  I  F  N  V  R  T  V  Q 99
697 gaatcatttgtttttccaaaagttggagacggctcaattaaaaaggtttatttcgataac
   E  S  F  V  F  P  K  V  G  D  G  S  I  K  K  V  Y  F  D  N 119
757 gaaagaagatatataaatccggtcgaaaagggtgaaatatatctttcaatagaattcgaa
   E  R  R  Y  I  N  P  V  E  K  G  E  I  Y  L  S  I  E  F  E 139
817 aaaaatgatattgaagacgttgaactacaagctaacgcatcttctatacaaaaatctgta
   K  N  D  I  E  D  V  E  L  Q  A  N  A  S  S  I  Q  K  S  V 159
877 atagagttcaataataccatccttttataggtttcacgtatttaccgaagccgaagtttta
   I  E  F  N  N  T  I  L  Y  R  F  H  V  F  T  E  A  E  V  L 179
937 aagtatagatttttgatccacgatagcgaagaaataatatacggtttcaacggaacagaa
   K  Y  R  F  L  I  H  D  S  E  E  I  I  Y  G  F  N  G  T  E 199
997 gagtttttgaattcgactttaatcatcctataatttcttattttgatataccagaatgg
   E  F  F  E  F  D  F  N  H  P  I  I  S  Y  F  D  I  P  E  W 219
1057 tcaaaaggaaggatctattatcaaatatttcctgatagattcagaaatggtgatacttcc
     S  K  G  R  I  Y  Y  Q  I  F  P  D  R  F  R  N  G  D  T  S 239
1117 aacgatccgcaagggacctatagttggaacggccctcacaacagaaattctctttctttt
     N  D  P  Q  G  T  Y  S  W  N  G  P  H  N  R  N  S  L  S  F 259
1177 ggtttttatggtggagatcttcaggggtcattgattcaattgaccacttagaatacatt
     G  F  Y  G  G  D  L  Q  G  V  I  D  S  I  D  H  L  E  Y  I 279
1237 ggggtggaagcgatctacttcaaccccatttttgaagctcaaactccccataaatacgat
     G  V  E  A  I  Y  F  N  P  I  F  E  A  Q  T  P  H  K  Y  D 299
1297 acaactgattatttaaaaattgatgattctttcggtaacgaagaggtcttttctaatatg
     T  T  D  Y  L  K  I  D  D  S  F  G  N  E  E  V  F  S  N  M 319
1357 atagaggcgttacatgaatcagatatcaaagtaatcttagatggtgtattcaatcatact
     I  E  A  L  H  E  S  D  I  K  V  I  L  D  G  V  F  N  H  T 339
1417 ggaactgaattcttcgccatgaaagaaaacttttctcaaacaagaaaaatccaattatttg
     G  T  E  F  F  A  M  K  E  N  F  L  K  Q  E  K  S  N  Y  L 359
1477 gattggtattatatcaaatcgtttcctatcaaaaaatccacagaaagttacgaaggttgg
     D  W  Y  Y  I  K  S  F  P  I  K  K  S  T  E  S  Y  E  G  W 379
1537 catggatacgctgatctccctcaattaaacaatgaaaattccgaagtaagggcatacata
     H  G  Y  A  D  L  P  Q  L  N  N  E  N  S  E  V  R  A  Y  I 399
1597 aatcaggtaattggcaaatggatgagttttgggatagatggatggagaatggatgcggtc
     N  Q  V  I  G  K  W  M  S  F  G  I  D  G  W  R  M  D  A  V 419
1657 gatcaactccctgaaacttattggtcagctctttacgagaatattaaaaacatagaccaa
     D  Q  L  P  E  T  Y  W  S  A  L  Y  E  N  I  K  N  I  D  Q 439
1717 gaagccctagttgtgggagaattttggagagatgccacttcttattttgaagatccaagt
     E  A  L  V  V  G  E  F  W  R  D  A  T  S  Y  F  E  D  P  S 459
1777 ttcgactcggttatgaattacattttcagagatgcggctattgcatatgccaaaggtggg
```

RBS

Start codon of amyA

↑ Vertical arrow: signal site

amyA

Conserved region 1

Conserved region 2 (D : catalytic residue)

Conserved region 3 (E: catalytic

Figure 3.9. The complete nucleotide sequence of *P. mexicana* 64G3 α-amylase gene and its deduced amino acid residues (in shaded area).
The putative RBS is boxed. The four highly conserved regions of GH13 enzymes are shaded light gray. Three catalytic residues (Asp417, Glu446 and Asp511) are in bold, italic and black shaded letters. The putative processing site for the signal peptide is indicated by a vertical arrow↑. Upstream and downstream regions are also presented, showing the two incomplete ORFs.

Three catalytic residues including Asp417, Glu446 and Asp511 corresponding to Asp206, Glu230 and Asp297 of Taka amylase A (Takuji et al. 1996) were contained in conserved regions 2, 3 and 4, respectively (Fig. 3.9). A potential ribosome binding site (RBS), 5'-AGGGGG-3', is located nine basepairs upstream of the translational initiation codon, ATG. To identify a putative signal peptide, the sequence of the first 50 amino acid residues was processed by SignalP 3.0 (see 5.2.4). The result indicated a putative signal sequence of 25 residues in length with cleavage between Leu25 and Tyr26 (Fig. 3.9). The 60 and 15 bp non-coding regions upstream and downstream the ORF of *amyA* contained no potential promoters or transcription terminator motifs.

3.1.7. The expression of *amyA* gene in *E. coli*

3.1.7.1. Construction of an expression vector in *E. coli*

amyA-DNA sequence corresponding to the mature protein was obtained by PCR amplification using two primers, CuAmyEfet22 and CuAmyEret22 (see Table 5.3) and *P. mexicana* 64G3 genomic DNA as template. A 1950 bp PCR product (Fig. 3.10 A) was purified and cloned into the *BamH*I-*Xho*I restriction sites of the vector pET22b(+) (Novagen), creating the pET/a*myA* plasmid (Fig. 3.10 B, lane 2). *E. coli* Rosetta (DE3)plysS was transformed with pET/*amyA* and was designated Rosetta/a*myA*.

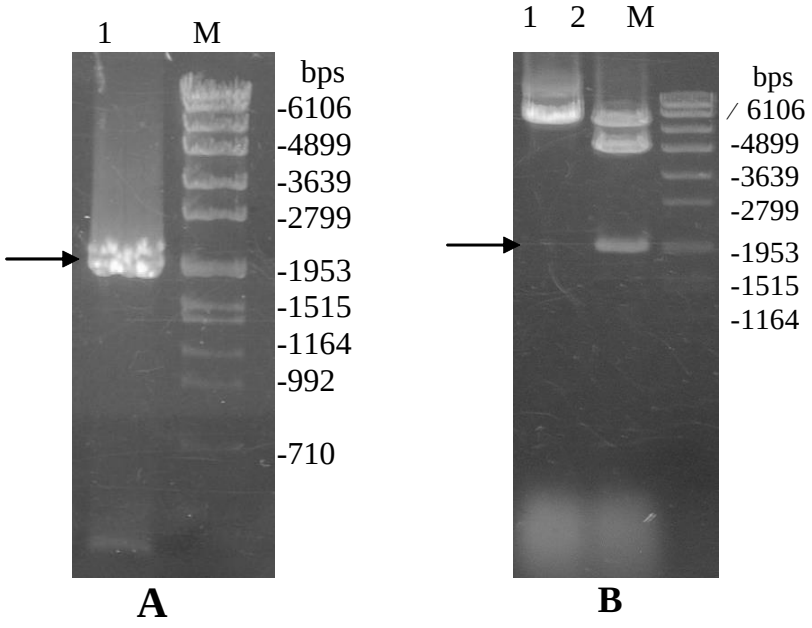

Figure 3.10. PCR amplification of *amyA* gene (A) and restriction analysis of pET/*amyA* with *BamH*I and *Xho*I (B)
(A). Lane 1, *amyA* gene; lane M, DNA marker VII
(B). Lane 1, linear pET22b(+); lane 2, pET/*amyA* digested by *BamH*I and *Xho*I. An arrow indicates *amyA* insert; lane M, DNA marker VII.

3.1.7.2. Expression of *amyA*

3 h after induction of Rosetta/*amyA* culture with 1 mM IPTG at 30°C, the supernatant and debris fractions from cell lysate were separated. Supernatant fractions of induced-cells showed higher activity, observed on starch containing agar, than that of non-induced cell which produced a native *E. coli* amylase (Fig. 3.11). During various temperature incubations, highest amylase activities were observed at 42°C whereas a significant loss of activities appeared at 60°C (Fig. 3.11).

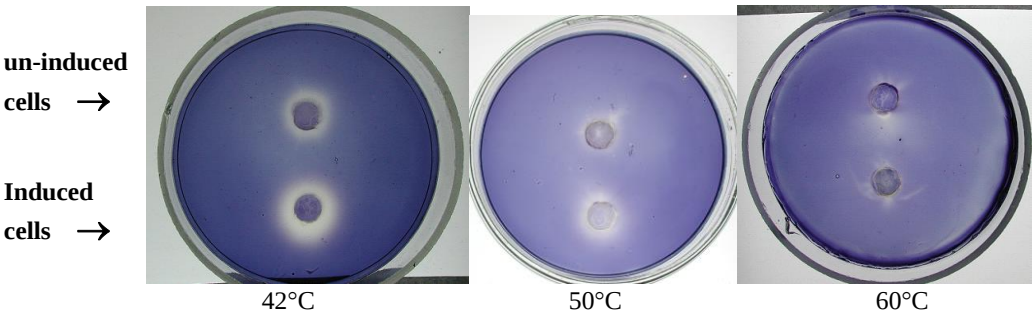

Figure 3.11. Amylase activity of cell lysate at different temperatures (on starch agar)

The supernatant and debris fractions from cell lysate were separated and subjected to SDS-PAGE analysis. The results showed the appearance of a protein with a molecular weight of approximately 77 kDa which was absent in the un-induced culture (Fig. 3.12 A, lane 1, 2). Identification of this protein band as recombinant AmyA (rAmyA) was confirmed by matrix-assisted laser desorption-ionization time-of-flight mass spectrometry (MALDI-TOF MS). This clearly indicated that rAmyA was produced in *E. coli*. However, most of the enzyme (estimated to be about 90%) aggregated into the debris fraction (known as inclusion bodies) (Fig. 3.12 A, lane 3).

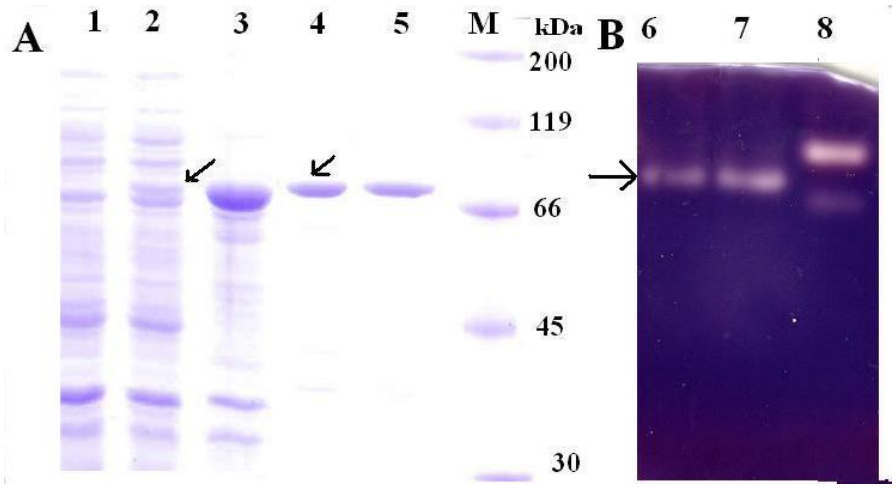

Figure 3.12. SDS-PAGE of the protein samples obtained during the expression and after purification steps (A) and active staining of purified rAmyA (B)

(**A**). Lane: 1. The supernatant of un-induced Rosetta/*amyA*; Lane 2 and 3, supernatant and debris fractions of induced Rosetta/*amyA*, respectively; Lane 4 and 5, purified rAmyA from supernatant and debris fractions respectively; M, molecular mass markers (in kDa). The arrows indicate a band of rAmyA in supernatant fraction

(**B**). Active staining of purified rAmyA. Lane 6 and 7: activities of rAmyA from supernatant and debris fractions respectively; lane 8: crude extract of strain 64G3

The total yield of purified rAmyA amounted to 14.3 mg per 100 mg of the host soluble cellular protein. The rAmyA in the supernatant fraction was purified to homogeneity as a single protein band with mobility corresponding to a molecular mass of about 77 kDa (Fig. 3.12 A, lane 4 and 5). The purified rAmyA in the supernatant fraction showed a specific activity of 0.5 U mg^{-1}. Active staining of the purified rAmyA revealed one active band (Fig.3.12 B, lane 6).

3.1.7.3. Optimization of expression of AmyA in soluble form

In the first approach, production of rAmyA was carried out at 37°C for 3 h with 1mM IPTG as inducer. However, most amylase was produced as inclusion bodies, resulting in the inactive enzyme. In order to obtain a higher amount of active rAmyA, two strategies were applied: (i) optimisation of expression conditions, and (ii) refolding of insoluble amylase into its native form.

(i) Optimisation of the expression conditions

* *Effect of IPTG concentration:* different concentrations of IPTG ranging from 0.01 mM to 1 mM were tested. The production of rAmyA was conducted for 3 h at 30°C and levels of the enzyme produced in both supernatant and debris fractions were analysed using SDS PAGE. Results showed that the highest amounts of enzyme (in both forms) were observed with 1 mM of IPTG as inducer (Fig. 3.13). In both fractions, the amounts of rAmyA increased with higher concentrations of IPTG. However, in all cases, the portion of insoluble rAmyA remained much higher.

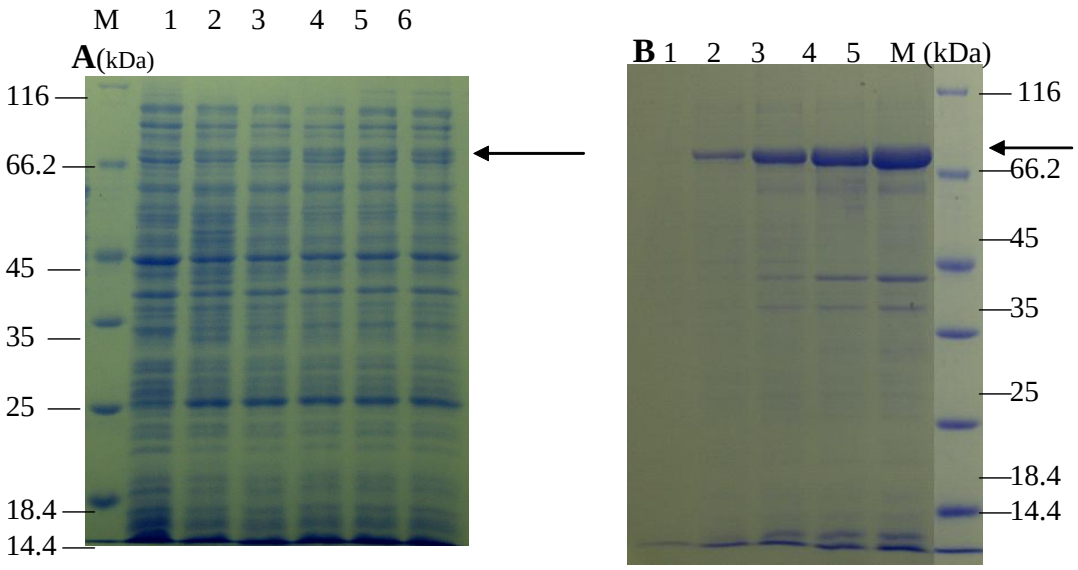

Figure 3.13. Effect of IPTG concentration on production of rAmyA

(**A**). SDS PAGE of intracellular supernatant. Lane M: protein marker; Lane 1: non-induced cell; lane 2, 3, 4, 5 and 6: cells were induced at 0.01, 0.05, 0.1, 0.5 and 1 mM IPGT, respectively. The arrows indicate rAmyA bands.

(**B**). SDS PAGE of debris fraction. Lane M: protein marker; lane 1: non-induced cell; lane 2, 3, 4 and 5: cells were induced at 0.05, 0.1, 0.5 and 1 mM IPTG respectively. The arrow indicate rAmyA bands.

* *Effect of induction periods on expression of amyA*

The expression of *amyA* gene was carried out as mentioned previously, using 1 mM ITPG and cell samples were harvested after induction at various time intervals (1, 2, 3 and 5 h). Fig. 3.14 shows that increasing amounts of rAmyA correlate with prolonged induction. However, the enzyme was distributed almost exclusively as inclusion bodies. Within 3 h, production of rAmyA correlated with increasing induction period. Whereas a longer induction (5 h) did not result in more rAmyA, as expressed by the similar yields of rAmyA produced after 3 and 5 h (Fig. 3.14, lane 3 and 4).

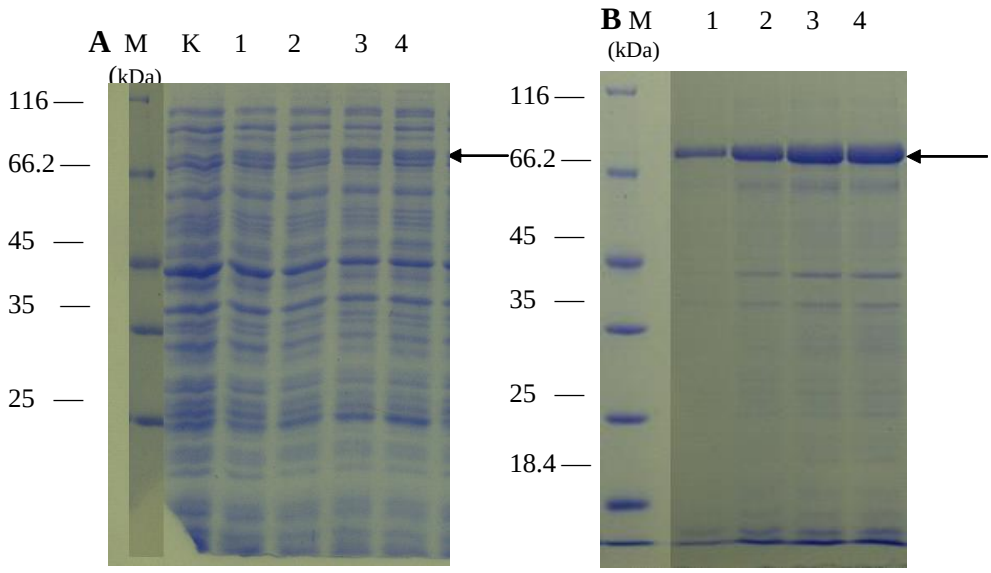

Figure 3.14. Effect of the induction periods on the production of rAmyA.

(**A**). SDS PAGE of soluble fraction. Lane M: protein marker; lane K: non-induced cell, 3h after reaching $OD_{600\ nm}$ of 1; lane 1, 2, 3 and 4: induction periods of 1, 2, 3 and 5 h respectively. The arrows indicate rAmyA bands.

(**B**). SDS PAGE of debris fraction. Lane M: protein marker; lane 1, 2, 3 and 4: induction periods of 1, 2, 3 and 5 h, respectively. The arrows indicate rAmyA bands.

** Effect of temperature on rAmyA expression*

Growth experiments within a temperature range from 16-37°C were carried out using 1mM of ITPG as inducer followed by continued cell growth for three hours. The results of growth-temperature variations on rAmyA expression is shown in Fig. 3.15. Level of soluble rAmyA produced in cells grown at 16 and 22°C appeared to be higher in comparison to the cells grown at 30 and 37°C. The amount of insoluble rAmyA, at lower growth- temperatures (16°C and 22°C), was notably lower compared to those of cells grown at 30°C and 37°C (Fig. 3.15 B). Thus, the amount of soluble rAmyA increased with decreasing temperatures.

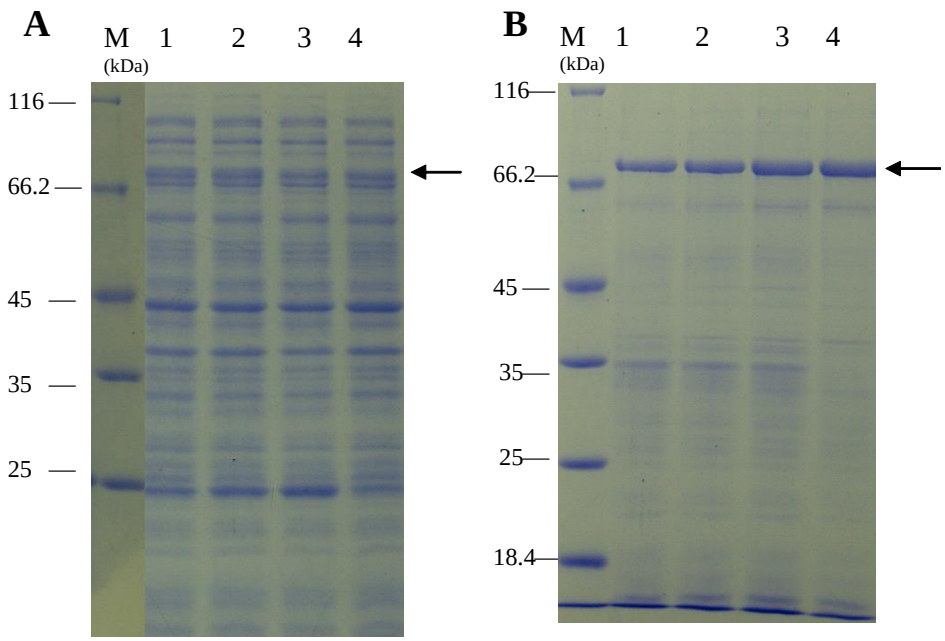

Figure 3.15. Effect of growth- temperatures on the rAmyA production

(A). SDS PAGE of intracellular supernatant. Lane M: protein marker; lane 1, 2, 3 and 4: cells induced at 16, 22, 30 and 37°C respectively. rAmyA is indicated by the arrow.

(B). SDS PAGE of debris fraction. Lane M: protein marker; lane 1, 2, 3 and 4: cells induced at 16, 22, 30 and 37°C respectively. rAmyA is indicated by the arrow.

(ii) Refolding of insoluble rAmyA

Although various expression conditions were applied as discribed above, a much higher amount of amylase as inclusion bodies still remained. By using the Protein refolding kit (Novagen), insoluble rAmyA easily became water soluble and its activity was obtained after dialysis of solublized rAmyA against a working buffer of pH 6.8. The purified, refolded amylase showed a specific activity on starch with a value of 0.18 U mg^{-1}, lower than that of soluble rAmyA purified from cellular supernatant (0.5 U mg^{-1}). Active staining of the refolded rAmyA also showed an active band similar to that of soluble rAmyA (Fig 3.12 B, lane 6 and 7). The mass ratio of rAmyA purified from the supernatant versus those from debris fractions was about 9:91.

Because the purified, refolded rAmyA showed a remarkably lower activity, all subsequent studies with this enzyme were carried out using rAmyA purified from supernatant fraction.

3.1.8. Characterization of enzymes

3.1.8.1. Effect of temperature on enzyme activity

Temperature optimum of rAmyA was studied within the range of 30°C to 65°C in 50 mM sodium phosphate buffer pH 6.5. The enzyme was active at temperatures between 30-55^{o}C, with an optimum at 45^{o}C (Fig. 3.16). Activity rapidly declined at 55^{o}C and no activity was detected at 60°C.

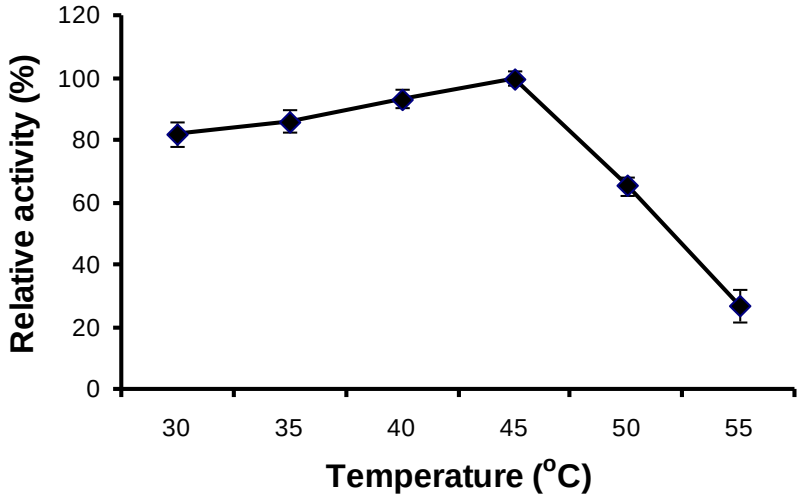

Figure 3.16. Effect of temperature on rAmyA activity

Thermostability results, as displayed in Fig. 3.17, showed that the enzyme was relatively stable at 55°C, with 80% of its activity remaining after 1 h-treatment at the respective temperature. Incubation of the enzyme at 60°C for 30 min caused the loss about 55% of its activity. The enzyme was completely inactive after being treated at 65°C for 30 min. However, the presence of 10 mM Ca^{2+} in the enzyme solution reconstituted 36.1% of activity. The optimal temperature for rAmyA was 45°C, 30°C below that of starch hydrolysis by strain 64G3 extract (highest activity at 75^{o}C, Fig. 3.4 A). This result can be attributed to the activation of other extremely thermophilic amylase(s) in the crude extract.

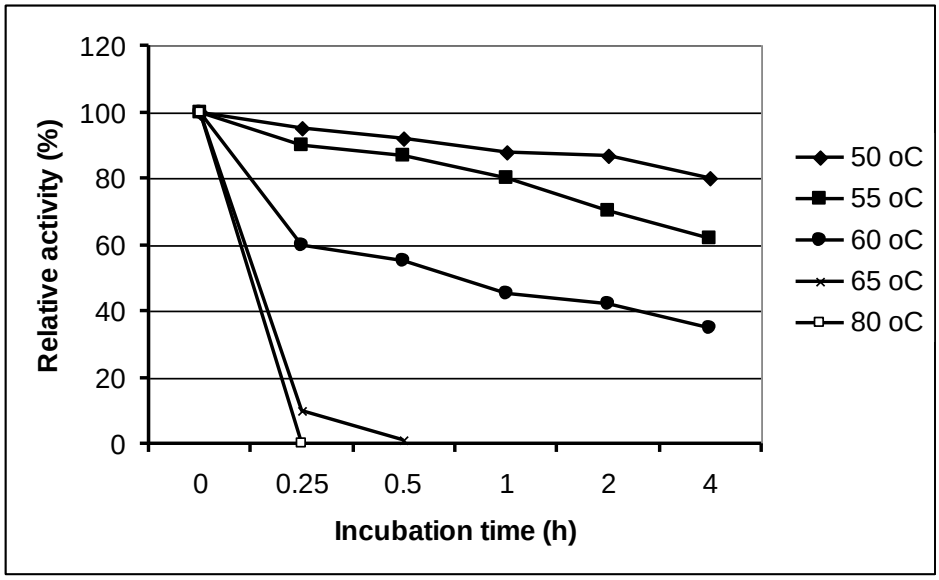

Figure 3.17. Thermostability of rAmyA

The enzyme was incubated at the given temperature and residual activity was measured after indicated incubation periods.

3.1.8.2. Effect of pH on enzymatic activity

The effect of pH on the activity was studied in 50 mM sodium phosphate buffer (pH 5.5 to 8.0) and in 50 mM acetate buffer (pH 3.0 to 5.5). The enzyme was active over a pH range from 4.5 to 8.0, with an optimum at pH 6.5 (Fig. 3.18). Its activity rapidly decreased below pH 5.0 and above pH 8.0.

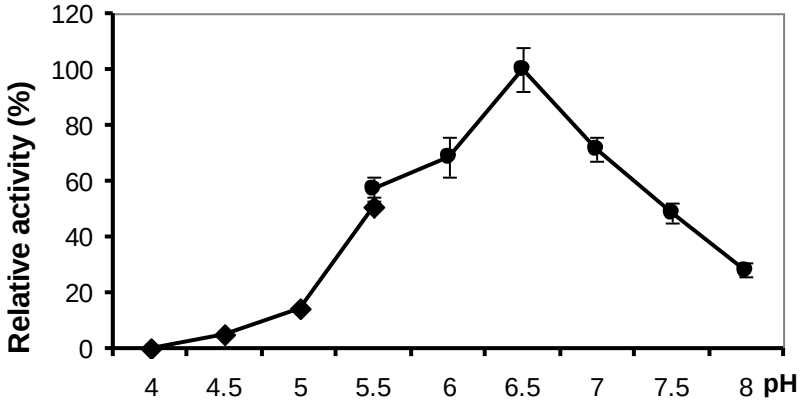

Figure 3.18. Effect of pH on the enzyme activity. in an acetate buffer pH 3-5.5 (♦) and phosphate buffer pH 5.5 to 7.8 (•)

3.1.8.3. Effect of different divalent ions on rAmyA activity

The enzyme activity was measured in presence of various divalent ions at a final concentration of 1 mM in the reaction solution. Of all the metal ions tested, Cu^{2+} and Ni^{2+}showed remarkable inhibitory effects because they reduced the enzyme activity by 75.4 and 52.9%, respectively (Table 3.1). Ca^{2+}, Mn^{2+}, Fe^{2+} and Co^{2+} showed stimulating effects of 19.6, 23.5, 37.2 and 58.8%, respectively, whereas Mg^{2+} and Zn^{2+} had no effect on enzymatic activity. Treatment of rAmyA with 5 mM or 20 mM EDTA, an inhibitor of metallo-enzymes, caused a similar loss of 58.8%. However, the presence of 10 mM Ca^{2+} or Mg^{2+} in the EDTA treated enzyme reaction retained 85 and 62% of activity, respectively. This result demonstrates that rAmyA is a metal ion dependent amylase, like most other known bacterial amylases.

Table 3.1. Effect of metal ions on rAmyA activity

Metal ions	Relative activity (%)
None	100
Ca^{2+}	119.6
Mg^{2+}	102.1
Fe^{2+}	137.2
Mn^{2+}	123.5
Co^{2+}	158.8
Zn^{2+}	100
Ni^{2+}	47.1
Cu^{2+}	24.6

3.1.8.4. Substrate specificity and mode of starch degradation

The hydrolysis of various substrates by rAmyA is shown in Table 3.2. The enzyme hydrolyzed soluble starch and amylose to produce maltose as the major end-product, maltotriose and glucose to a lesser extent (Fig. 3.19 A and B). Glycogen and amylopectin were hydrolyzed by this enzyme (Table 3.2). Maltotetraose and longer oligosaccharides were not recognized on the TLC plate.

Table 3.2. Substrate specificity of rAmyA

Substrate	Relative activity (%)
Starch	100
Amylopectin	110
Amylose	74
Glycogen	30
Pullulan	1
α-Cyclodextrin	0
β-Cyclodextrin	0
γ-Cyclodextrin	0

rAmyA did not hydrolyze pullulan and any types of tested cyclodextrins. It also showed a weak activity on glycogen. The rAmyA did not cleave maltose or pNPG (p-nitrophenyl-α-D-glucopyranoside), substrates of α-glucosidase and glucoamylase. Glucose released during hydrolysis of starch by rAmyA was due to the subsequent cleavage of maltotriose. Other oligosaccharides from maltotriose to maltoheptaose were hydrolyzed by rAmyA to form shorter oligosaccharides (data not shown).

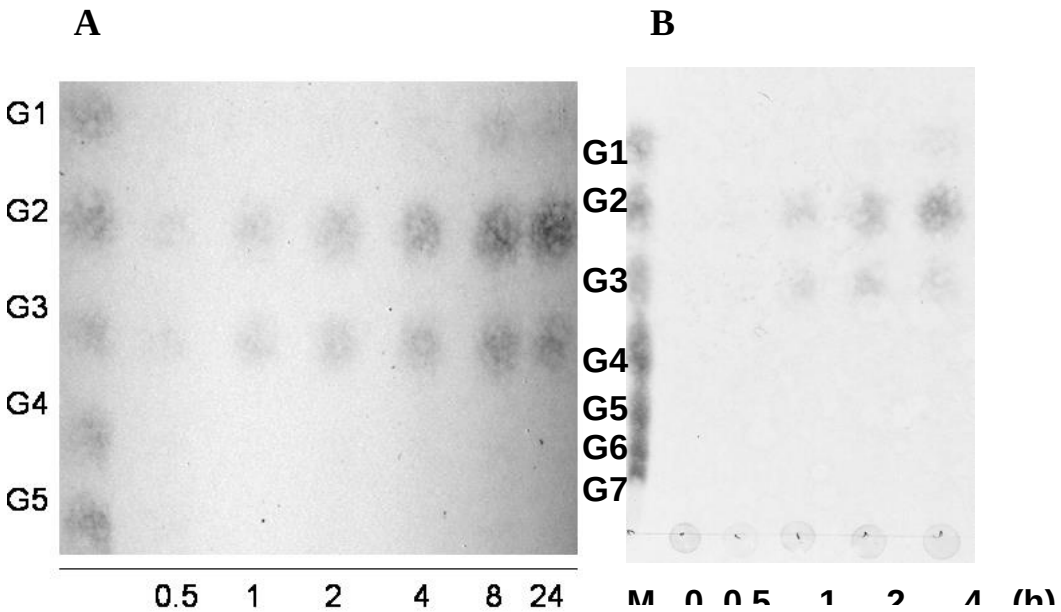

Figure 3.19. Hydrolysis patterns of rAmyA analyzed by TLC.

(**A**) and (**B**): soluble starch and amylose as substrates respectively. Reaction samples were collected at various points during incubation (h). G1–G7: represents a standard mixture of malto-oligosaccharides ranging from G1 (glucose), G2 (maltose), G3 (maltotriose) to G7 (maltoheptanose).

On the basis of the primary structure, the substrate specificities and the hydrolysis pattern, rAmyA was classified as an endo-acting α-amylase (EC. 3.2.1.1).

3.2. Cloning and expression of a chaperonin (*cpn*) operon in *B. subtilis*

3.2.1 Subcloning of *cpn10/60* operon into *E. coli* using pJET1

The *O. antarctica cpn10/60* operon (sequence presented in appendix B) was previously constructed in pPst26 and its monocistronic mRNA was successfully translated in *E. coli*, resulting the synthesis of Cpn10 and Cpn60 protein (Ferrer et al. 2004b). This plasmid was used as the template for PCR amplification of *cpn10/60* operon. Since it can not be excluded that the native ribosome binding site (RBS) of *cpn60* gene does not work properly in *B. subtilis* (McLaughlin et al. 1981), two alternative operons were used in this study: (i) *cpn10/60* operon with its native RBS of *cpn60* gene, designated as nativeRBS operon, and (ii) *cpn10/60* operon with the substitution of the native RBS of *cnp60* gene with RBS of amylase promoter (P_{amyQ}) of *B. amylolyquefaciens* (Takkinen et al. 1983), designated as changedRBS operon. The cloning strategy for both operons is illustrated in Fig. 3.20.

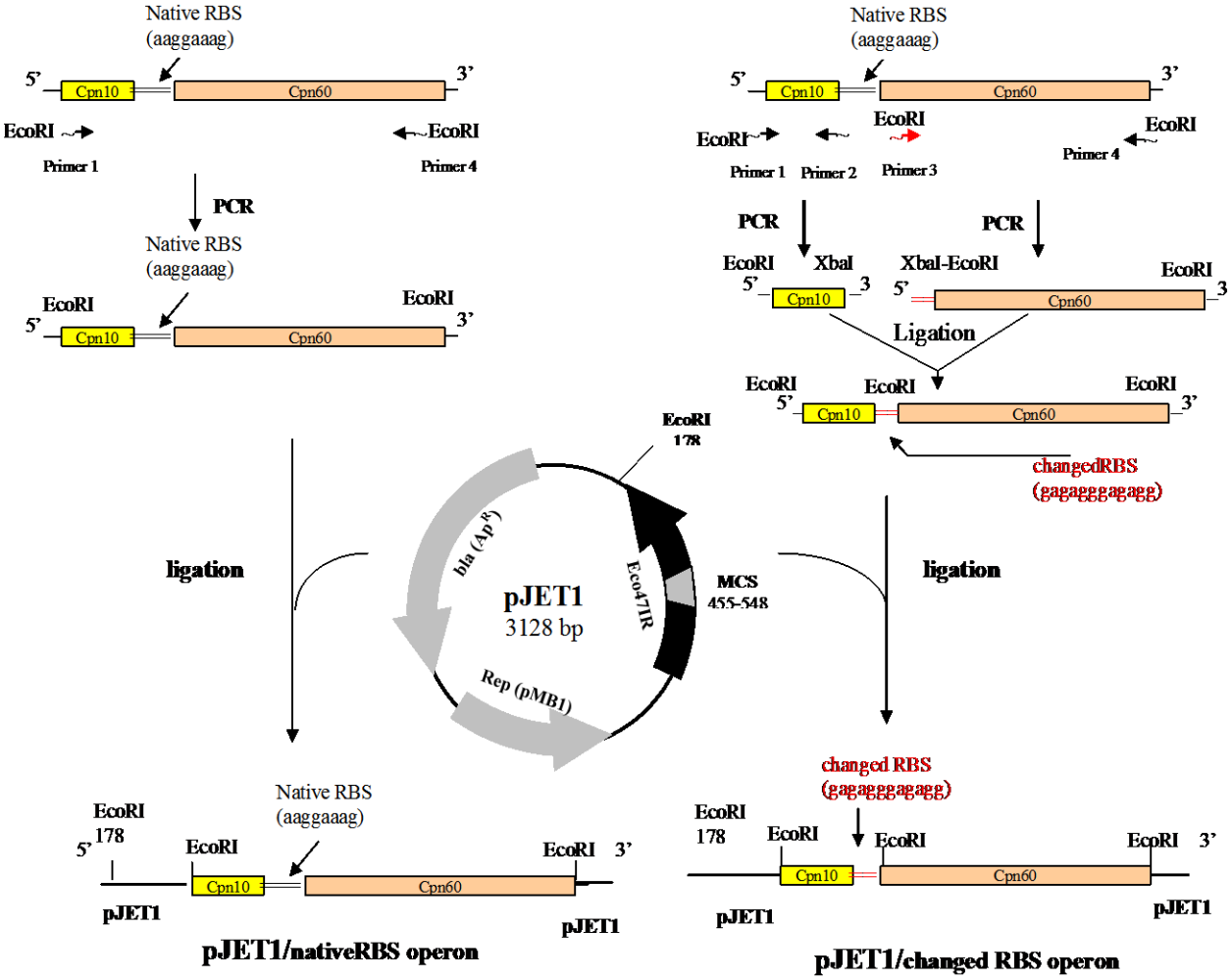

Figure 3.20. Schematic representation of both cpn operons amplified and cloned in pJET1. Red letters indicate sequence of the RBS of P_{amyQ}

(i) Amplification of the nativeRBS operon resulted in a PCR product which matchs the size of the *cpn10/60* operon (1989 bp, Fig. 3.21, lane 3). This operon was directly cloned in pJET1, a linearized blunt-end cloning vector, and transformed in *E. coli* DH5α. The successful cloning of the nativeRBS operon in pJET1 was verified by *EcoR*I digestion of plasmids isolated from a selected ampicillin resistant clone. The result of restriction analysis revealed two bands: a ~2 kb band (contains *cpn* operon) as insert and a 2.8 kb band, a pJET1 backbone (Fig 3.22 A).

(ii) In order to obtain the changedRBS operon with modified RBS preceding the *cpn60* gene (1647 bp), *cpn60* gene was PCR amplified using primer Os-GroEL2f with a modified RBS introduced at its 5' end and primer Os-GroELr (Fig. 3.21, lane 2). The PCR product (*cpn60* gene) was ligated with *cpn10* gene (294 bp) (Fig. 3.21, lane 1) at *Xba*I site to produce the changedRBS operon which was then cloned into pJET1 and transformed in *E. coli* DH5α.

The successful cloning of the changedRBS operon in pJET1 was verified by a separate PCR amplification of *cpn60* (~1,700 bp), *cpn10* (~297 bp) and changedRBS operon (~2.0 kb, a fusion of two genes) using the plasmid isolated from a selected transformant as template (Fig. 3.22, B).

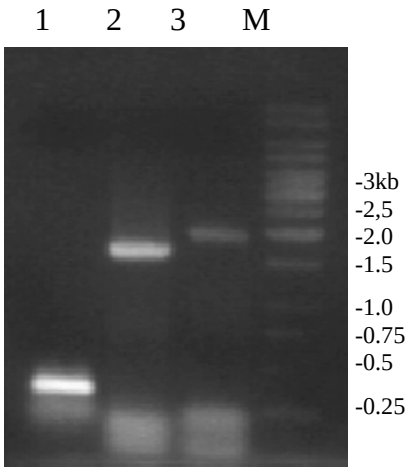

Lane 1: Amplification of *cpn10* gene (~297 bp).
Lane 2: Amplification of changedRBS *cpn60* gene (~1.7 kb)
Lane 3: Amplification of nativeRBS operon, with an expected band ~ 1,989 bp.
Lane M: marker DNA 1 kb.

Figure 3.21. PCR amplification of *cpn10, cpn60 gene* and nativeRBS operon.

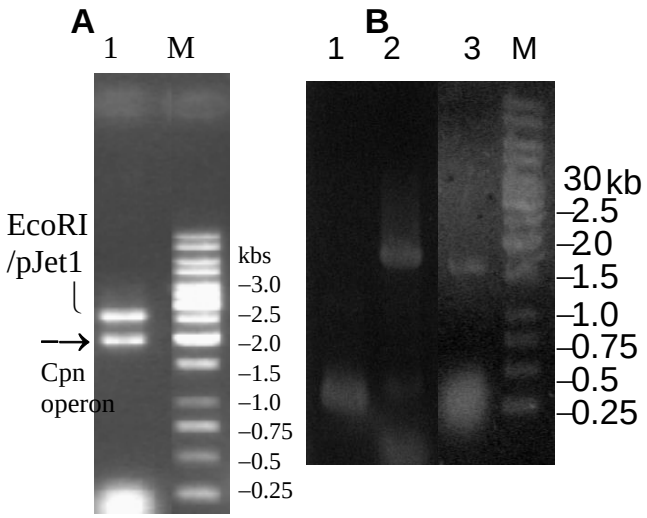

Figure 3.22. Analysis of pJET1 carrying *cpn10/60* operons

A: *Eco*RI digestion of plasmid
Lane 1: pJET1 carrying nativeRBS operon. Lane M: DNA marker 1kb. The arrow indicates the cpn operon as insert.
B: PCR amplification of *cpn10* (lane 1), *cpn10/60* (lane 2) and *cpn60* gene (lane 3). Lane M: DNA marker.

3.2.2. Sub-cloning of the two *cpn* operons in pKTH290 and transformation in *B. subtilis*

Plasmid pKTH290 (see appendix A for the partial sequence) was previously constructed based on the vector backbone of pUB110 which replicates in *B. subtilis* or other *Bacillus* species at 30-50 copies per cell. Both *Eco*RI digested *cpn* operons were purified and subcloned into pKTH290 thereby replacing the *porA* gene (1120 bp) in the vector backbone. (illustrated in Fig. 3.23). The resulting plasmids were designated pKTH/nativeRBS and pKTH/changedRBS respectively. Integration of both *cpn* operons into *Eco*RI site of pKTH290 was confirmed by *Eco*RI digestion (Fig. 3.24 A) and orientation of both *cpn* operons in pKTH290 was elucidated by *Cla*I digestion. The correct insertion resulted in three DNA fragments with sizes of 4.3, 1.09 and 0.40 kb (Fig 3.24 B lane 3 and 4) whereas an opposite orientation of the operon resulted in a different DNA band profile with sizes of 3.95, 1.09 and 0.845 kb (Fig 3.24 B, lane 1 and 2).

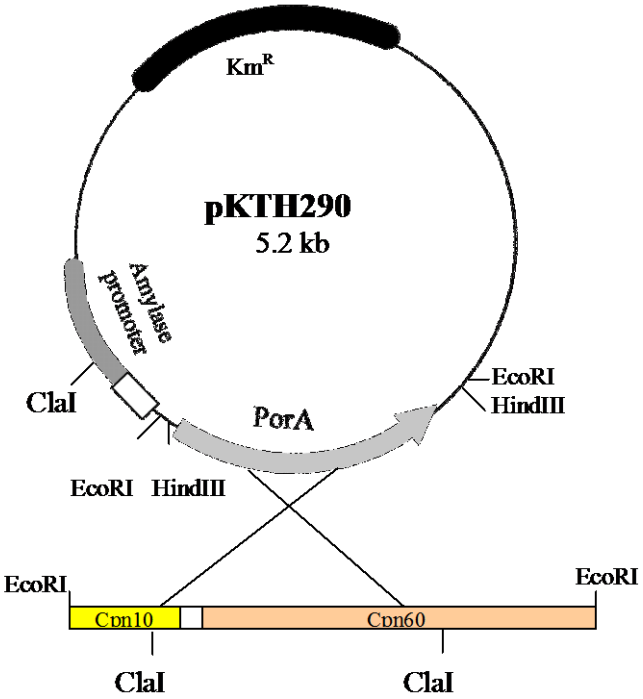

Figure 3.23. Schematic map of pKTH290 and the replacement of *porA* with the *cpn* operon

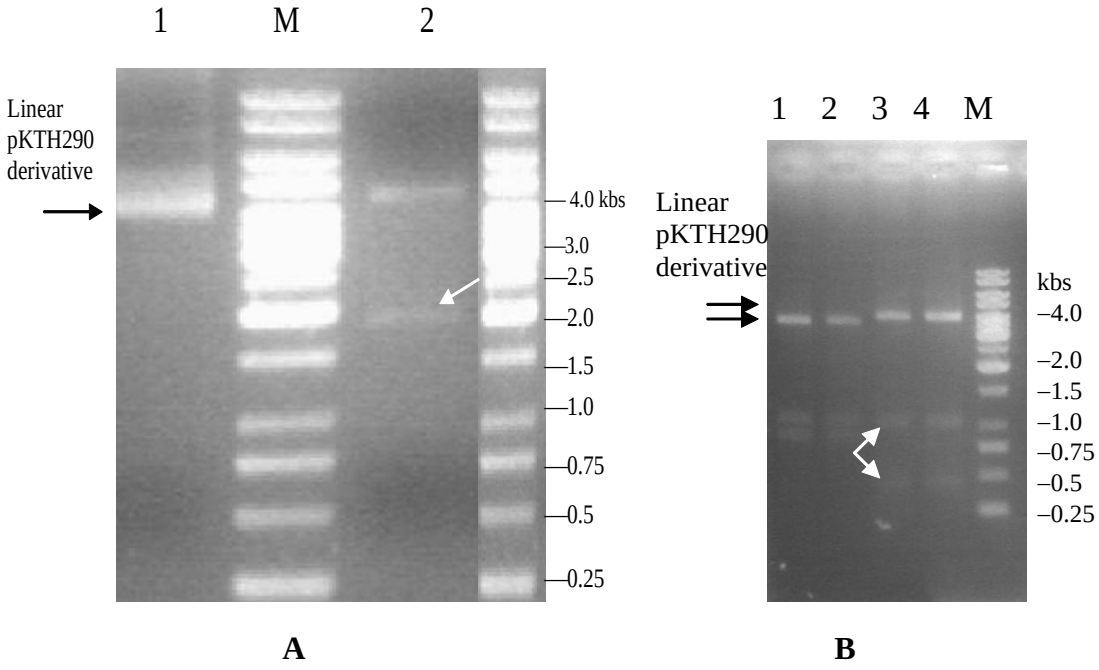

Figure 3.24. Enzymatic digestion of pKTH/nativeRBS and pKTH/changedRBS.

(A). *Eco*RI digestion. Lane 1: linear backbone of pKTH290 (4.1 kb); lane 2: pKTH/ nativeRBS operon (insert of ~2 kbs, indicated by a white arrow). (**B**). *Cla*I digesion of pKTH/nativeRBS and pKTH/changedRBS. Lane 1 and 2: *cpn* operon in antisense direction; Lane 3 and 4: *cpn* operons in correct orientation. Lane M: DNA marker.

3.2.3. Expression of *cpn* operons in *B. subtilis*

The P_{amyQ} in pKTH290 is active without any supplemental inducer. Expression of genes controlled by P_{amyQ} would result in the synthesis of intracellular proteins because of the truncated signal peptide (Nurminen et al. 1992). Cells harboring pKTH/nativeRBS and pKTH/changedRBS were designated as *B. subtilis* NTI and *B. subtilis* CHA respectively. They were cultivated at 30°C and cell samples for protein analysis were harvested throughout the experiment. The soluble cellular fractions were subjected to SDS PAGE analysis (Fig 3.25 A). Both *B. subtilis* NTI and *B. subtilis* CHA produced a distinct protein band with an estimated Mw of 12-14 kDa which was absent in the control strain carrying a pKTH290 backbone without the *cpn* operon (*B. subtilis*/pKTH). This result indicates the synthesis of Cpn10 protein. Additionally to Cpn10, *B. subtilis* CHA also produced a protein with an estimated Mw of 60 kDa which matches the size of the Cpn60. Thus Cpn10 and Cpn60 were both synthesized in cells CHA and the highest amounts of Cpn60 accumulated during a stationary growth phase (Fig 3.25 B). In contrast, *B. subtilis* NTI failed to produce the Cpn60 protein. Probably due to inefficency of the native RBS of *cpn60* gene in *B. subtilis*.

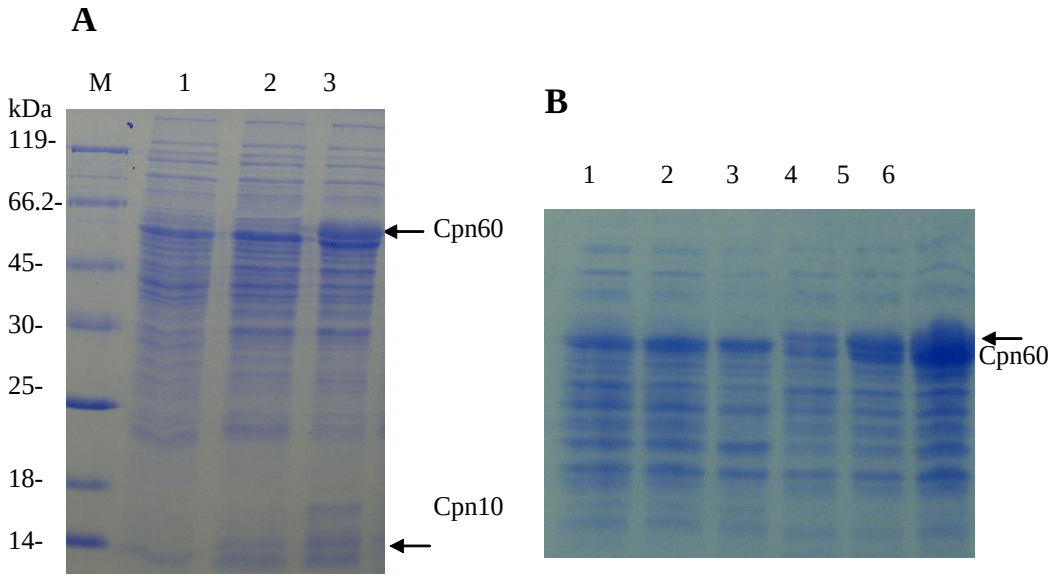

Figure 3.25. SDS PAGE of soluble cellular fraction of cells carrying *cpn* operon

(A): Expression of *cpn10/60* operons
Lane1: *B. subtilis* /pKTH without *cpn* operon
Lane2: *B. subtilis* NTI
Lane3: *B. subtilis* CHA
Lane M: Protein marker
(The arrows indicate Cpn10 and Cpn60 proteins)

(B): Production of Cpn60 at various growth phases
Lane 1, 2, 3: *B. subtilis* /pKTH without *cpn* operon at 12, 16 and 20 h of cultivation
Lane 4, 5, 6: *B. subtilis* CHA at 12, 16 and 20 h of cultivation respectively. The arrow indicates Cpn60

3.2.4. Growth of *B. subtilis* carrying pKTH/changedRBS at low temperatures and the impact of psychrophilic chaperonin on cold-adaptation of the host

A better growth of *E. coli* at low temperature (10°C) was supported by either *O. antarctica* Cpn60/10 (Ferrer et al. 2004b), or even a C-terminal domain of the Cpn60 from *Pseudoalteromonas haloplanktis* (Nakamura et al. 2004). Our experiments were carried out in order to evaluate the growth supporting function of *O. antarctica* chaperonin to *B. subtilis* at low temperature conditions.

B. subtilis CHA was grown at 15°C with shaking at 200 rpm until OD_{600nm} reached 0.2. The cell culture was divided into two equal portions. One continued to grow at 15°C and the other grew at 10°C. The growth of strain CHA was compared to that of control strain, *B. subtilis* /pKTH. Fig. 3.26 A, B show a comparable growth of the host carrying the *cpn* operon and the control strain for both temperatures. A slightly reduced growth of *B. subtilis* CHA at 10°C (Fig. 3.26 A) may be attributed to the expression of the *cpn* operon. The growth capacity on LB agar plates at 4°C was also examined. Cells were spreaded on agar plates and incubated at 15°C for 2 days, followed by incubation at 4°C for 5 days. No difference in the growth of *B. subtilis* CHA with that of *B. subtilis* /pKTH could be observed (Fig. 3.27). At 10°C, the Cpn60 protein was produced in a lower amount as compared to 28°C, but clearly visualized on SDS gels (Fig. 3.28). Production of Cpn60 was stable and quite similar between the late exponential and stationary phases (Fig 3.28).

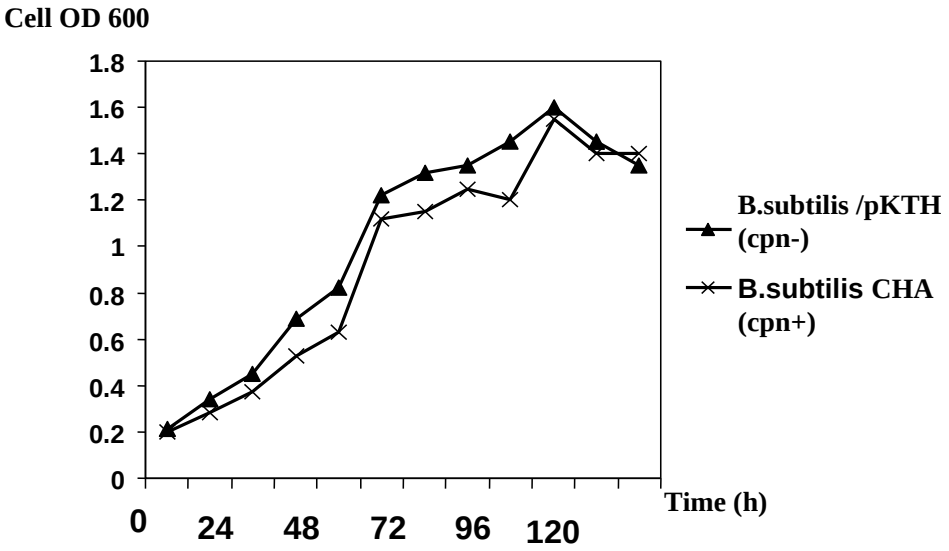

Figure 3.26 A. Growth of *B. subtilis* at 10°C. Samples were collected every 12 h

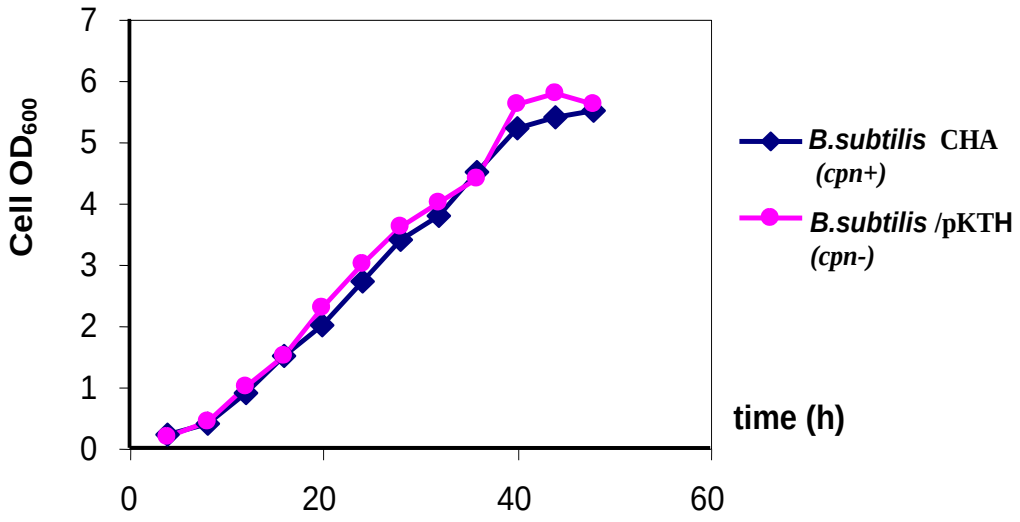

Figure 3.26 B. Growths of *B. subtilis* strains at 15°C. Samples were collected every 4 h

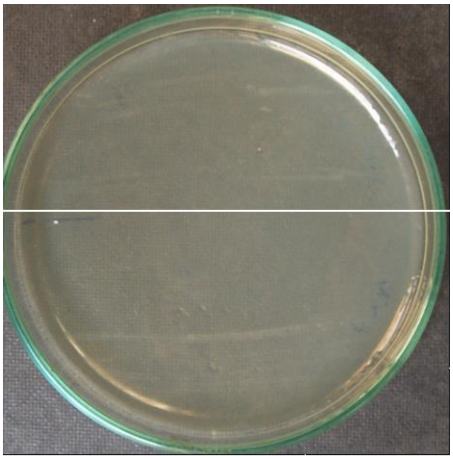

Figure 3.27. Cell growth on LB–agar at 4°C for 5 days after 2 day pre-incubation at 15°C

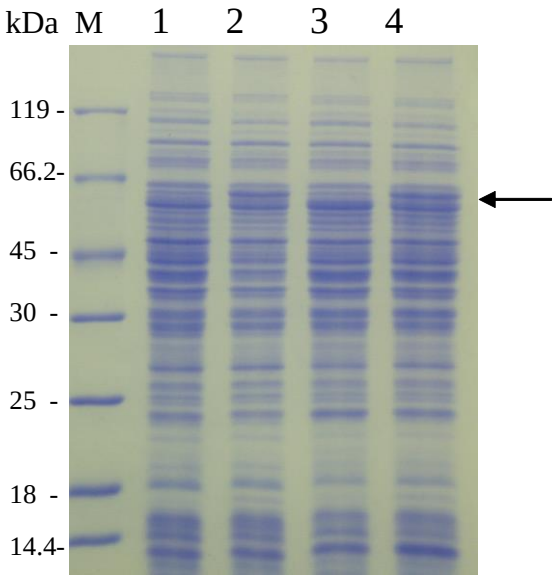

Figure 3.28. Production of Cpn60 protein in *B. subtilis* grown at 10°C.
Lane 1 and 3: cells at late exponential and stationary growth phases of *B .subtilis* /pKTH (*cpn*-)
Lane 2 and 4: cells at late exponential and stationary growth phases of *B. subtilis* CHA (*cpn*+)
The arrow indicates the Cpn60 protein. Cpn10 was not detected

3.2.5 Construction of *B. subtilis* carrying a single chromosomal copy of the *cpn* operon

3.2.5.1. Subcloning of changedRBS operon in pAC5

In this experiment, plasmid pAC5 (Fig. 3.29) was used for cloning and subsequent integration of the changedRBS operon into the *amyE* locus of the *B. subtilis* chromosome.

pKTH/changedRBS was used as template for amplification of *cpn* operon fused with P_{amyQ} using a set of primers *amyQ*/Os-GL and *Sac*I/term (see Table 5.3). The digested PCR product (~ 2.3 kb), designated as PamyQ/*cpn* was ligated into the *Sma*I/*Sac*I sites of pAC5 and *E. coli* DH5α was transformed with the recombinant plasmid, pAC5[PamyQ/*cpn*].

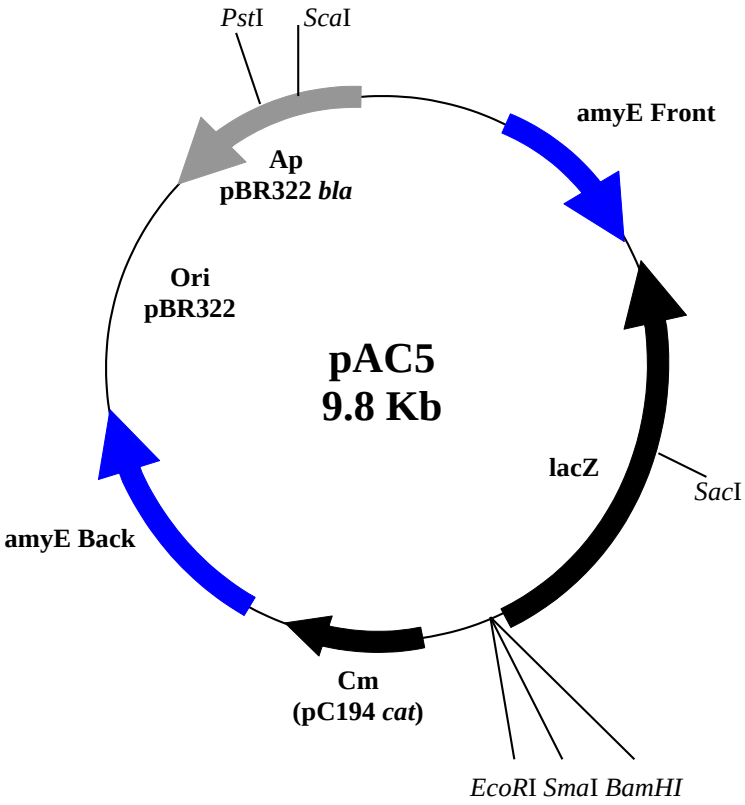

Figure 3.29. Map of the integration vector pAC5. Adapted from Verstraete et al. (1992)

The most relevant features are highlighted.

3.2.5.2. Integration of a single copy of the *cpn* operon into *B. subtilis* chromosome

The pAC5[PamyQ-*cpn*] isolated from a selected *E. coli* transformant was linearized by *Sca*I and introduced into the *B. subtilis* genome. Integration of PamyQ/*cpn* resulted in the knockout of the chromosomal *amyE* gene, causing a loss of amylase activity (Fig.3.30).

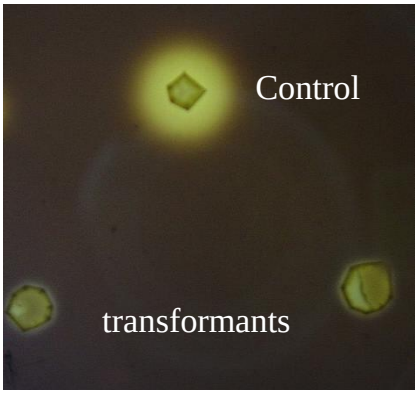

Figure 3.30. Amylase activity of *B. subtilis*.
Control: *B. subtilis* 168 showed clear halo zone of amylase activity. Transformants: *B. subtilis* with PamyQ/*cpn* inserted into *amyE* locus, designated as *B. subtilis* Cpn+, showed no amylase activity.

In order to confirm the integration of the PamyQ/*cpn* into *amyE* locus, an amylase-negative transformant was selected (named as *B. subtilis* Cpn+) and additionally verified by PCR amplification of PamyQ/*cpn* fusion using chromosomal DNA as template (Fig. 3.31).

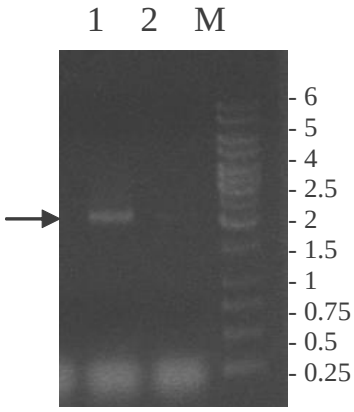

Figure 3.31. PCR amplification of the PamyQ/cpn using chromosomal DNA as template
Lane1: PCR product, using chromosomal DNA of *B. subtilis* Cpn+ as template
Lane2: PCR product, using chromosomal DNA of *B. subtilis* 168 as template (Cpn– or control)
LaneM: marker DNA

B. subtilis Cpn+ was grown in 5 mL LB medium at 28°C at 200 rpm overnight. Analysis of soluble cell lysate by SDS PAGE showed that the *B. subtilis* Cpn+ clearly produced an approximately 60 kDa protein that was absent in the soluble lysate of the Cpn^- cells (Fig. 3.32). This protein band indicates the presence of the Cpn60 protein.

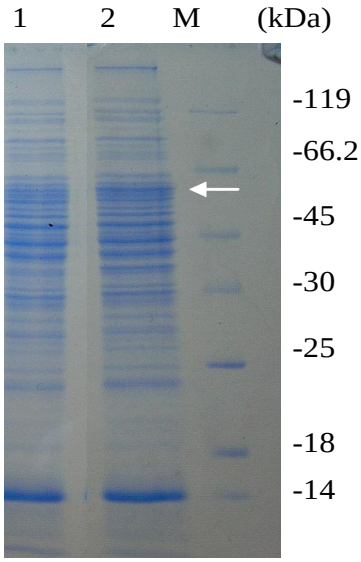

Figure 3.32. Expression of *cpn* operon in *B. subtilis* Cpn+

Lane 1: soluble cell lysate of the *B. subtilis* 168 (Cpn^- control)
Lane 2: soluble cell lysate of the *B. subtilis* Cpn+. The arrow indicates the Cpn60 protein band
LaneM: Protein marker

3.2.6. Expression of yeast α-glucosidase gene in *B. subtilis*

Yeast α-glucosidase, designated as PI, was chosen for co-production with *O. antarctica* Cpn60/10 protein because it was previously reported that PI was a "difficult" protein, with a maximal amount of 1% produced as inclusion bodies in *E. coli* under normal conditions (Kopetzki et al. 1989). In addition, the non-native PI required chaperonins for its folding into native form (Holl-Neugebauer et al. 1991; Xu et al. 1996).

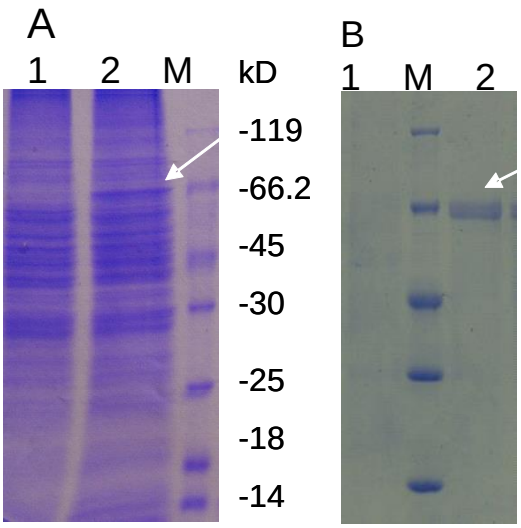

Figure 3.33. SDS PAGE of cellular fractions of the *B. subtilis* YPI
(**A**): Soluble cellular fraction. Lane 1: *B. subtilis* /pKTH (control); Lane 2: *B. subtilis* harboring pKTH/*gluc*PI ; Lane M: Protein marker
(**B**): In soluble cellular fraction. Lane 1: *B .subtilis* /pKTH; Lane 2: *B. subtilis* pKTH/*gluc*PI; Lane M: Protein marker

In this study, PI structural gene (*glucPI*) previously cloned in pKK177-3/GLUCPI (Kopetzki et al. 1989) was PCR-amplified and subcloned in pKTH290 plasmid at unique *Hind*III sites, resulting in pKTH/*glucPI*. This plasmid was then transformed in *B. subtilis* 168 and *B. subtilis* Cpn+, resulting *B. subtilis* YPI and *B. subtilis* Cpn+PI respectively. The recombinant PI produced intracellularly by *B. subtilis* YPI has a molecular mass of about 66,950 Da (Fig. 3.33). The soluble fraction of *B. subtilis* YPI showed PI activity at 37^{o}C when using 5 mM p-nitrophenol as substrate (Fig.3.34).

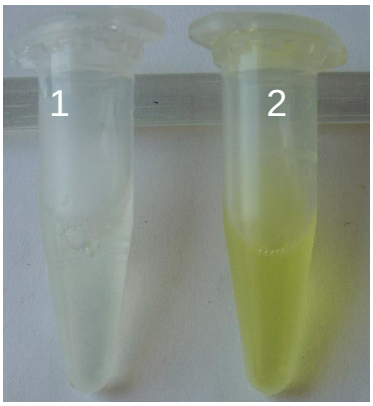

Figure 3.34. Activity of PI upon incubation with p-nitrophenol

Tube1: Cellular lysate of *B. subtilis* /pKTH

Tube2: Cellular lysate of *B. subtilis* YPI

PI activities determined at various temperatures (15°C, 25°C, 30°C and 37°C) are shown in Fig. 3.35. Highest PI activities (up to 5.2 U mg^{-1}) were observed during production at 25°C (Fig 3.35, solid squares) whereas activity values at 37°C remained very low, about 0.2 U mg^{-1} (Fig 3.35, open dots). For the given temperatures, higher activities were observed when cells enter mid-log growth phase. The soluble and corresponding insoluble fractions were subjected to SDS PAGE, displaying their distribution in the cell. As illustrated in Fig. 3.36 B the highest amount of insoluble PI can be detected at 30°C and it decreased upon the production at lower temperatures.

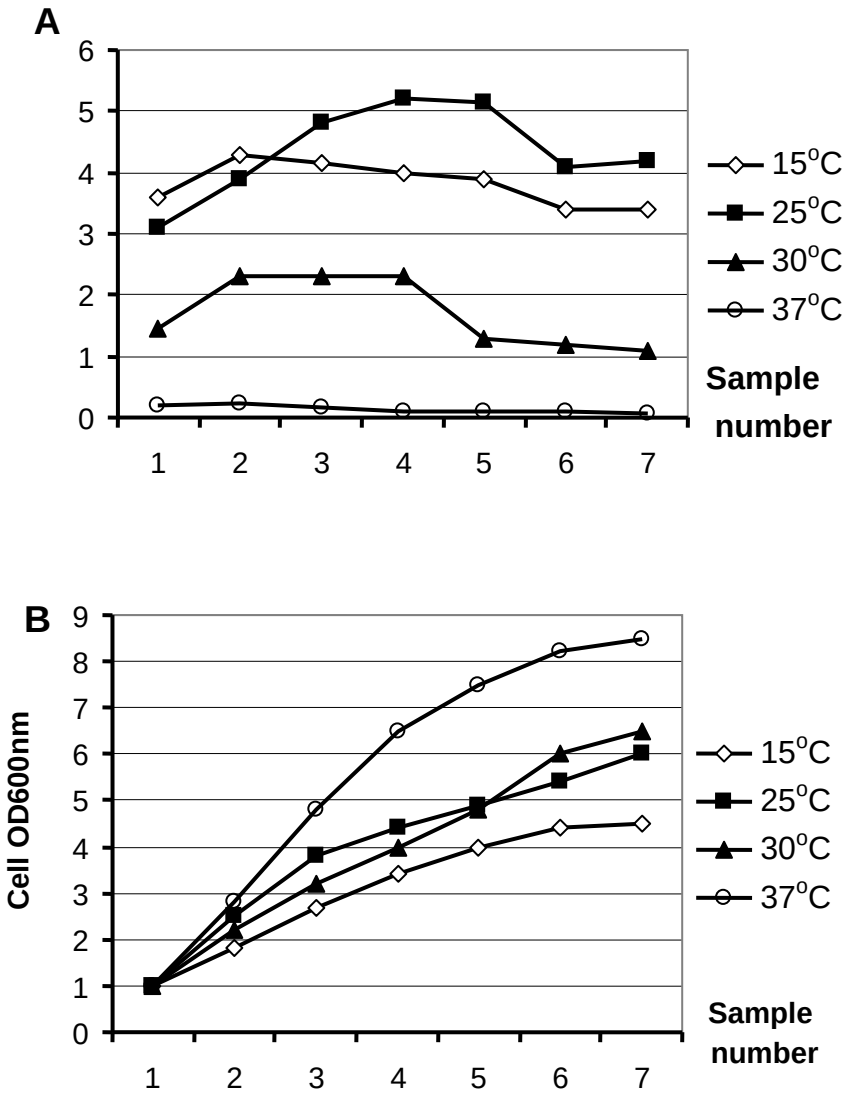

Figure 3.35. Pattern of PI activities during cell growth of *B. subtilis* YPI at various temperatures
(**A**): PI activity; (**B**): Cell OD_{600nm}
After reaching an optical density (OD_{600}) of 1.0, cells were harvested every 1 h for growth at 37°C and 30°C, 2 h for growth at 25°C and 4 h for growth at 15°C.

We were especially interested in the level of PI produced at 15°C at which the psychrophilic Cpn60 displayed the high folding activity both *in vivo* and *in vitro* (Ferrer et al. 2004). The amount of insoluble PI was produced at 15°C remained at a relatively low level (Fig. 3.36 A), but sufficient enough for assessment of the activity and solubility in the *in vivo* refoding experiment.

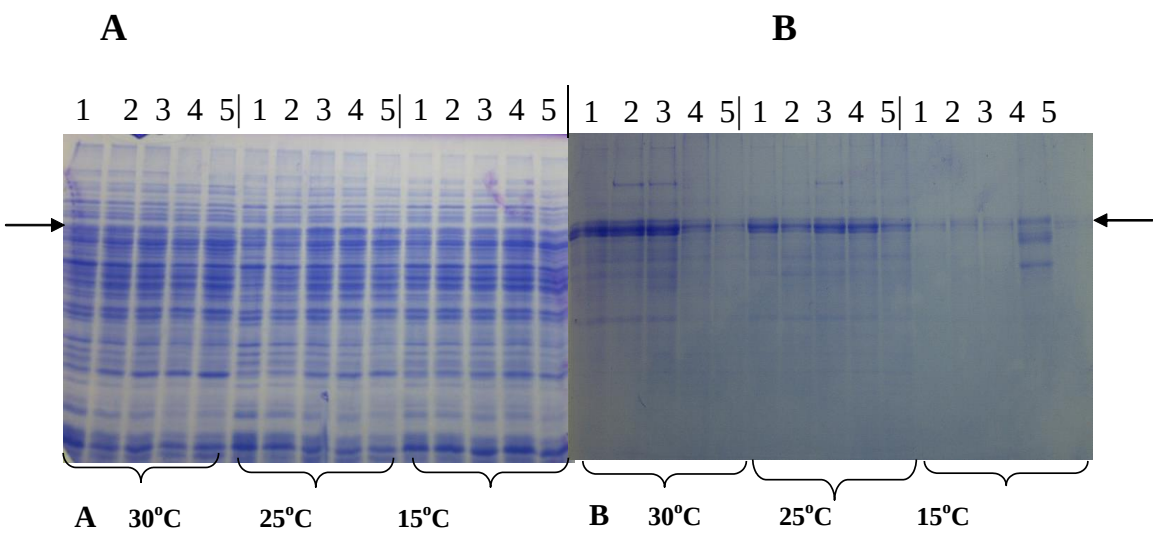

Figure 3.36. Distribution of PI produced by *B. subtilis* YPI at various growth temperatures.
(**A**): Soluble cellular fraction and (**B**): insoluble cellular fraction.
Lane 1: Cell samples were taken at cell OD_{600} of 1.0
Lane 2, 3, 4 and 5: Cell samples were taken every 1 h for growth at 30°C, 2 h for growth at 25°C and 4 h for growth at 15°C after OD_{600nm} of 1.0, respectively.
Arrows indicate the PI bands.

3.2.7. Impact of chaperonin co-expression on PI activity

In this study, the impact of chaperonin co-expression on PI activity was investigated in *B. subtilis* at 15°C. pKTH/gluc*PI* was transformed in *B. subtilis* Cpn+. The recombinant strain carrying the *cpn* operon and the pKTH/*glucPI* expression vector was designated as *B. subtilis* Cpn+PI. Activity of PI produced by *B. subtilis* Cpn+PI was measured and compared to the *B. subtilis* YPI, served as control cells.

Fig. 3.37 demonstrates that the patterns of PI activity in both strains were in general identical. At an OD_{600nm} of 1.0, the specific activity of PI amounted to 3.5 U mg^{-1}, and increased up to 4.4 U mg^{-1} when cells entered the mid-log growth phase. In both strains, PI activities decreased at the early stationary phase.

Production of recombinant PI was also analyzed on SDS-PAGE (Fig. 3.38). Both strains were cultivated at 15°C and aliquots of samples were collected every 4 h after the cells reached an OD_{600nm} of 1.0. Sampling was continued until cells entered the mid-stationary growth phase

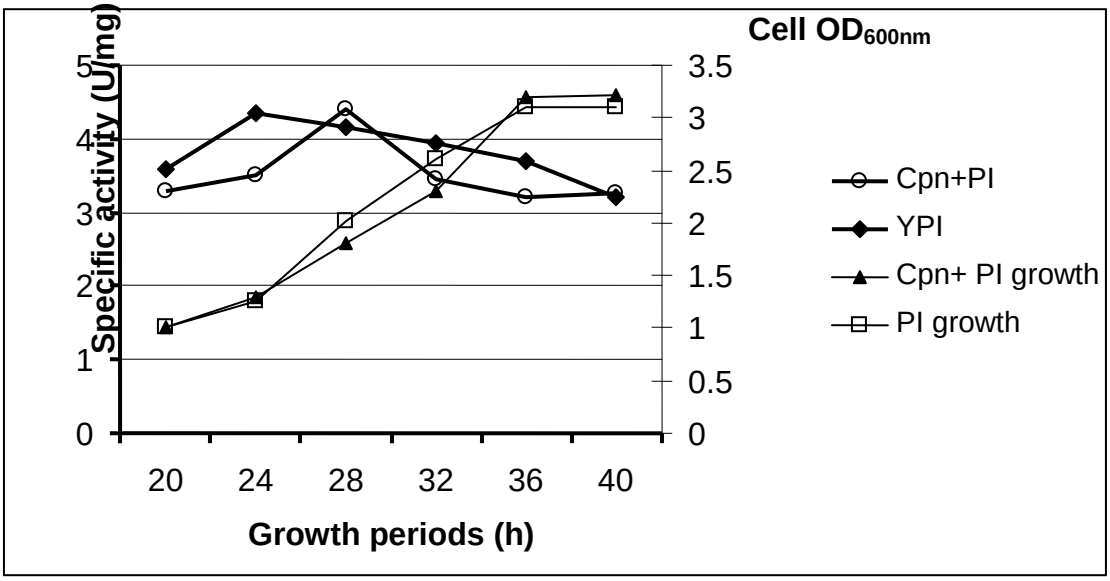

Figure 3.37. Cell growth and PI activity of *B. subtilis* Cpn+PI and YPI grown at 15°C

Cells were harvested every 4 h after cell OD_{600nm} reached 1.0

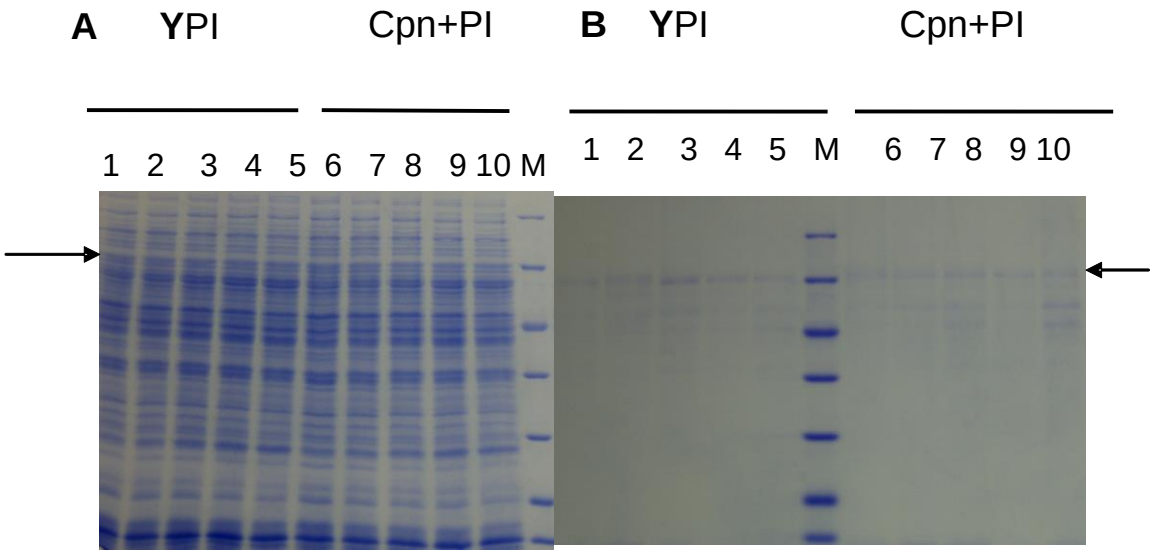

Figure 3.38. SDS PAGE of PI distribution in soluble (A) and insoluble (B) cellular fractions

Lane 1–5: PI produced in *B. subtilis* YPI; Lane 6–10: PI produced in *B. subtilis* Cpn+PI.
In both strains, 5 cell samples were the first 5 samples as indicated in Fig. 3.37

As illustrated in Fig. 3.38 A and B, the amounts of soluble and insoluble PI produced by *B. subtilis* Cpn+PI were comparable to the YPI cell (cpn negative strain). This result indicates no improvement of PI synthesis and activity by co-expression of *cpn* operon at 15°C.

IV- DISCUSSION

4.1. Taxonomy of the strain 64G3

Petroleum reservoirs embody an unusual combination of environmental conditions including temperature, pressure, pH, salinity and heavy metal. They are unique and linked to the deep subsurface. In such an environment, a wide variety of microbes has been isolated or detected using molecular based techniques. Some members of the order *Themotogales* (e.g. *Thermotoga*, *Geotoga* and *Petrotoga*), considered as exclusively thermophilic bacteria, are known as common inhabitants of petroleum reservoirs. Other Thermotogales members such as *Fervidobacterium*, *Thermosipho* (Urios et al. 2004) were isolated from continental springs and hydrothermal vents, respectively. Especially, up to now, all members of genus *Petrotoga* have been retrieved only from deep oil reservoirs (Miranda-Tello et al. 2007).

The this study, strain 64G3 was isolated in water/oil mixture of the oil reservoir offshore Vung Tau province, Vietnam. The sequence similarities of 16S rDNA with 16S rRNAs of *Petrotoga* members, including *P. mexicana* (identity: 99.3%, accession number: NR029058), *P. halophila* (98.6%, AY800102) *P. olearia* (98.1%, NR028947), *P. sibirica* (97.8%, NR025466), *P. mobilis* (97.4 %, CP000879) and *P. miotherma* (96.6%, L10657), indicated that strain 64G3 is closely related to the genus *Petrotoga.* The GC-content of the DNA was 33.4%, falling into the range of 31–36.1% for the six known members of the *Petrotoga* genus (Miranda-Tello et al., 2007). The genomic DNA-DNA relatedness of the strain 64G3 with *P. mexicana* (DSM 14811) (Miranda-Tello et al. 2004) yielded a value of 74.7%, which is above the threshold of 70% recommended for definition of bacterial species (Wayne et al. 1987). This strain was assigned to *P. mexicana* species. Dispite of a high similarity (99.3%) with *P. mexicana* DSM 14811, the DNA-DNA relatedness between these two species is relatively low (74.7%). This demonstrates that the two strains could have distinct bio-physical characteristics.

4.2. Biological and biophysical characteristics of the strain 64G3

Temperature, salinity and pH of the formation waters can also limit the bacterial activity (Magot et al. 2000). Different types of data indicated that the presence of indigenous bacteria in oil fields could be limited to a threshold temperature between 80–90°C. Moderately thermophilic members of the *Thermotogales* consist of the genera *Geotoga*, *Petrotoga* and *Marinitoga*. In this study, strain 64G3 was assigned to genus *Petrotoga*, since its optimum growth temperature is about 55°C and like other members of the *Thermotogales*, strain 64G3 is strictly anarerobic. An outer sheath like structure (called “toga”), a feature typical of the *Thermotogales* was also found in strain 64G3.

Morphologically**,** strain 64G3 is an anaerobic, rod-shaped and thermophilic organism. The cells varied widely in size from small ones of only 1μm in length to those with a length of 40–60 μm which is the highest size within the genus *Petrotoga*. The width of the cells also varied from 0.6–1.2μm. The cells could appear single, in pairs or chains, sometimes with more than 40 small cells per sheath. The higher number of cells per chain is a notable characteristic of this strain, in comparison to other members of *Petrotoga* (from 1–20 cells, Table 4). The strain is not motile and no flagella were detected. In contrast, mobility was observed for *P. mobilis*, *P. olearia*, *P. sibilica*, *P. halophila* and even the same species, *P. mexicana* DSM 14811 (Table 4).

The optimal pH for cell growth of this strain was pH 6.5-7.0, similar to most members of *Petrotoga*, except for *P. sibirica* which has optimal pH for growth at akaline pH 8.0 (Haridon, 2002). The strain 64G3 grew in a wide range of salinity, ranging from 1–10% NaCl, with an optimum at 3%. The ability of reducing sulfur compounds was different in the genus *Petrotoga* (Table 4). In addition to thiosulfate, strain 64G3 could reduce S^{o} to S^{-2}. So far, all members of *Petrotoga* could not reduce sulfate (Miranda-Tello et al. 2007). This makes the *Petrotoga* genus differ from the sulfate reducing group which commonly inhabit oil reservoirs.

Strain 64G3 used various carbohydrate compounds as sole carbon source for growth, including glucose, galactose, ribose, xylose, maltose, starch and xylan.

Table 4.Characteristics useful for differentiating between strain 64G3 and phylogenetically related *Petrotoga* species (Miranda-Tello et al. 2007)

Characteristics	***P.miotherma***	***P. mobilis***	***P. olearia***	***P.sibirica***	***P. mexicana***	***P. halophila***	**Strain 64G3 (this study)**
Source	Petroleum reservoir	Hot oilfield water	Petroleum reservoir	Petroleum reservoir	Oil well water	Oil well water	Oil well water
Cell size (μm)	0.6×2.0-7.5	0.5-1.5×1-50	0.3-0.6×0.9-2.5	0.3-0.6×0.9-2.5	0.5-0.7×1.4-30	0.5-0.7×2-45	0.6-1.2x1-60
Cells per sheath (n)	1-5	1-20	1-2	1-2	1-10	1-5	1-40
Motility	–	+	+	+	+	–	–
Spherical bodies	+	–	+	+	+	+	+
Range (optimum) for growth							
Temperature (°C)	35-65 (55)	40-65 (58)	37-60 (55)	37-55 (55)	30-65 (55)	45-65 (60)	30-65 (55)
pH	5.5-9.0 (6.5)	5.5-8.5 (6.5-7.0)	6.5-8.5 (7.5)	6.5-9.4 (8.0)	5.9-8.5 (6.6)	5.6-7.8 (6.7-7.2)	4.5-8.0 (7.0)
NaCl (%)	0.5-10 (2)	0.5-9 (3-4)	0.5-8 (2)	0.5-7 (1)	1-20 (3)	0.5-9 (4-6)	1-10 (3)
Reduction of thiosulfate	+	+	–	–	+	–	+
G+C content (mol%)	34.2a/32b	34a/31b	35b	33b	36.1a	34.6a	33.4
Substrate utilization							
Arabinose	+	+	+	–	+	+	ND
Cellobiose	ND	+	+	–	+	+	ND
Galactose	+	+	–	+	+	+	+
Xylan	–	+	+	+	+	+	+
Xylose	+	+	+	–	+	+	+

Determined by: a, HPLC method; b, thermal denaturation method. ND: no data available

4.3. Amylase and the cloning of amylase coding gene

Several members of the order *Thermotogales* were found to produce amylolytic enzymes and these characterized enzymes were all thermophilic. The strain 64G3 used soluble starch as sole carbon source, indicating the presence of amylolytic enzymes. Activity staining of cell extract revealed two active bands, suggesting that strain 64G3 produced at least two amylases. In this study, most amylase activity was found to be inside the cell or associated with the "toga", i.e. the outer sheath of the cell. The strain produced at least one thermophilic amylase with the highest activity at 75°C.

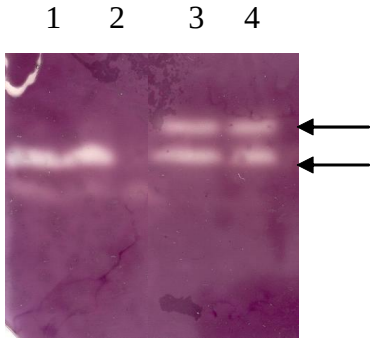

Figure 4.1. Native PAGE of the cellular extract of strain 64G3

Lane 1 and 2: 64G3 cell extract without heat treatment
Lane 3 and 4: 64G3 cell extract with heat treatment for 5 min at 70 and 80°C respectively. Higher bands indicate partially denatured protein.

It is known that bacteria can produce multiple amylases (Kobayashi et al. 1988). However, it was unknown how many different amylase genes are encoded in the genome of strain 64G3. Thus, degenerate primers were used in order to amplify potential amylase genes. Out of six alternative combinations of 5 degenerate primers, only a set of GA5f and GA2r resulted in an amplification of one DNA band. In theory, to amplify a specific gene, PCR conditions need to be properly adjusted to specifically obtain individual genes. In this study, one fragment of an amylase gene (*amyA*) was successuflly amplified and consequently, the complete *amyA* gene was sequenced and analysed. The 1,992 bp *amyA* gene encoding 663 amino acid residues is flanked by two other incomplete ORFs. The matches with the highest sequence identities were found to a glycosidase (45%) of an uncultured *Thermotogales* strain (GenBank accession number CAJ75719), a cyclomaltodextrinase (41%) of *Laceyella sacchari* (AAX29990) and an amylase (40%) of *Kosmotoga olearia* (ACR80687).

Three catalytic residues Asp417, Glu446 and Asp511 corresponding to Asp206, Glu230 and Asp297 of Taka amylase A (Oyama et al. 1996) are located in conserved regions 2, 3 and 4, respectively (Fig. 3.9). A potential ribosome binding site (RBS), 5'-AGGGGG-3', is located nine base pairs upstream of the translational initiation codon, ATG. A putative signal sequence of 25 residues in length with cleavage between Leu25 and Tyr26 was found. Sequence analysis of the regions upstream and downstream of the *amyA* gene revealed two other truncated ORFs (339 and 354 bp), encoding polypeptides which are homologous to P-loop NTPase and Primosomal protein N' (replication factor Y) families respectively. P-loop NTPase domain superfamily contained the ASCE (additional strand catalytic E) class which includes ATPase Binding Cassette (ABC) that are involved in carbohydrate metabolisms. The involvement of primosomal protein N' in carbohydrate metabolisms remains unknown.

The 60 and 15 bp non-coding regions upstream and downstream the ORF of the *amyA* gene contained no potential promoters or transcription terminator motif. Thus, the *amyA* gene and the two adjacent ORFs are located within one operon (all three ORFs have the same polarity). It suggested that the *amyA* gene formed a gene cluster with the two truncated ORFs, which would benefit from a translational coupling mechanism. An α-amylase coding gene of *Pyrococcus furious* was reported to be flanked closely by two other ORFs of unknown function (Laderman et al. 1993) and no promoter and transcription terminator motif for the gene was found. It was common that the function related protein coding genes were located in one cluster. A cluster of five genes involved cyclomaltodextrin metabolism was found in *Thermococcus* sp. They are involved in degrading, synthesizing, binding and transporting of carbohydrate (cyclodextrin) (Hashimoto et al. 2001). The closely related species, *T. neapolitana* also has a gene cluster with at least 3 genes involved in glucan metabolism. Out of them, one putative α-amylase gene (*amyB*) was sequenced (Yernool et al. 2000).

During expression and characterization of the rAmyA, the sequence of a complete DNA genome of *P. mobilis* JS95 was deposited (YP_001568457). A very high identity of 94% between deduced AmyA of the isolate 64G3 with *P. mobilis* SJ95 α-amylase was observed, reflecting a close phylogenetic relationship between the two species. Moreover, the upstream and downstream ORFs of *P. mobilis* amylase gene showed high homologies to the *amyA* flanking upstream and downstream regions of strain 64G3.

4.4. The expression of *amyA* gene and the enzyme characteristics

4.4.1. Expression of *amyA*

During expression of *amyA* at 37°C a large portion of rAmyA was produced in form of inclusion bodies (inactive form). This phenomenon is very common for expression of foreign genes in *E. coli*, such as amyC of *T. maritima* (Ballschmiter et al. 2006). The yield of soluble rAmyA could be improved by optimization of production, including lowering induction temperature and increasing IPTG concentration. It is well known that, a lower rate of protein synthesis increases the efficiency of protein folding and results in a higher amount of active protein. The activity recovered from insoluble rAmyA, however, could be obtained by chaperone-free refolding of the insoluble form. In this study, specific activities recovered from refolding were lower than those of soluble rAmyA (0.18 Umg^{-1} vs 0.5 Umg^{-1}). Therefore, it is obvious that the refolding conditions should be studied in order to obtain a full amylase activity.

4.4.2. Bio-characteristics of rAmyA

Various amylase genes of hyperphilic members of the genus *Thermotogales* were expressed and characterized, such as amylase gene of *T. maritima* (Ballschmiter et al. 2006; Liebl et al. 1997; Lim et al. 2003; Bibel et al. 1998), *T. neapolitana* (Park et al. 2010), *F. pennavorans* (Bertoldo et al. 1999). They were all optimally active at extreme temperatures, between 70 and 90°C. It seems that enzymes of hyperthermophiles possess thermostable and thermoactive properties (Vieille and Zeikus 2001). Strain 64G3, a moderate thermophile, optimally grows at 55°C. The rAmyA has a temperature optimum at 45°C. It was surprising that the enzyme showed a thermal sensitivity like enzymes from mesophiles. Its activity declined rapidly at 55°C and was completely inactive at 60°C. rAmyA functioned at neutral pH, like most bacterial amylases (Liu et al. 2010; Kim et al. 1992; Laderman et al. 1993). An intracellular α-amylase C of *T. maritima*, however, was reported to be optimally active at remarkbly high pH (pHopt 8.5) (Ballschmiter et al. 2006), whereas the other two α-amylase of the same species had pH optima at neutral pH (both at pH 7.0) (Liebl et al. 1997; Lim et al. 2003).

rAmyA showed activity on linear α-1,4-D glucosidic linkages in soluble starch, amylose, amylo-pectin and other related oligosaccharides. The enzyme did not cleave α-1,6 linkages in pullulan and cyclic α-1,4 D-glucosidic linages in cyclodextrins. This demonstrates that rAmyA is a real α-amylase, differing from subgroups of α-amylase including maltogenic amylase, cyclomaltodextrinase, neopullulanase which degrade starch as well as pullulan and

cyclodextrin (Turne et al. 2005; Tang et al. 2008; Cha et al. 1998). The hydrolysis pattern of rAmyA was quite different from those of other typical α-amylases, such as amylase from *B. licheniformis* and *P. furiosus* which hydrolyzed starch in an endo-acting fashion to release oligosaccharides of different degrees of polymerization (Dong et al. 1997). A noteworthy property of rAmyA was that the enzyme produced mainly maltose and maltotriose but minor amounts of glucose. The hydrolysis pattern of rAmyA was similar to that of the related *T. neapolitana* exo-amylase in that both enzymes hydrolyzed maltotriose and formed maltose as the major product of starch hydrolysis. However, *T. neapolitana* amylase did not produce maltotriose during starch hydrolysis. Additionally, the enzyme formed final products differing from those of starch hydrolysis by maltogenic amylases (EC.3.2.1.133) and maltotriose producing amylases which produce maltose and maltotriose as the major product, respectively. α-Amylases of micro-organisms such as *Aspergillus awamori* KT-11 showed hydrolysis pattern on starch similar to rAmyA in terms of final products (maltose as majority) (Matsubara et al. 2004). An intracellular amylase of a related species, *T. neapolitana*, degraded starch and formed maltose as sole product (Park et al. 2010).

The specific activity of rAmyA towards starch was remarkably low, about 0.5 U mg^{-1}. Generally, microbial amylases have specific activities ranging from 14 to 3,000 U mg^{-1} on starch. To our knowledge, the highest activity was 5,600 U mg^{-1} as recorded for *T. maritima* α-amylase (Liebl et al. 1997). However, this strain also produced another amylase, AmyC, with a very low specific activity about from 0.3–1.0 U mg^{-1} (Ballschmiter et al. 2006). In this study the low activity (0.5 U mg^{-1}) of rAmyA on starch is unknown. It may be due to the nature of AmyA or the involvement of the host environment during folding or starchy substrate difficulty.

4.5. Cloning and expression of *cpn* operon in *B. subtilis* and impact of *O. antarctica* chaperonin in cold adaptation of the host.

The successful transformation of a pKTH290 backbone carrying the *O. antarctica cpn* operons into *B. subtilis* was obtained using protoplast transformation method. *B. subtilis* cells carrying pKTH/nativeRBS operon produced only Cpn10, whereas the cells carrying pKTH/changedRBS operon produced both Cpn10 and Cpn60 proteins. This result indicates that the RBS sequence of native *cpn60* gene does not work properly in *B. subtilis*. The differences in RBS sequence between gram-negative and -positive bacteria are well documented elsewhere (Francis et al. 2000). Soluble Cpn60 was produced at high levels in the range of growth temperature from 25–28^{o}C (Fig. 3.25), but at a reduced level at 10°C. So, the high production of soluble psychrophilic chaperonin at a wide range of temperature is a successful achievement, which would be applied in subsequent studies.

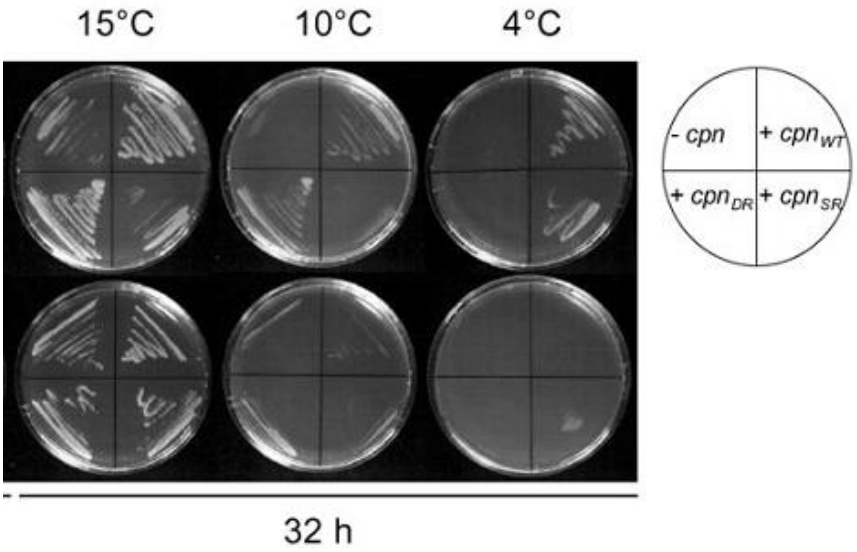

Figure 4.2. Cell viability of parental and engineered *E. coli* strains at different temperatures. Adapted from Ferrer et al (2004b)

Cold-adaptation of *E. coli* caused by psychrophilic chaperonins has been observed earlier (Fig. 4.2) (Ferrer et al. 2004; Nakamura et al. 2004). However, no similar data for *Bacillus* have been reported. In this study, the *O. antarctica cpn* operon was highly expressed using a multi-copy plasmid (pKTH290). The experimental results indicate no clear support of *B. subtilis* cell growth at 10°C and 15°C mediated by this chaperonin (Fig. 3.26 A and B). The growth profiles between the *cpn*-positive and *cpn*-nagative strains at these temperature

conditions were comparable. The psychrophilic chaperonin failed to support the cold-adaptation of the host although they were overproduced.

Willimsky et al. (1992) reported that the cold shock protein (CspB) of *B. subtilis* clearly supported the cell viability of *B. subtilis* in freezing conditions (–80°C) but the impact of this protein on cell growth adaptation to cold conditions has not been discussed.

Recently Endo et al. (2006) demonstrated that the replacement of *B. subtilis cpn60* gene by its homologue from *E. coli* and a psychrophilic *Pseudomonas* sp. *cpn60* gene clearly resulted in different thermal adaptations of *B. subtilis*, depending on *cpn60* gene sources. Being replaced with *Pseudomonas* sp. and *O. antarctica cpn60* genes, *B. subtilis* was unable to grow at elevated temperature, 51 and 48°C respectively, but the wild type strain grew well (Endo et al. 2006). The authors suggested that this might be due to lack of native *B. subtilis* Cpn60 rather than the involvement of recombinant Cpn60 from *Pseudomonas*. Unfortunately, a report on the impact of *Pseudomonas* sp. Cpn60 on cold-adaptation of *B. subtilis* was not presented, but they stated that *O. antarctica cpn60* replacement showed no differences on *B. subtilis* growth at low temperature (10°C) and that one copy of psychrophilic *cpn60* gene was not enough to support a cold adapation. In our study, *O. antarctica* Cpn60 and Cpn10 proteins were produced in *B. subtilis* at a high level using a multi-copy plasmid. However, production of Cpn60 and its co-chaperonin Cpn10 from *O. antarctica* did not improve cold adaptation of the host. It is known that cold adaptation of the wild type strain of *B. subtilis* is supported by the cold-inducible synthesis of cold shock proteins (CSPs) B, C and D (Graumann and Marahiel 1999). In response to cold shock the cytosolic protein pattern and composition changes markedly in *B. subtilis*. Thus, key proteins or molecular mechanisms involving in a better cold adaptation of *B. subtilis* remain unknown unless a cold adapted strain of *B. subtilis* is constructed and analysed by means of genetic and proteomic engineering.

Strocchi et al (2006) compared the proteomic profile of *E. coli* K-12 expressing *O. antarctica cpn* operon with the parental strain grown at 18°C and 4°C and found the involvement of 22 house-keeping proteins in system failure of *E. coli* at low temperatures. Among these proteins, four key cold-sensitive proteins including DnaK, ClpB, Dps and RpsB were reactivated by the *O. anrctatica* chaperonin. Besides the direct folding activity of O.

antarctica chaperonin, there existed also the possibility of an indirect effect of this chaperonin on the expression levels of the proteins (Strocchi et al. 2006).

4.6. The heterologous production of yeast α -glucosidase (PI) in *B . subtilis*

Yeast α-glucosidase (EC.3.2.1.20) belongs to the GH13 family. The enzyme was considered as a "difficult" protein during heterologous production in *E. coli* because of the formation of inclusion bodies (Kopetzki et al. 1989). The enzyme was in *vitro* renatured by GroE(S)L from *E. coli*, psychrophilic *Colwellia psychrerythraea* (Yamauchi et al. 2012) and *Bacillus* sp. (Xu, 1996).

In our study, *glucPI* gene was cloned and successfully expressed in *B. subtilis* (Fig. 3.33). The specific activity amounted to 5 U/mg which was comparable to the activities measured after intracellular production in *E. coli* (Kopetzki et al. 1989; Le Thanh and Hoffmann 2005) or in yeast (Kopetzki et al. 1989). Our result showed that most PI accumulated in inclusion bodies when being produced at 25 and 30°C (Fig. 3.36), whereas at 15°C, the yield of PI aggregation was remarkably reduced. An active PI was produced at temperatures ranging from 15 to 30°C, but not at 37°C. This result indicates an incomplete folding of PI in the host, *B. subtilis*. To date, no definitive correlation has been established between the amino acid sequence of a protein and its propensity to aggregation *in vivo*. Generally, for optimal production of so called "difficult" proteins in their native forms, several strategies should be applied, including the configuration of expression system, transcriptional and translational regulation, protein targeting, use of fusion protein, co-expression of chaperones, codon usage, mutation of target proteins and optimization of fermentation conditions (Makrides 1996; Betiku 2006).

Thus, as one attempt to improve the amount of soluble PI, co-expression of *O. antarctica cpn* operon at a low temperature was investigated.

4.7. Integration of *O. antarctica cpn* operon in the *B. subtilis* chromosome

The integration of a single copy of the *O. antarctica cpn* operon into the *amyE* locus of *B. subtilis* chromosome was carried out using the integrative plasmid pAC5. This vector does not contain any promoter and terminator sequence for the expression of the gene to be inserted. Thus, we combined *amyQ* promoter, *cpn* operon and a transcriptional terminator of *B. subtilis* amylase gene together using pKTH/changedRBS as template for the PCR-amplification. Transformants (*B. subtilis* Cpn+) could not degrade starch due to the knock out of its chromosomal amylase gene (Fig. 3.30).

The host Cpn+ produced the Cpn60 protein at a lesser extent as compared to that of the host carrying pKTH/changedRBS (multi-copy plasmid). Endo et al. (2006) also reported the integration and expression of psychrophilic *Pseudoalteromonas* sp. *cpn60* gene in *B. subtilis*, but no detail data on the impact of this chaperonin on cold adaptation of the host was revealed.

4.8 Co-expression of α-glucosidase gene and *O. antarctica cpn* operon, the impact of psychrophilic chaperonins on enzyme activity

PI activity and the cellular distribution of PI from the Cpn+ and Cpn– cells (served as control) was assayed and compared. PI activity obtained from Cpn+ cells was not increased when compared with those of the Cpn– cells. SDS PAGE of cellular extracts displayed PI aggregation in both strains with an equal amount (Fig.3.38) and the amounts of soluble enzyme were not increased in Cpn+ strain. This result suggested that the *O. antarctica* chaperonin had no positive effect on both the production and the activity of PI in *B. subtilis*. This finding might be due to: (i) folding incapacity of the *O. antarctica* chaperonin towards PI, (ii) low yield of the *O. antarctica* chaperonin, (iii) upper limited level of soluble PI in cells, (iv) the bottleneck from upstream host chaperone (for instance TF, DnaK, GrpE) or (v) other unknown reasons.

Xu et al. (1996) reported that GroEL of *Bacillus* sp. C125 protected yeast PI from aggregation and folded this enzyme *in vitro*. The reactivation of thermally denatured PI was no spontaneous process but mediated by the GroE system or GroEL alone which recovered enzyme activity from the non-native form (Yamauchi et al. 2012; Neugebauer and Rudolph 1991). Le Thanh (2005) reported that higher amount of active PI produced in *E. coli* after a temperature down-shift from 42°C to 24°C was due to the involvement of DnaK and ClpB proteins in disaggregation of PI inclusion bodies which in turn have been reactivated. A PI homologue, *B. thermoglucsidasius* α-1,6 glucosidase produced in *E. coli* was the protein substrate for *B. thermoglucsidasius* chaperonin, but not for DnaK system (Watanabe et al. 2002).

Overexpression of *B. subtilis groE* and *dnaK* resulted in an increase in the secreted recombinant SCA (antidigoxin single chain antibody) by 60% and intracellular soluble SCA by 70% (Wu et al. 1998). The inclusion bodies of SCA were also significantly reduced. Beside GroE and DnaK, another *B. subtilis* chaperone, PrsA, also showed a positive effect on SCA solubility with a two fold increase from 17 to 38% of the total protein (Wu et al. 1998). In our study, expression of one set of *O. antarctica* Cpn60/10 may be not sufficient for re-activation of yeast PI. Another chaperone, GrpE, is involved in transferring a protein substrate to

GroEL/ES and was shown to be required for a folding process of rhodanase enzyme by GroEL/ES (Langer et al. 1992).

It was demonstrated previously that *O. antarctica* chaperonin can efficiently refold denatured proteins *in vitro* (i.e., rhodanase, lactate dehydrogenase, DnaK) (Ferrer et al. 2004b; Strocchi et al. 2006). However, so far, the molecular mechanism of *in vivo* folding activity of psychrophilic Cpn60/Cpn10 towards recombinant proteins is not well understood. The efficient production of active proteins by co-expression of *O. antarctica cpn* operon in *E. coli* at low temperature was documented elsewhere (Hartinger et al. 2010; Lin et al. 2012). Ferrer et al. (2004a) observed that *O. antarctica* chaperonin did not refold *O. antarctica* esterase neither by co-expression in *E. coli* nor by folding *in vitro*. Thus, an increase in the active protein level produced by commercial cold-adapted *E. coli* (known as ArcticExpress^{Tm}) might be due to the cold adaptation of the host mediated by *O. antarctica* chaperonin rather than their direct folding activity towards target proteins (Hartinger et al. 2010).

Yasukawa et al. (1995) investigated the effect of co-production of *E. coli* GroE on the solubility of eight *E. coli* produced eukaryotic recombinant proteins. They revealed that GroE improved solubility of several recombinant proteins such as *myb* proto-oncogene product (cMyb) and Ser/thr kinases but it did not increase the solubility of other proteins such as *myc* proto-oncogene product (Myc) adenovirus oncogene product (E1A). Proudfoot et al. (1996) observed that *E. coli* chaperonins folded *Candida albicans* phosphomannose isomerase (PMI) *in vitro* but failed to fold this enzyme *in vivo*.

The productive folding of a given protein may not correlate with chaperonin level and a high level of overproduction of chaperones might eventually show undesirable side effects regarding protein yield and quality (Martinez-Alonso et al. 2010). Overproduction of other chaperone likes IbpAB, resulted in reduced amounts of the major chaperones such as DnaK, GroEL, ClpB (Le Thanh et al. 2005). As observed by Watanabe (2002), an excess co-production of *B. thermoglucosidasius* GroEL remarkably decreased α-1,6 glucosidase activity from 29.9 to 9.46 U mg^{-1} protein after production in *E. coli*. Thus, the over-production of chaperones might trigger undesired proteolytic activities which is detrimental with regards to recombinant protein stability, quality and yield (Martinez-Alonso et al. 2010).

Understanding the mechanisms and substrate specificities of the major chaperones and their roles in the chaperone-network will provide ideas for rational choice of the chaperone(s) for co-expression. An enhanced concentration of an individual chaperone above physiological levels can result in down-regulation of other heat shock proteins (Le Thanh 2005). In order to efficiently fold a protein the chaperone network must work in a well-balanced way (Langer et

al. 1992). Generally, an increase in the yield of a specific chaperone does not guarantee a better folding of a foreign protein because the protein folding is driven by syngeristic actions of several chaperones such as TF, DnaK/DnaJ/GrpE and GroEL/ES systems (Langer et al. 1992) or non-chaperon factors (Das et al. 2008). Thus, a selection of the appropriate set of folding chaperones is still a trial and error process.

V- MATERIALS AND METHODS

5.1. Materials

5.1.1. Bacteria

Table 5.1. Bacterial strains used in this study

Bacteria	Relevant genotype/phenotype	Reference/ source
Isolate 64G3	unknown	Oil reservoir, Vietnam
E. coli DH5α	F^- *end*A1 *hsd*R17(rk^-, mk^+) *sup*E44 *thi*-λ^- *gyr*A96 *rel*A1 Δ(*arg*F- *laczya*)U169 (for cloning)	Invitrogen, Germany
E. coli Rosetta(DE3)pLysS	F^- *ompT hsdS*$_B$(r_B^- m_B^-) *gal dcm lacY1* (DE3) pLysSRARE6 (Cm^R) (for expression of genes)	Invitrogen, Germany
E. coli Rossetta/*amyA*	*E. coli* Rosetta (DE3)pLyS contains pET22b(+)/*amyA* For expression of *amyA* gene	This study
B. subtilis 168	*TrpC2*	(Kunst et al. 1997)
B. subtilis /pKTH	*B. subtilis* 168 contains pKTH290 Δ*porA*	This study
B. subtilis NTI	*B. subtilis* contains pKTH/nativeRBS	This study
B. subtilis CHA	*B. subtilis* contains pKTH/changedRBS	This study
B. subtilis YPI	*B. subtilis* 168 contain pKTH/*glucPI*	This study
B. subtilis Cpn+	*B. subtilis amyE*::P_{amyQ}/*cpn*	This study
B. subtilis Cpn+pI	*B. subtilis* Cpn+ contains pKTH/*glucPI*	This study

5.1.2. Plasmids

Table 5.2. Plasmids used in this study

Plasmids	Relevent genotype Description/purpose	Reference/ source
pUC19	*bla*, *lacZ*, P_{lac} Cloning plasmid for *E. coli*	Fermentas
pET22b(+)	*bla*, T7 promoter Expression plasmid for *E. coli* (DE3)pLysS	Novagen, Germany
pJET1	*bla*, linearized cloning plasmid for *E. coli*.	Fermentas
pET22b(+)/*amyA*	pET22b(+) *amyA*	This study
pKTH290	*Kn*, P_{amyQ}/*porA* Expression plasmid for *B. subtilis.*	(Nurminen et al. 1992)
pKTH	pKTH290 Δ*porA*	This study
pKTH/*glucPI*	pKTH290 Δ*porA*::*glucPI*	This study
pKTH/nativeRBS	pKTH290 Δ*porA*:: native *cpn*	This study

pKTH/changedRBS	pKTH290 Δ*porA*::*cpn10-rbs-cpn60*	This study
pAC5	*amyE* front *lacZ Cm amyE* back Integration vector for *B. subtilis*.	Verstraete et al. (1992)
pAC5/P_{amyQ}-*cpn*	pAC5 Δ*lacZ*::P_{amyQ}/*cpn*	This study
pPst26	Containing *O. anrctatica cpn* operon.	(Ferrer et al. 2004b)

5.1.3. Oligonucleotides

Table 5.3. Primers used for PCR reactions

Primer name	Use/purpose	Sequence (from 5' to 3' end)
GA1f, forward	Coressponds to sequence coding for conserved region 1 of GH13	ATIGAYYTIGTIMTYAAYCA*
GA2f, forward	Corresponds to sequence coding for conserved region 2	GTHGATGGITKCMGAMTIGA*
GA2r, reverse	Corresponds to sequence coding for conserved region 2	ARCARCRTCIATKCKSAAICC*
GA4r, reverse	Corresponds to sequence coding for conserved region 4	GAAGWMICKTKSIWYRTCRTG*
GA5r, reverse	Corresponds to sequence coding for conserved region 7	GCCIWKYTCITCICCITRRTA*
CuAmyEfet22, forward	Amplification of gene coding for mature α-amylase	AGACGGATCCATATTCGAAAG AAGCGAC (*BamH*I, underlined)
CuAmyEret22	Amplification of gene coding for mature α-amylase	GCCGCTCGAGCTCGCTAACAA GTACAAGA (*Xho*I underlined)
Cyaf, forward	Amplification of partial 16S rRNA gene	CAGAGTTTGATCCTGGCTCAG
Cyar, reverse	Amplification of partial 16S rRNA gene	TACCTTGTTACGACTTCACC
SgamylF, forward	Amplification of Digoxigenin labeled 210 bp fragment for southern hybridization	TCGACTCGGTTATGAATTAC
SgamyR, reverse	Amplification of Digoxigenin labeled 210 bp fragment for southern hybridization	CAGCTAATTTCGTTCGTTGT
Os-GroES1f, forward	Amplification of *O. anrctatica cpn10*	TTAGAATTCGAAGCTTATGAA AATCCGTCCATTAC (*Eco*RI, H*ind*III, underlined)
Os-GroES1r,	Amplification of *O. anrctatica cpn10*	ATCTCTAGAAAGCTTAAGCCT CTAAACGCCGT (*Xba*I and

reverse		*Hind*III, underlined)
amyQ/Os-GL, forward	Amplification of *O. anrctatica cpn* operon fused with amyQ promoter)	ATGAATTCGCCCCGCACATAC GAAAAG (*EcoR*I, underlined)
*Sac*I/termi, reverse	Amplification of *O. anrctatica cpn* operon (introduced termination sequence from *B. subtilis)*	AGAGCTCAAAAAGAAACCATC ATTGATGGTTTCTTTCGGTAAC ATCATGCCAGGC (*Sac*I, underlined)
Os-GroEL2f, forward	Amplificaiton of changed/RBS *O. anrctatica cpn60*	ATTCTAGATGAATTCGTATAA GAAAATGAGAGGAAACATGGC TGCTAAAG (*Xba*I and *EcoR*I underlined)
Os-GroEL2r/Ter.	Amplification of *O. anrctatica cpn* operon (introduced termination sequence from *B. subtilis)*	AGAGCTCAAAAAGAAACCATC ATTGATGGTTTCTTTCGGTAAC ATCATGCCAGGC (*Sac*I, underlined)
FOGLUI, forward	Amplification of yeast glucosidase gene	ACCTCAAGCTTGATATGACTAT TTCTGGATCATC (*Hind*III, underlined)
REGLUI, reverse	amplification of yeast glucosidase gene	ATAATAAGCTTTTACCGGCGA GGT (*Hind*III, underlined)

* B, D, H, K, M, R, S, V, W, Y and I denotes bases c/t/g; a/t/g; a/c/t; t/g; a/c; a/g; c/g; a/c/g; a/t; c/t and all four bases respectively.

5.1.4. Chemicals and buffers

5.1.4.1. Chemicals and buffers for isolation of plasmids

Buffer S1		Buffer S2		Buffer S3	
Tris-HCl	50 mM	NaOH	0.2 N	Sodium acetate	3 M
EDTA	10 mM	SDS	1%	pH = 5.5	
Rnase A pH 8.0	100 µg mL^{-1}				

5.1.4.2. Chemicals for gel electrophoresis of DNA

Buffer TAE (Tris-acetate EDTA)		DNA loading buffer (5X)	
Tris-acetate	40 mM	Bromophenol blue	0.25 % (w/v)
EDTA	2 mM	Cylene cyanol	0.25 % (w/v)
		EDTA	50 mM
		Glycerol	30 %
		Tris-HCl pH 7.5	10 mM

5.1.4.3. Chemicals and buffers for *B. subtilis* protoplast transformation

SMM buffer	SMMP medium	PEG solution (40%, w/v)
Sucrose 0.5 M Maleate 0.02 M $MgCl_2$ 0.02 M pH 6.5 adjusted with NaOH	An equal volume of: 4 ×PAB 2 ×SMM	PEG 6000: 40 g 2 × SMM buffer: 50 mL dH20 up to 100 mL.

5.1.4.4. Chemicals and buffers for SDS-PAGE

Chemicals and buffers for SDS-PAGE

Sample loading buffer 4×		10 × running buffer
0.5 M Tris-HCl (pH 6.8): 6.6 mL Glycerol: 7.5 mL SDS 10 % (w/v): 12 mL Bromophenol blue 2 %: 0.5 mL dH_2O up to 25 mL		Tris-HCl (pH 8.4): 30.3 g Glycine: 144.1 g SDS: 10 g dH_2O up to 1 L
Coomassie staining solution		Destaining solution
Coomassie blue R250: 1.5 g Methanol: 455 mL Acetic acid: 80 mL dH_2O up to 1 L		Methanol: 50 mL Acetic acid: 70 mL dH_2O up to 1 L
Separating gel (12%)		Stacking gel (4%)
dH_20	3.35 mL	dH_20	3.05 mL
TrisHCl (pH 8.8) 0.5M	2.5 mL	TrisHCl (pH 8.8) 0.5M	-
Tris HCl (pH 6.8) 0.5M	-	Tris HCl (pH 6.8) 0.5M	1.25 mL
SDS 10% (w/v)	100 µl	SDS 10% (w/v)	50 µl
Acrylamide/Bis 30% (w/v)	4 mL	Acrylamide/Bis 30%	665 µl
APS (w/v) 10%	50 µl	APS (w/v) 10%	25 µl
TEMED	5 µl	TEMED	5 µl

5.1.4.5. Chemicals and buffers for immunochemiluminescent detection

Denaturation buffer 1.5 M NaCl 0.5 M NaOH	Neutralization buffer pH 5.5 1 M Tris-HCl 3 M NaC
20 × SSC 3 M NaCl 0.3 M Na-citrate; pH 7.0	Hybridization buffer 5 × SSC, 0.1% (w/v) N-lauroylsarcosine 0.02% SDS 1 × blocking solution
Pre-hybridization buffer 5 × SSC 0.5% SDS 50% formamide 0.1% N-laurilsarcosine 2% blocking reagent (Roche) 50 mM sodium phosphate pH 7.0	Low stringency buffer 2 × SSC 0.1% SDS High stringency buffer 0.5 × SSC 0.1% SDS
Maleic acid buffer pH 7.5 0.1M maleic acid 0.15M NaCl	Blocking solution 1% blocking reagent (Roche) Maleic acid buffer
Antibody solution 75 mU mL^{-1} anti-Digoxigenin – AP dissolved in blocking solution (1:10,000)	Washing buffer Maleic acid buffer 0.3% Tween 20
Detection buffer pH 9.5 100 mM Tris-HCl, 100 mM NaCl	

5.1.4.6. Chemical components in protein refolding kit

10 × wash buffer	10 × solubilization buffer	50 × dialysis buffer
200 mM Tris-HCl, pH 7.5 100 mM EDTA 10% Triton X-100	500 mM CAPS pH 11.0 30% N-lauroylsarcosine	1 M Tris-HCl, pH 8.5 1 M DTT

5.1.4.7. Chemical componets in His bind purification kit

8 × binding buffer	8 × wash buffer	4 × elute buffer	4 × strip buffer	8 × charge buffer
4 M NaCl 160 mM Tris-HCl 40 mM imidazole pH 7.9	4 M NaCl 480 mM imidazole 160 mM Tris-HCl pH 7.9	4 M imidazole 2 M NaCl 80 mM Tris-HCl pH 7.9	2 M NaCl 400 mM EDTA 80 mM Tris-HCl pH 7.9	400 mM $NiSO_4$

5.1.5. Media

5.1.5.1. Luria-Bertani (LB) broth

Substance	Quantity
Bacto-trypton	10 g
Yeast extract	5 g
NaCl	10 g
ddH_2O	to 1 L

5.1.5.2. SOC (super optimal broth with catabolic repression)

SOC medium	
Bacto-tryptone 20 g	$MgCl_2$ 20 mM
Yeast extract 5 g	$MgSO_4$ 20 mM
NaCl 0.5 g	Sterile glucose 0.2%
KCl 2.5 mM	ddH_20 to 1L

5.1.5.3. Media for protoplast transformation of *B. subtilis*

PAB	SMMP	DM3	TBY
PAB: 16.5 g ddH_2O to 1L	An equal volume of: 4× PAB 2× SMM buffer	Agarose 4%: 200 mL Sodium succinate 1 M (pH 7.3): 500 mL Difco casamino acids 5%: 100 mL Difco yeast extract 10%: 50 mL K_2HPO_4 3.5%, KH_2PO_4 1.5%: 100 mL Glucose 20%: 25 mL $MgCl_2$ 1M: 20 mL Bovine serum albumin 2%: 5mL (added to DM3 medium 50-60°C) ddH_2O to 1L	Tryptone: 10 g, yeast extract: 5 g NaCl: 5 g ddH_2O to 1L

5.2. Methods

5.2.1. Microbiological methods

5.2.1.1. Enrichment and isolation of strain 64G3

The strain 64G3 was isolated from oil/water mixtures taken from production well-heads of a petroleum reservoir located in Vung Tau city of Vietnam. The *in situ* temperature was 50-55°C. The samples were collected anaerobically in sterile glass containers and transported to the laboratory at ambient temperature. A 10% volume sample of oil/water mixture was inoculated into 25 mL Hungate tubes containing basal medium supplemented with 0.5% (w/v) starch. The enrichments were then incubated anaerobically for five days at 50°C. For isolation, the culture was plated on the same medium solidified with 4% phytagel. The plates were then incubated in anaerobic jars at 50°C for 5 days. Single colonies were picked and the isolation procedure was repeated three times to obtain pure strains. The strain 64G3 was stored at -80°C in a 50% (v/v) glycerol: medium solution.

5.2.1.2. Cultivation conditions

Strain 64G3 was routinely grown in basal medium containing (g L^{-1}): glucose: 5.0; $MgSO_4$: 3.0; $(NH_4)_2SO_4$: 0.5; $CaCl_2$: 0.5; K_2HPO_4: 0.2; NaCl: 30; yeast extract: 1.0. Prior to inoculation, the medium was reduced with a sterile stock solution of 10% $NaHCO_3$ and 10% $Na_2S.9H_20$ to obtain final concentrations of 0.04% and 0.1%, respectively. One mL of mixed vitamins (Wolin et al. 1963) was added to 1 L of the medium and the pH was adjusted to 7.0 with 10% $NaHCO_3$. The strain was cultured anaerobically in 25 mL Hungate tubes by transferring of a 10% (v/v) inoculation to fresh medium and incubated for 3 days at 50°C. Growth experiments were performed in duplicate.

E. coli DH5α and Rosetta (DE3)plysS (Invitrogen, Germany) were used for gene cloning and expression respectively. *E. coli* strains were aerobically grown in LB broth or agar containing 1% bacto-trypton (w/v), 0.5% yeast extract (w/v), 0.5% NaCl (w/v), supplemented with ampicillin (100μg mL^{-1}) or chloramphenicol (30 μg mL^{-1}) if needed.

B. subtilis was grown in LB broth or agar containing appropriate antibiotics (if needed).

Unless stated otherwise normal bacterial growth in LB broth was carried out at 37°C with virogous shaking at 200 rpm.

5.2.1.3. Scanning Electron Microscopy

Cells were fixed in the medium with 3% glutaraldehyde and 25 mM sodium azide. After 1 hour incubation, cells were harvested by centrifugation and resuspended in a small

volume of medium containing 25 mM sodium azide. Samples were bound for 10 min onto gold and poly-L-lysine coated glass slides. After washing with a washing buffer (50 mM cacodylate pH 7.4, 25 mM sodium azide, 1 mM $CaCl_2$ and 0.9% NaCl) followed by distilled water, cells were stained for 20 seconds with 1% urany acetate and air dried. The glass slides with cells were mounted onto stubs and sputtered with 10 nm gold with a Polaron SC7640 sputter coater (VG Microtech, East Sussex, UK) applying 1 kV and 13 mA. The samples were examined in a ZEISS DSM 940A scanning electron microscope (Oberkochen, Germany) at 7 kV and a working distance of 4 mm. Photographs were taken with an equipment of Point Electronic (Halle, Germany).

5.2.2. Molecular methods

5.2.2.1. Isolation of bacterial chromosomal DNA

Strain 64G3 was grown overnight in basal medium at 50°C for 2 days. Five mL of culture were harvested by centrifugation for 5 min at 4°C, 5,000 ×g. Cells were resuspended in 0.5 mL of 50 mM Tris-HCl and 10 mM EDTA buffer, pH 7.5 (TE buffer) containing 100 µg mL^{-1} lyzozyme. The mixture was incubated at 37°C for 15 min. Then, 30 µL of 10 % SDS and 6 µL of protease K 20 mg mL^{-1} were added and the incubation was carried out at 56°C for 2 h. The cell lysate appeared translucent and viscous. An equal volume of TE saturated phenol was added and mixed gently. The sample was centrifuged at 10,000 ×g for 10 min at 4°C to separate two phases (organic/aqueous). The aqueous layer was transferred into a new tube and washing step was repeated twice. For extraction of DNA, an equal volume of chloroform/isoamyalcohol (24:1, v/v) was added and mixed gently by inversion of the tube. The tube was centrifugated at 10,000 ×g for 10 min at 4°C. The supernatant (aqueous layer) was transferred to a new tube. Two volumes of absolute ethanol were added and precipitated for 1 h at -20°C. To pellet the DNA, centrifugation was performed at 10,000 ×g for 10 min at 4°C. Ethanol was discarded and the pellet was washed with ethanol 70%. The pellet was air-dried for 5 min and resuspended in 100 µL of TE buffer pH 7.5. DNA was stored at -20°C.

5.2.2.2. Isolation of plasmid DNA

The mini-preparation of plasmid-DNA of *E. coli* and *B. subtilis* was done following the method described by Birnboim & Doly (1979). Five mL of LB medium containing appropriate antibiotics were incubated with a fresh single colony and cultivated overnight at 37°C with shaking at 200 rpm. To collect cells, 1.5 mL of cell culture was centrifuged for 5 min at 6,000 ×g. Cell pellets were resuspended in 200 µL buffer S1 and then incubated at 37°C for 5 min. For *B. subtilis* cells, buffer S1 was supplied with 0.5 mg mL^{-1} lysozyme and the incubation

was extended up to 30 min. Afterwards, 200 µL of lysis buffer (S2) were added and the tubes were mixed gently by inversion and incubated on ice for 5 min, then for another 5 min after adding 150 µL buffer S3. The cell lysates were subjected two times to chloroform/isoamyalcohol (24:1, v:v) extraction by adding 500 µL chloroform/isoamyalcohol, mixed gently and centrifuged at 10,000 ×g for 15 min. The upper phase was transferred to a new tube and mixed with two volumes of 100 % ice-cold ethanol to precipitate the DNA at -20°C for 1 h. The DNA pellet was obtained by centrifugation at 10,000 ×g at 4°C for 15 min. The pellet was washed with 70% ice-cold ethanol, centrifuged, air dried and dissolved in 50 µL TE or dH_20.

5.2.2.3. Polymerase chain reaction (PCR)

The PCRs were carried out in order to amplify a specific DNA fragment. For the standard PCR, components listed below were pipetted in a PCR test tube.

PCR components	Final concentration
10 × Tag polymerase buffer: 5 µL	1 ×
dNTP mix (each 2.5 mM): 2µL	0.1 mM
$MgCl_2$ (or $MgSO_4$) 25 mM: 2 µL	2 mM
Primer 1: 1 µL	100 pmol
Primer 2: 1 µL	100 pmol
DNA polymerase (Vent, Tag): 0.5 µL	1 U
dH_2O was adjusted to 50 µL	

The cyclic reaction, composed of three steps (denaturation at 94°C, annealing 50-55°C, and extension at 72°C), was repeated up to 25 times in a thermocycler. The annealing temperature, in particular, was calculated depending on the DNA fragment to be amplified. For standard PCR the annealing temperature was set at 55°C. A standard PCR condition was set up as below.

Initial denaturation		94°C 4min
25 cycles	Denaturation Annealing Extension	94°C 30 s 55°C 60 s 72°C (1 min/1 kb size)
Final extension Store		72°C 5 min 4°C

5.2.2.4. Restriction endonuclease digestion

To create compatible DNA ends for ligation as well as for restriction analysis, DNA was cleaved in the presence of 10-20 U of selective restriction endonuclease/μg DNA. The concentration of DNA used in each experiment was variable depending on the molecular size of DNA fragments and experimental purpose. Generally, to obtain complete digestion, tubes were incubated for 3 h at 37°C. For uncomplete digestion, the reaction was stopped at indicated time points and the nuclease was inactivated by addition of 10 mM EDTA and 1% SDS to the tube and the tube was heated at 75°C for 10 min. If required, 1% BSA (100 mg mL^{-1}) could be added to the reaction. The digested product was analyzed on 0.8% agarose gel by electrophoresis.

5.2.2.5. Dephosphorylation of linearized DNA fragments

To avoid self-ligation of digested plasmids, caft intestinal alkaline phosphatase (CIP) was used to remove 5' phosphate residues at the ends of digested plasmid. The reaction tube was placed at 37°C for 30 min, followed by the addition of another volume of the fresh enzyme and the incubation continued for 30 min. After that, the enzyme was inactivated by heating the tube to 65°C for 10 min. The dephosphorylated DNA was then purified by QIAquick gel extraction Kit.

Reaction components:

Dephosphorylation buffer 10 ×	10 μL
DNA plasmid	1 μg
Alkaline phosphatase	10U–20 U
dH_2O	to 100 μL

5.2.2.6. DNA Ligation

For ligation of DNA fragments and plasmid together, the bacteriophage T4 ligase was used. The molar concentration of the insert DNA exceeded the DNA plasmid concentration at least 3-fold. The ligation mixture was prepared on ice with the following components.

DNA plasmid	1 µL
DNA fragment	3 µL
10 × ligation buffer	2 µL
T4-DNA ligase	0.5 µL (~0.5 U)
dH_20	up to 20 µL

The ligation reaction was incubated at 16°C overnight.

5.2.2.7. Agarose gel electrophoresis of DNA

DNA electrophoresis was performed in a horizontal mini gel apparatus. The concentration of agarose was prepared at 0.8–1% (w/v). The electrophoresis was run in 1 ×TAE buffer at a constant voltage 100 V for 20-30 min. Gel was stained in an ethidium bromide solution (1.0 µg mL^{-1} of water) for 15 min, followed by washing with distilled water. The DNA was visualized under UV light. The size of DNA was estimated by using 1 kb DNA ladder (Fermentas) loaded on the same gel.

5.2.2.8. Purification of DNA fragment from agarose gels and from solution

From agarose gels

DNA fragments were isolated from agarose gels after electrophoresis using QIAquick gel extraction Kit. One piece of gel containing a desired DNA fragment was cut off the gel plate and placed in a clean tube. Three volumes of buffer QG were added to one volume of the gel. The tube was incubated at 50°C for 10 min with gentle vortexing until the gel was completely dissolved. The sample was then loaded to the QIA quick column and was centrifuged at 13,000 ×g for 1 min. The flow-through was discarded and the column was centrifuged for additional 1 min. For washing, 0.75 mL of PE buffer was added to the column followed by centrifugation 1 min at 13,000 ×g. The column was then placed into a clean 1.5 mL tube. The DNA was eluted by adding 50 µL of dH20 or buffer TE pH 8.0, followed by centrifugation at 13,000 ×g.

From aqueous solution

DNA in aqueous solution was purified using the QIAquick gel extraction kit. Three volumes of buffer QG were added to one volume of DNA solution. The subsequent procedures were performed in the same way as described above for agarose gels.

5.2.2.9. Transformation

5.2.2.9.1. Electrotransformation

The electrotransformation was used in order to achieve high-efficiency transformation of plasmid DNA in bacteria. A volume of 250 mL LB medium was inoculated with 2 mL of overnight culture. The inoculated flask was shaken vigorously (250 rpm) at 37°C until an OD_{600nm} of 0.5 (*E. col*i) or 1.0 (*B. subtilis*). After chilling on ice for 15 min, cells were pelleted by centrifugation 10 min 5,000 ×g. Cell pellet was washed twice with 100 mL of cold sterile dH_20 and resuspended in 2.5 mL ice-cold 10% glycerol (for *E. coli*) or 2.5 mL of ice-cold 30% PEG 6,000 (for *B. subtilis*). 60 µL of each cell suspension was transferred into a pre-chilled tube. The cells can be directly used or stored at –80°C for next use. 1–2 µL of solution containing 0.05–0.5 µg plasmid DNA were added to 60 µL of fresh competent or thawed cells. The mixture was placed on ice for 15 min and afterwards transferred into a pre-chilled cuvette (2 mm gap size). Electrotransformation was performed with 2,500 V, 25 µF, and 200 Ohms. Immediately, the transformed cells were diluted by addition of 1mL of ice-cold SOC (super optimal broth with catabolic repression) medium and incubated for 30–60 min at 37°C. 150 µL of transformation culture were spreaded on LB-agar plates containing appropriate antibiotic(s) and incubated overnight at 37°C.

5.2.2.9.2. *B. subtilis* protoplast transformation (Chang and Cohen 1979)

A 5 mL tube of TBY medium was inoculated with a fresh single colony and the tube was shaken overnight at 37°C. The overnight culture was diluted 50-fold into 50 mL of fresh Penassay broth (PAB) medium and grown at 37°C at 200 rpm until the OD_{600} reach 1.2 to 1.5. The cells were harvested by centrifugation at 3500 ×g at RT for 10 min. The cell pellet was resuspended in 5 mL of SMMP solution containing 2 mg mL^{-1} lysozyme and incubated at 37°C with shaking at 50 rpm for 2 h. Cells were examined under the microscope after 30 min and thereafter in 15 min intervals. The incubation was continued until 99% of the cells was converted into protoplasts (globular appearance). The protoplasts were pelleted by

centrifugation at 4,000 ×g for 15 min at RT, washed once with SMMP solution and pelleted a second time. The pellet was resuspended in 2 mL of SMMP and ready for uptake of DNA.

For transformation, 1–10 µL of DNA (0.2 µg) were mixed with equal volume of 2X SMM solution in a sterile tube, followed by an addition of 0.5 mL protoplast suspension. Immediately, 1.5 mL of 40% PEG in 1X SMM was added, and the tube was mixed gently. After 2 min exposure to PEG, 5 mL of SMMP medium was added to the mixture to dilute the PEG. Protoplasts were recovered by centrifugation for 10 min at 3,000 ×g. The treated protoplasts were resuspended in 1 mL of SMMP and were incubated for 1.5 hour at 30°C to enable phenotypic expression of genetic determinants carried by the plasmid. The protoplasts were then plated onto a DM3 agar plate containing kanamycin (100 µg mL^{-1}). Colonies appeared after incubation for 2–4 days at 37°C.

5.2.2.10. Construction of *P. mexicana* 64G3 genomic DNA library

The genomic library was constructed using pUC18 as the cloning vector and procedures as described by Lim et al. (2003). Genomic DNA of the strain 64G3 was partially digested with *Sau*3*A*I for 5–10 min and the fragments with sizes from 2 to 5 kb were pooled and purified from agarose gel. The obtained fragments were then ligated to *BamH*I-digested and dephosphorylated pUC19 (at 16°C, overnight). The ligated mixture was used to transform *E. coli* DH5α by electroporation. The genomic library containing approximately 20,000 white colored clones was stored in a deep freezer until screening.

5.2.2.11. DNA Base composition analysis

The GC-content of the DNA was determined at the DSMZ (Germany). DNA was isolated and purified on hydroxyapatite according to the procedure of Cashion et al. (1997). DNA was hydrolyzed with P1 nuclease and the nucleotides dephosphorylated with bovine alkaline phosphatase (Mesbah et al. 1989). The resulting deoxyribonucleosides were analyzed by HPLC (Shimadzu, Japan). GC determination was calculated from the ratio of deoxyguanosine (dG) and thymidine (dT), using non-methylated Lambda DNA (GC-content 49.85 mol %) as a reference (Mesbah et al. 1989).

5.2.2.12. PCR DIG Probe Synthesis

The DNA probe was labeled with DIG -UTP (digoxigenin-UTP) in the PCR using the PCR DIG Probe Synthesis Kit (Roche, Germany). Primers SgamyF and SgamyR were used for probe synthesis using genomic DNA of strain 64G3 as template. PCR volume consisted of 3 µL 10 × PCR buffer with $MgCl_2$, 3 µL 2 mM dNTPs, 3 µL each of primers (100 pmol mL^{-1}), 1 µL Taq polymerase and 1 µL template genomic DNA. dH_2O was added to make a total volume of 30 µl. The PCR cycling conditions were the same as described above. After amplification by PCR, a specific band of about 210 bp was purified from agarose gel.

5.2.3. Protein and biochemical methods

5.2.3.1. Determination of protein concentration

The concentration of proteins in samples were determined using the method of Bradford (Bradford, 1976). A protein sample with unknown concentration was diluted in ddH_20 to the volume of 200 µL, followed by addition of 800 µL 1X Roti-nanoquant working solution (Roth, Germany) to make a total volume of 1 mL. The tubes were gently mixed by inversion and placed at RT for 5 min. The absorption was measured at A595nm. The blank sample was prepared similarly using 200 µL of dH_20 instead of protein solution. The protein concentration was estimated based on the linear dependence between the A595nm and the protein concentration. For the calibration curve, duplicate volumes of 20 to 200 µL of Bovine Serum Albumin (BSA) standard solution (0.1 mg mL^{-1}) were prepared, and dH_20 was added to each tube to make a final volume of 200 µL. A volume of 800 µL of 1 ×Roti-nanoquant solution was added to each tube. A graph of A595 nm for the protein standards was recorded. Determine the best fit of the data to a straight line in the form of the equation "y = mx + b" where y = A595nm value and x = protein concentration. This equation was used to calculate the concentration of the protein sample based on the measured absorbance of sample.

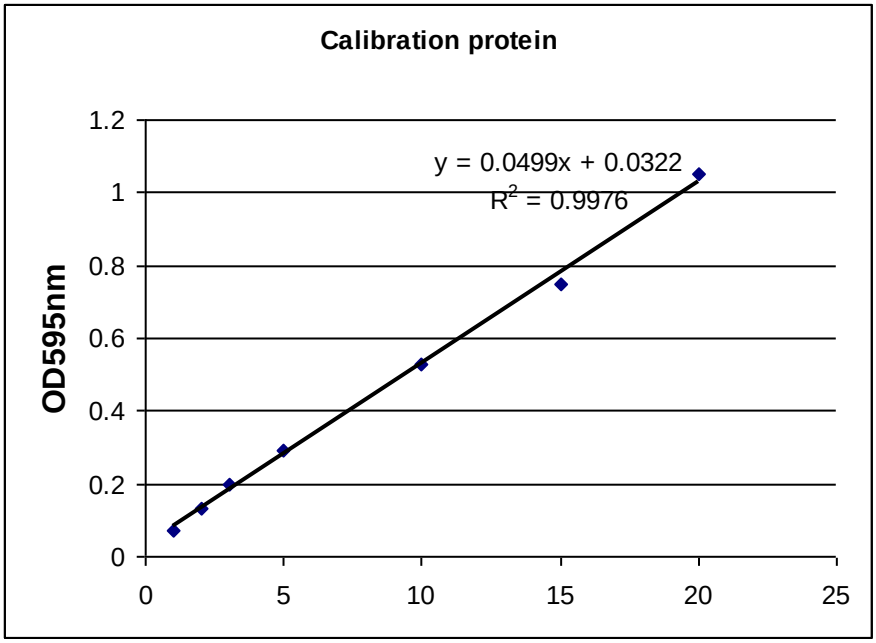

The dilution of BSA stock (0.1 mg mL^{-1}) to desired concentrations								
Volume (µL) of stock BSA 0.1 mg mL^{-1}	2.5	5	10	20	30	40	50	60
Volume (µL) of dH_20 added	197.5	195	190	180	170	160	150	140
Final conc. BSA (µg mL^{-1})	1.25	2.5	5	10	15	20	25	30

5.2.3.2. Polyacrylamide gel electrophoresis (SDS-PAGE)

SDS-PAGE was used to analyse the protein composition of complex protein mixtures such as crude cell extracts or to analyse the purity of proteins during purification or refolding experiments. The technique is based on separation of proteins according to their molecular weights under denature conditions (Laemmli 1970).

SDS gels were set up and run in a minigel electrophoresis unit (mini-PROTEAN II; BioRad), using 7.3 cm × 10.2 cm glass plates and 0.75–1.0 mm spacers. The stacking and separating gel solutions were premixed (stored at 4°C) with absence of APS and TEMED. The

APS and TEMED were added immediately before preparing the gels. Gels were run in an electrophoresis chamber flooded with 1× running buffer.

Protein samples were mixed with 1/4 volume of loading buffer and then heated for 5 min at 100°C to denature proteins. The mixtures were then centrifuged at 10,000×g for 3 min and protein samples were loaded into wells (8–10 μg protein per lane). The electrophoresis was run at constant current (25 mA/gel) until the bromphenol blue dye reached the bottom of the gel. The gel was removed and stained with Coomassie blue by agitating for 1 h at RT, followed by washing with a destaining solution for at least 1 h. Washing steps were repeated by changing the destaining solution until protein bands were clearly visible.

Molecular weight of analysed proteins was estimated by comparison with a standard protein marker mixture separated on the same gel.

5.2.3.3. Activity staining – native PAGE

Protein samples were separated by (SDS) polyacrylamide gel electrophoresis (PAGE) with a 12% (w/v) gel. Non-denaturing PAGE was performed under the same conditions except for the absence of SDS and no heat treatment of the proteins. Amylase activity staining was performed by non-denaturing PAGE with the following protocol: gels were rinsed with distilled water for 10 min at room temperature and washed for 30 min in 50 mM sodium phosphate buffer pH 6.5 with gentle agitation. The washed gels were then soaked in a fresh buffer containing 0.5% soluble starch and the incubation was performed for 5–6 h at 45°C to express hydrolytic activity. The gels were then treated with a lugol solution (0.5% of I_2 and 0.5% KI) to stop the enzymatic reaction. Zones of amylase activity were visualized as a light band against a dark blue background of uncleaved starch.

5.2.3.4. Southern blotting

Three μL of plasmid solutions was blotted on a Whatman 3MM paper and dried at RT. The paper was then submerged in denaturing solution for 5–10 min, followed by soaking in neutralization solution for 5 min. A nitrocellulose membran (positive charged) which was pre-weted with 20 × standard sodium citrate (SSC) was placed in contact with the Whatman 3MM paper. A stack of absorbent paper towels was placed on top and air trapped between the membrane and paper was removed by rolling a glass tube over the membrane. The transfer of DNA from the gel to the membrane by capillarity took about 6 hours. After tranfer, DNA was fixed to the membrane by incubation at 80°C for 2 h.

5.2.3.5. Southern hybridization

The prehybridization buffer was prewarmed at 68°C. The membrane was then incubated in the pre-hybridization buffer at 68°C for 30 min in a hybridization bottle using the hybridization oven.

The DIG-labeled DNA probe (5–25 ng mL^{-1}) was denatured at 100°C for 10 min and immediately chilled on ice. The pre-hybridization buffer was then poured off and the denatured probe was added to an appropriate volume of standard hybridization buffer (1 membrane ≈ 4 mL) and the membrane was incubated in this mixture overnight at 68°C.

5.2.3.6. Immunochemiluminescent detection

After overnight incubation, the membrane was washed twice for 5 min in low stringency buffer at RT and twice for 15 min at 68°C with high stringency buffer. To avoid unspecific hybridization signals, the membrane was incubated for 30 min in a blocking solution and another 30 min in the same buffer containing anti-dioxygenin conjugated with AP (akaline phosphatase). The membrane was then washed twice (each for 15 min) with a washing buffer and rinsed with detection buffer for 2 min.

The membrane was incubated for 5 min in detection buffer contaning CDP-star (Roche, Germany) (diluted 1:100), followed by a wash with washing buffer for 15 min to remove unbound antibody. Afterthat, the membrane was exposed to X-film for 5–10 min in a dark room. The film was soaked in developing solution until signals were visible and then rinsed in water and soaked in fixation solution for 2 min.

5.2.3.7. Overexpression of *amyA* and purification of rAmyA

Two mL of the Rosetta/*amyA* culture was used to inoculate 200 mL of LB broth contaning ampicillin and chloramphenicol in a 1L glass flask which was agitated at 37°C until an OD_{600nm} of 0.5–0.7 was reached. The cells were induced with 0.5 mM isopropyl-thio α-D galactopyranoside (IPTG) and futher incubated at 30°C with agitation for 3 h. Cells were harvested by centrifugation (6,000 ×g, 10 min, 4°C), resuspended in 10 mL of binding buffer (40 mM Tris-HCl pH 7.9, 0.5 M NaCl and 10 mM imidazole), and disrupted by sonication at 4^oC. Clear supernatant and debris fractions were separated by centrifugation (10,000 ×g, 20 min, 4°C).

The soluble rAmyA in the clear supernatant fraction was purified using the His bind purification kit (Novagen, Germany) according to the supplier's protocol (TB054).

Preparation of column: The polypropylene columns containing 2.5 mL settled resin can be used to purify up to 20 mg of target protein. Bottle containing His•Bind Resin was mixed gently by inversion until resin was completely suspended. A desired amount of slurry was transfered to column (e.g. 100 µL slurry yields 50 µL resin for settled bed volume of 50 µL). Resin was allowed to pack under gravity flow. The column was charged and equilibrated using the following runs with indicated buffers:

a) 3 volumes of sterile deionized water

b) 5 volumes of 1 × charge buffer

c) 3 volumes of 1 × binding buffer

Purification of protein:

After sonication the cell lysate was loaded onto the prepared column which was then washed with 10 volumes of 1 × binding buffer, followed by washing with 6 volumes of 1 × wash buffer. The bound protein was eluted with 6 volumes of 1 × elute buffer. Alternatively, 6 volumes of 1 × strip buffer may be used to remove protein by stripping Ni^{2+} from column. The eluate was captured in 1 mL fractions.

The flow rate was set about 0.5 mL/min in all steps. The collected elution fraction was then dialyzed 3 times against 50 mM phosphat buffer pH 6.5 at 4°C to remove imidazole from samples.

5.2.3.8. Refolding of cellular inclusion bodies

Insoluble cellular fraction contaning rAmyA was refolded using Protein Refolding Kit (Novagen, Germany). The refolding procedure is described below:

The solubilization buffer was supplemented with 0.3% N-lauroylsarcosine and 1 mM DTT (dithiothreitol). The solution was then added to the inclusion bodies (at concentration 10–20 mg mL^{-1}) and mixed gently. The mixture was incubated at RT for 15 min and centrifuged at 10,000 ×g for 10 min. Supernatant containing the solubilized protein was tranfered into a dialysis tube and the dialysis was carried out as below:

+ The tube was dialyzed for 3–6 h at 4°C in at least 50 times the volume of protein sample (with addition of 0.1 mM DTT). The fresh buffer was changed at least three times

+ Dialysis was continued through two additional changes (3 h each) with the dialysis buffer lacking DTT.

+ The dialyzed protein solution was centrifuged at 10,000 × g for 10 min at 4°C and the supernatant containing refolded enzyme was stored at 4°C until next usage.

5.2.3.9. Preparation of cellular fractions of *B. subtilis*

A volume of the cell culture corresponding to 1 mL of culture at OD_{600} of 1.0 was obtained. Cells were collected by centrifugation at 5000 ×g for 5 min. The pellet was washed twice with 50 mM sodium phosphate buffer pH 7.0. The cells were re-suspended in 200 µL of the same buffer supplemented with 2 mg mL^{-1} lyzozyme, followed by incubation at 37°C for 15–30 min. The cells were placed on ice for 15 min and were disrupted by sonication for 10s on ice. The soluble and insoluble fractions were separated by centrifugation at 13,000 ×g for 15 min. The insoluble fractions were washed twice with sodium phosphate buffer containing 0.5% Triton X-100 to remove the membrane-bound proteins. The insoluble proteins were solubilized in 200 µL of protein loading buffer containing 6 M urea and subjected to SDS-PAGE electrophoresis.

5.2.3.10. Amylase activity assay

The activity was assayed by measuring the amount of reducing sugars released, as described by Miller (1959). 50 µL of the enzyme was added in 450 µL sodium phosphate buffer 50 mM (pH 6.5) containing 0.5 % (w/v) soluble starch and the enzyme reaction mixtures were incubated at 45^{o}C for 60 min. Addition of 500 µL of DNS solution will stop enzymatic reaction. The mixture was heated in boiling water for 10 min to develop color. The blank sample was prepared using dH_2O instead of enzyme solution. The absorbance of the coloured solution was measured spectrophotometrically at 530 nm. One unit (U) of amylase activity was defined as the amount of the enzyme that released a reducing sugar equivalent to 1 µmol of maltose per min under the defined conditions.

Amount of released reducing sugar was estimated based on the linear dependence between the OD_{530nm} and maltose concentration. A standard curve made up with 0 to 1 µmol maltose (diluted from 10 mM maltose as stock.) was used as a reference.

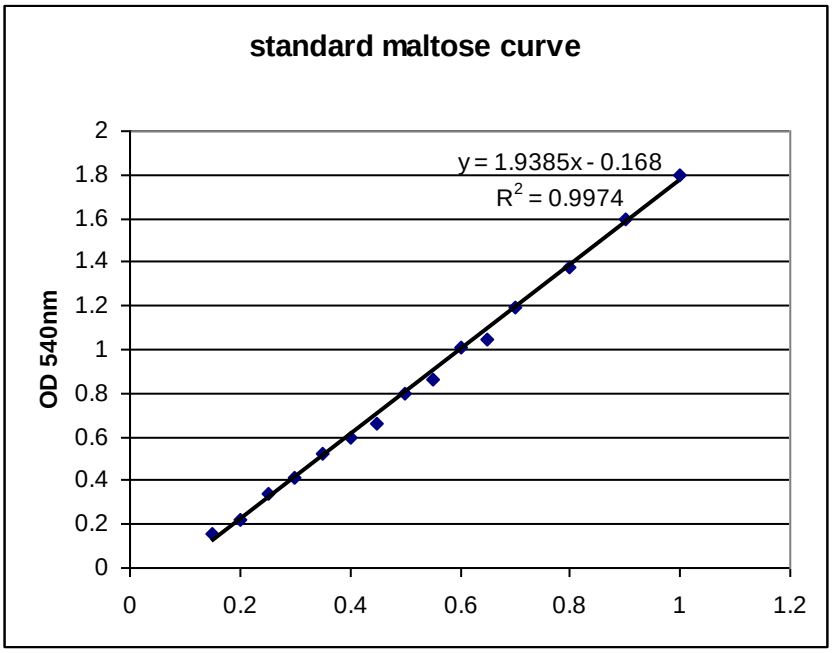

The dilution of maltose stock solution (10 mM) to desired concentrations											
Volume (µL) of maltose (10 mM)	20	25	30	35	40	45	50	60	70	80	100
Volume (µL) of d H_20	480	475	470	465	460	455	450	440	430	420	400
Final maltose (mM)	0.4	0.5	0.6	0.7	0.8	0.9	1.0	1.2	1.4	1.6	2.0

Specific activity of amylase per mL

$$U/mL = \frac{[(OD_{test} - OD_0) + 0.168] * n}{V * 1.9385 * T}$$

OD_{test}: $OD_{530\ nm}$ of the enzymatic reaction

OD_0 : $OD_{530\ nm}$ of the blank sample (dH_20 used instead of enzyme)

V: volume of amylase (mL)

n: Reaction volume (mL)

T: Reaction time (min)

5.2.3.11. α- Glucosidase activity assay

α-Glucosidase activity was assayed with α-pNPG (p-nitrophenyl α- D glucopyranoside) as the substrate (Guffanti and Corpe 1975). The release of p-nitrophenol from α-pNPG by glucosidase was used to estimate the activity. 10 µL of the soluble cell fraction were added to 490 µL 2 mM pNPG in 50 mM sodium phosphate buffer pH 7.0 (pre-warmed). The reaction mixture was incubated at 37°C for 15 min. The reaction was stopped by the addition of 500 µL 1 M Na_2CO_3. The absorption of yellow p-nitrophenol released was measured at A410 nm. One unit (U) of enzyme activity was defined as the amount of enzyme that released one µmol of p-nitrophenol per minute under the standard conditions. A standard curve was constructed using series of known concentrations of p-nitrophenol (5–30 µM). The blank sample containing water instead of enzyme solution was treated the same way.

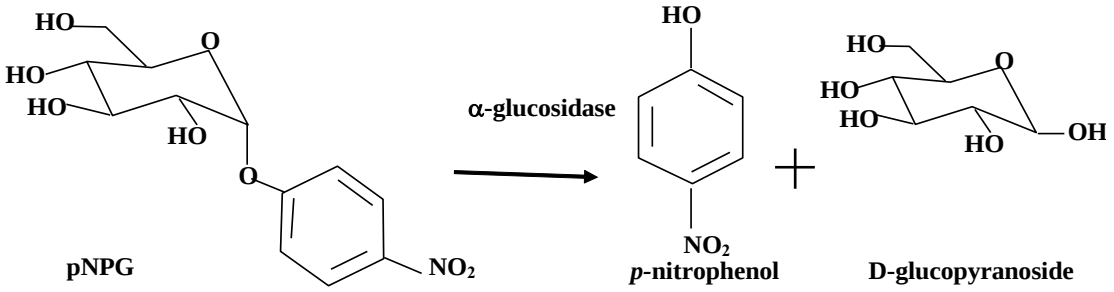

p-NPG is cleaved by α- glucosidase

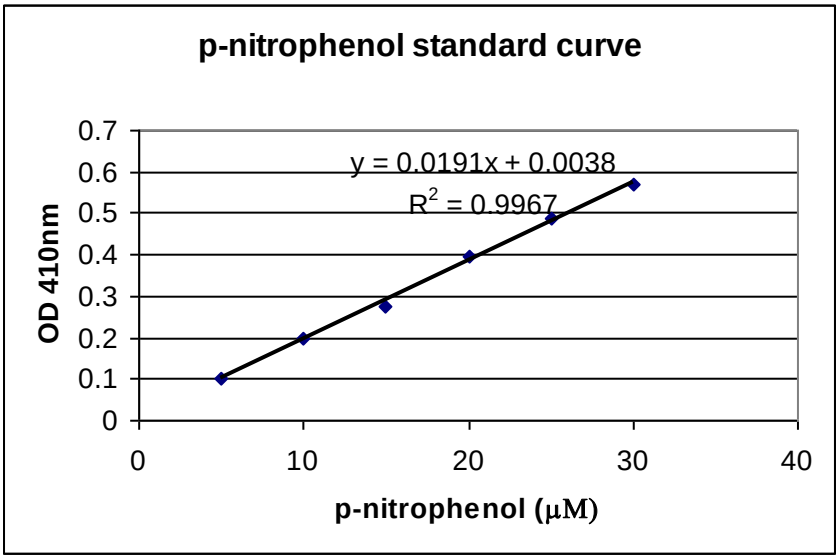

The dilution of p-nitrophenol (100 mM) to desired concentrations						
Volume (μL) of p-nitrophenol strock (100 mM)	25	50	75	100	125	150
dH20 (μl)	475	450	425	400	375	350
Final p-nitrophenol conc. (mM)	5	10	15	20	25	30
p-nitrophneol (μmol)	2.5	5.0	7.5	10	12.5	15

5.2.3.12. The effect of divalent metal ions on rAmyA activity

Amylase activity was examined following pre-incubation of the purified rAmyA with various metal ions at a final concentration of 1.0 mM at room temperature for 10 min. The samples were cooled on ice and assayed for the residual activity.

5.2.3.13. Substrate specificity of rAmyA

Substrate specificity of the enzyme was determined by incubating the purified rAmyA with a variety of substrates, including malto-oligosaccharides, soluble starch, amylose, amylopectin, cyclodextrins and pullulan. The activities towards these substrates were measured using a standard assay. The released sugars from the starch degradation were also identified by thin-layer chromatography (TLC).

5.2.3.14. Analysis of hydrolysis products by TLC

The reaction products were centrifuged and spotted on Whatman K5F silica gel plates (Whatman, Maidstone, United Kingdom), developed in isopropyl alcohol-ethyl acetate-water (3:1:1, v/v/v) as the solvent system (Yang et al. 2006). For visualization of spots, the plates were dried, sprayed with a solution containing 0.3% (w/v) *N*-(1-naphthyl) ethylenediamine and 5% (v/v) H_2SO_4 in methanol and then heated for 10 min at 110°C.

5.2.4. Computational analysis

Searches for sequence similarities and open reading frame (ORF) were conducted with BLAST provided by the National Center for Biotechnology Information (*www.ncbi.nlm.nih.gov/*). The signal peptide cleavage and a potential transcription termination site were predicted using the programes SignalP 3.0 (Niesel, 1997) and Mfold 3.2 (Zuker M.,

2003), respectively. The structure display and free energy calculation of sequence was conducted with the mfold web server (http://mfold.rna.albany.edu/?q=mfold/Structure-display-and-free-energy-determination).

5.2.5. Nucleotide sequence accession number

The partial 16S rDNA sequence of the investigated strain (*P. mexicana* 64G3), the complete nucleotide and the deduced sequences of AmyA were deposited in the GenBank database under the accession number JQ417660 and DQ985807, respectively.

VI. REFERENCES

Agashe V. R. and F.U. Hartl (2000). "Roles of molecular chaperones in cytoplasmic protein folding." Semin Cell Dev Biol **11**(1): 15–25.

Albanese V., A.Y. Yam, et al. (2006). "Systems analyses reveal two chaperone networks with distinct functions in eukaryotic cells." Cell **124**(1): 75–88.

Anfinsen C.B. (1972). "The formation and stabilization of protein structure." Biochem J **128**(4): 737–49.

Anfinsen C.B. (1973). "Principles that govern the folding of protein chains." Science **181**(96): 223–30.

Anfinsen C.B. and H.A. Scheraga (1975). "Experimental and theoretical aspects of protein folding." Adv Protein Chem **29**: 205–300.

Ayling A. and F. Baneyx (1996). "Influence of the GroE molecular chaperone machine on the in vitro refolding of *Escherichia coli* β-galactosidase." Protein Sci **5**(3): 478–87.

Baldwin R.L. (1989). "How does protein folding get started?" Trends Biochem Sci **14**(7): 291–4.

Ballschmiter M., O. Futterer, et al. (2006). "Identification and characterization of a novel intracellular alkaline α-amylase from the hyperthermophilic bacterium *Thermotoga maritima* MSB8." Appl Environ Microbiol **72**(3): 2206–11.

Banner D.W., A.C. Bloomer, et al. (1975). "Structure of chicken muscle triose phosphate isomerase determined crystallographically at 2.5 angstrom resolution using amino acid sequence data." Nature **255**(5510): 609–14.

Barth T. (1991). "Organic acids and inorganic ions in water from petroleum reservoirs, Norwegian continental shelf: a multivariate statistical analysis and comparison with american reserrvoir formation waters." Appl Geochem **6**: 1–15.

Berg B., R.J. Ellis, et al. (1999). "Effects of macromolecular crowding on protein folding and aggregation." EMBO J **18**(24): 6927–33.

Bertoldo C. and G. Antranikian (2002). "Starch-hydrolyzing enzymes from thermophilic archaea and bacteria." Curr Opin Chem Biol **6**(2): 151–60.

Bertoldo C., F. Duffner, et al. (1999). "Pullulanase type I from *Fervidobacterium pennavorans* Ven5: cloning, sequencing and expression of the gene and biochemical characterization of the recombinant enzyme." Appl Environ Microbiol **65**(5): 2084–91.

Betiku E. (2006). "Molecular chaperones involved in heterologous protein folding in *Escherichia coli*." Biotechnol Mol Biol Rev **1**(2): 66–75.

Bhutani N. and J.B. Udgaonkar (2002). "Chaperonins as protein-folding machines." Curr Sci **83**(11): 1337–51.

Bibel M., C. Brettl, et al. (1998). "Isolation and analysis of genes for amylolytic enzymes of the hyperthermophilic bacterium *Thermotoga maritima*." FEMS Microbiol Lett **158**(1): 9–15.

Birnboim H.C. and J. Doly (1979). "A rapid alkaline extraction procedure for screening recombinant plasmid DNA." Nucleic Acids Res **7**(6): 1513–23.

Boel E., L. Brady, et al. (1990). "Calcium binding in α-amylases: an X-ray diffraction study at 2.1-A resolution of two enzymes from Aspergillus." Biochemistry **29**(26): 6244–9.

Boisvert D.C., J. Wang, et al. (1996). "The 2.4 A crystal structure of the bacterial chaperonin GroEL complexed with ATP gamma S." Nat Struct Biol **3**(2): 170–7.

Bonilha P.R.M., V. Menocci, et al. (2006) "Cyclodextrin glycosyltransferase from *Bacillus licheniformis*: optimization of production and its properties.". Braz J Microbiol **37**: 317–23.

Bradford M.M. (1976). "A rapid and sensitive method for the quantitation of microgram quantities of protein utilizing the principle of protein-dye binding." Anal Biochem **72**: 248–54.

Braig K., Z. Otwinowski, et al. (1994). "The crystal structure of the bacterial chaperonin GroEL at 2.8 A." Nature **371**(6498): 578–86.

Bukau B., E. Deuerling, et al. (2000). "Getting newly synthesized proteins into shape." Cell **101**(2): 119–22.

Cashion P., M.A. Holder-Franklin, et al. (1977). "A rapid method for the base ratio determination of bacterial DNA." Anal Biochem **81**(2): 461–6.

Cha H.J., H. G. Yoon, et al. (1998). "Molecular and enzymatic characterization of a maltogenic amylase that hydrolyzes and transglycosylates acarbose." Eur J Biochem **253**(1): 251–62.

Chang H.C., Y.C. Tang, et al. (2007). "SnapShot: molecular chaperones, Part I." Cell **128**(1): 212.

Chang S. and S.N. Cohen (1979). "High frequency transformation of *Bacillus subtilis* protoplasts by plasmid DNA." Mol Gen Genet **168**(1): 111–5.

Chaudhuri T. K., G.W. Farr, et al. (2001). "GroEL/GroES-mediated folding of a protein too large to be encapsulated." Cell **107**(2): 235–46.

Chen J. and W.E. Stites (2001). "Packing is a key selection factor in the evolution of protein hydrophobic cores." Biochemistry **40**(50): 15280–9.

Chen S., A.M. Roseman, et al. (1994). "Location of a folding protein and shape changes in GroEL-GroES complexes imaged by cryo-electron microscopy." Nature **371**(6494): 261–4.

Chen Y., F. Ding, et al. (2008). "Protein folding: then and now." Arch Biochem Biophys **469**(1): 4–19.

Chennubhotla C. and I. Bahar (2006). "Markov propagation of allosteric effects in biomolecular systems: application to GroEL-GroES." Mol Syst Biol **2**: 1–13.

Chuang J.L., R.M. Wynn, et al. (1999). "GroEL/GroES-dependent reconstitution of α2-β2 tetramers of humanmitochondrial branched chain α-ketoacid decarboxylase. Obligatory interaction of chaperonins with an α-β dimeric intermediate." J Biol Chem **274**(15): 10395–404.

Cordes M.H., A. R. Davidson, et al. (1996). "Sequence space, folding and protein design." Curr Opin Struct Biol **6**(1): 3–10.

Craig E., W. Yan, et al. (1999). "Genetic dissection of the Hsp70 chaperone system of yeast." In B. Bukau (ed.), Molecular chaperones and folding catalysts: regulation, cellular function and mechanisms. Harwood Academic Publishers, Amsterdam, The Netherlands: Harwood Academic Publishers; pp. 139–162

Das D., A. Das, et al. (2008). "Role of the ribosome in protein folding." Biotechnol J **3**(8): 999–1009.

Davey M.E., W. A. Wood, et al. (1993). "Isolation of three species of *Geotoga* and *Petrotoga*: two new genera, representing a new lineage in the bacterial line of descent distantly related to the *"Thermotogales"*." System Appl Microbiol **16**: 191–200.

Diderichsen B. and L. Christiansen (1988). "Cloning of a maltogenic α-amylase from *Bacillus stearothermophilus*." FEMS Microbiol Lett **56**: 53–60.

Dill K.A. (1990). "Dominant forces in protein folding." Biochemistry **29**(31): 7133–55.

Dill K.A. (1999). "Polymer principles and protein folding." Protein Sci **8**(6): 1166–80.

Dill K.A., K.M. Fiebig, et al. (1993). "Cooperativity in protein-folding kinetics." Proc Natl Acad Sci USA **90**(5): 1942–6.

Dong G., C. Vieille, et al. (1997). "Cloning, sequencing, and expression of the gene encoding extracellular α-amylase from *Pyrococcus furiosus* and biochemical characterization of the recombinant enzyme." Appl Environ Microbiol **63**(9): 3569–76.

Duilio A., M.L. Tutino, et al. (2004). "Recombinant protein production in antarctic Gram-negative bacteria." Methods Mol Biol **267**: 225–37.

Endo A., M. Sasaki, et al. (2006). "Temperature adaptation of *Bacillus subtilis* by chromosomal groEL replacement." Biosci Biotechnol Biochem **70**(10): 2357–62.

Fayet O., T. Ziegelhoffer, et al. (1989). "The groES and groEL heat shock gene products of *Escherichia coli* are essential for bacterial growth at all temperatures." J Bacteriol **171**(3): 1379–85.

Fenton W.A., J.S. Weissman, et al. (1996). "Putting a lid on protein folding: structure and function of the co-chaperonin, GroES." Chem Biol **3**(3): 157–61.

Ferrer M., T.N. Chernikova, et al. (2004a). "Expression of a temperature-sensitive esterase in a novel chaperone-based *Escherichia coli* strain." Appl Environ Microbiol **70**(8): 4499–504.

Ferrer M., H. Lunsdorf, et al. (2004b). "Functional consequences of single: double ring transitions in chaperonins: life in the cold." Mol Microbiol **53**(1): 167–82.

Fiebig K. M. and K. A. Dill (1993). "Protein core assembly processes." J Chem Phys **98**(4): 3475–87

Flynn G.C., J. Pohl, et al. (1991). "Peptide-binding specificity of the molecular chaperone BiP." Nature **353**(6346): 726–30.

Fisher J. (1987). "Distribution and occurence of aliphatic acid anions in deep subsurface waters." Geochim Cosmochim Acta **51**: 2459–2468.

Francis K.P., D. Joh, C.B. Kawahara, et al. (2000). "Monitoring bioluminescent *Staphylococcus aureus* infections in living mice using a novel *lux*ABCDE construct. Infect Immun. **68**(6): 3594–3600.

Frydman, J. (2001). "Folding of newly translated proteins in vivo: the role of molecular chaperones." Annu Rev Biochem **70**: 603–47.

Georgopoulos C.P., R.W. Hendrix, et al. (1973). "Host participation in bacteriophage lambda head assembly." J Mol Biol **76**(1): 45–60.

Gething M.J. (1997). "Protein folding. The difference with prokaryotes." Nature **388**(6640): 329–331.

Grassia G.S., K.M. McLean, et al. (1996). "A systematic survey for thermophilic fermentative bacteria and archaea in high temperature petroleum reservoirs." FEMS Microbiol Ecol **21**: 47–58.

Graumann P.L. and M.A. Marahiel (1999). "Cold shock response in *Bacillus subtilis*." J Mol Microbiol Biotechnol **1**(2): 203–9.

Guffanti A.A. and W.A. Corpe (1975). "Maltose metabolism of *Pseudomonas fluorescens.*" J Bacteriol **124**(1): 262–8.

Haber E. and C.B. Anfinsen (1962). "Side-chain interactions governing the pairing of half-cystine residues in ribonuclease." J Biol Chem **237**: 1839–44.

Haridon S.L. et al (2002). "*Petrotoga olearia* sp. nov. and *Petrotoga sibirica* sp. nov., two thermophilic bacteria isolated from a continental petroleum reservoir in Western Siberia." Int J Syst Evol Microbiol. **52**: 1715–1722.

Hartinger D., S. Heinl, et al. (2010). "Enhancement of solubility in Escherichia coli and purification of an aminotransferase from *Sphingopyxis* sp. MTA144 for deamination of hydrolyzed fumonisin B(1)." Microb Cell Fact **9**: 62.

Hartl F.U. and M. Hayer-Hartl (2002). "Molecular chaperones in the cytosol: from nascent chain to folded protein." Science **295**(5561): 1852–8.

Hartl F.U. and M. Hayer-Hartl (2009). "Converging concepts of protein folding in vitro and *in vivo*." Nat Struct Mol Biol **16**(6): 574–81.

Hashimoto Y., T. Yamamoto, et al. (2001). "Extracellular synthesis, specific recognition, and intracellular degradation of cyclomaltodextrins by the hyperthermophilic archaeon *Thermococcus* sp. strain B1001." J Bacteriol **183**(17): 5050–7.

Hecht M.H., A. Das, et al. (2004). "De novo proteins from designed combinatorial libraries." Protein Sci **13**(7): 1711–23.

Henrissat B. (1991). "A classification of glycosyl hydrolases based on amino acid sequence similarities." Biochem J **280 (Pt 2)**: 309–16.

Holl-Neugebauer B., R. Rudolph, et al. (1991). "Reconstitution of a heat shock effect in vitro: influence of GroE on the thermal aggregation of α-glucosidase from yeast." Biochemistry **30**(50): 11609-14.

Horwich A.L., W.A. Fenton, et al. (2007). "Two families of chaperonin: physiology and mechanism." Annu Rev Cell Dev Biol **23**: 115–45.

Horwich, A.L., K.B. Low, et al. (1993). "Folding in vivo of bacterial cytoplasmic proteins: role of GroEL." Cell **74**(5): 909–17.

Huang, Y.S. and D.T. Chuang (1999). "Mechanisms for GroEL/GroES-mediated folding of a large 86-kDa fusion polypeptide in vitro." J Biol Chem **274**(15): 10405–12.

Huber R., T.A. Langworthy, et al. (1986). "*Thermotoga maritima* sp. nov. represents a new genus of unique extremely thermophilic eubacteria growing up to 90°C." Arch Microbiol **144**: 324–333.

Hunt J.F., A.J. Weaver, et al. (1996). "The crystal structure of the GroES co-chaperonin at 2.8 A resolution." Nature **379**(6560): 37–45.

Huston A.L. (2008). "Biotechnological aspects of cold-adapted enzymes". In: Margesin R, Schinner F, Marx J-C, Gerday C (eds) Psychrophiles: from biodiversity to biotechnology. Springer-Verlag, Heidelberg, Germany, pp 347–363.

Ikai A. and C. Tanford (1971). "Kinetic evidence for incorrectly folded intermediate states in the refolding of denatured proteins." Nature **230**(5289): 100–2.

Janecek, S. (1997). "α-Amylase family: molecular biology and evolution." Prog Biophys Mol Biol **67**(1): 67–97.

Janecek S. (1997). "Domain evolution in the α-amylase family." J Mol Evol **45**: 322–331.

Janecek S., B. Svensson, et al. (2003). "Relation between domain evolution, specificity, and taxonomy of the α-amylase family members containing a C-terminal starch-binding domain." Eur J Biochem **270**(4): 635–45.

Joseph R.E. and A.H. Andreotti (2008). "Bacterial expression and purification of interleukin-2 tyrosine kinase: single step separation of the chaperonin impurity." Protein Expr Purif **60**(2): 194–7.

Kamtekar S., J.M. Schiffer, et al. (1993). "Protein design by binary patterning of polar and nonpolar amino acids." Science **262**(5140): 1680–5.

Katsuya Y., Y. Mezaki, et al. (1998). "Three-dimensional structure of *Pseudomonas* isoamylase at 2.2 A resolution." J Mol Biol **281**(5): 885–97.

Kerner, M.J., D.J. Naylor, et al. (2005). "Proteome-wide analysis of chaperonin-dependent protein folding in *Escherichia coli*." Cell **122**(2): 209–20.

Kim D.E., H. Gu, et al. (1998). "The sequences of small proteins are not extensively optimized for rapid folding by natural selection." Proc Natl Acad Sci U S A **95**(9): 4982–6.

Kim I.C., J. H. Cha, et al. (1992). "Catalytic properties of the cloned amylase from *Bacillus licheniformis*." J Biol Chem **267**(31): 22108–14.

Kim P.S. and R.L. Baldwin (1982). "Specific intermediates in the folding reactions of small proteins and the mechanism of protein folding." Annu Rev Biochem **51**: 459–89.

Kobayashi Y. et al. (1988). "Heat stable amylase complex produced by a strictly anaerobic and extremely thermophilic bacterium, *Dictyoglomus thermophilum*." Agric Biol Chem, **52**: 615–616.

Koch R., F. Canganella, et al. (1997). "Purification and properties of a thermostable pullulanase from a newly isolated thermophilic anaerobic bacterium, *Fervidobacterium pennavorans* Ven5." Appl Environ Microbiol **63**(3): 1088–94.

Kopetzki E., P. Buckel, et al. (1989). "Cloning and characterization of baker's yeast α-glucosidase: over-expression in a yeast strain devoid of vacuolar proteinases." Yeast **5**(1): 11–24.

Kopetzki E., G. Schumacher, et al. (1989). "Control of formation of active soluble or inactive insoluble baker's yeast α-glucosidase PI in *Escherichia coli* by induction and growth conditions." Mol Gen Genet **216**(1): 149–55.

Kramer G., D. Boehringer, et al. (2009). "The ribosome as a platform for co-translational processing, folding and targeting of newly synthesized proteins." Nat Struct Mol Biol **16**(6): 589–97.

Kunst, F., N. Ogasawara, et al. (1997). "The complete genome sequence of the gram-positive bacterium *Bacillus subtilis*." Nature **390**(6657): 249–56.

L'Haridon S., M.L. Miroshnichenko, et al. (2002). "*Petrotoga olearia* sp. nov. and *Petrotoga sibirica* sp. nov., two thermophilic bacteria isolated from a continental petroleum reservoir in Western Siberia." Int J Syst Evol Microbiol **52**(Pt 5): 1715–22.

Laderman K.A., K. Asada, et al. (1993). "α-Amylase from the hyperthermophilic archaebacterium *Pyrococcus furiosus*. Cloning and sequencing of the gene and expression in *Escherichia coli*." J Biol Chem **268**(32): 24402–7.

Laderman K.A., B.R. Davis, et al. (1993). "The purification and characterization of an extremely thermostable α-amylase from the hyperthermophilic archaebacterium *Pyrococcus furiosus*." J Biol Chem **268**(32): 24394–401.

Laemmli U.K. (1970). "Cleavage of structural proteins during the assembly of the head of bacteriophage T4." Nature **227**(5259): 680–5.

Langer T., C. Lu, et al. (1992). "Successive action of DnaK, DnaJ and GroEL along the pathway of chaperone-mediated protein folding." Nature **356**(6371): 683–9.

Le Thanh H. (2005). "Optimisation of active recombinant protein production, exploring the impact of small heat-shock proteins of *Escherichia coli*, IbpA and IbpB, on *in vivo* reactivation of inclusion bodies." Biochemistry and Biotechnology. Halle, Martin-Luther. PhD thesis**:** 125.

Le Thanh H., P. Neubauer, et al. (2005). "The small heat-shock proteins IbpA and IbpB reduce the stress load of recombinant *Escherichia coli* and delay degradation of inclusion bodies". Microb Cell Fact. **4**:6

Le Thanh, H. and F. Hoffmann (2005). "Optimized production of active α-glucosidase by recombinant *Escherichia coli*. evaluation of processes using *in vivo* reactivation from inclusion bodies." Biotechnol Prog **21**(4): 1053-61.

Lee S.C. and P.O. Olins (1992). "Effect of overproduction of heat shock chaperones GroESL and DnaK on human procollagenase production in *Escherichia coli*." J Biol Chem **267**(5): 2849–52.

Leemhuis H., L. Dijkhuizen (2003). “Hydrolysis and transglycosylation reaction specificity of cyclodextrin glycosyltransferase”. Jof Appl Glycosci **50**(2): 263–271.

Leveque E., S. Janecek, et al. (2000). "Thermophilic archaeal amylolytic enzymes." Enzyme Microb Technol **26**: 2–13.

Levinthal C. (1968). "Are there pathways for protein folding?" J Chim Phys **65**: 44–45.

Liebl W., I. Stemplinger, et al. (1997). "Properties and gene structure of the *Thermotoga maritima* α-amylase AmyA, a putative lipoprotein of a hyperthermophilic bacterium." J Bacteriol **179**(3): 941–8.

Lien T., M. Madsen, et al. (1998). "*Petrotoga mobilis* sp. nov., from a north sea oil-production well." Int J Syst Bacteriol **48 Pt 3**: 1007–13.

Lim W.J., S.R. Park, et al. (2003). "Cloning and characterization of a thermostable intracellular α-amylase gene from the hyperthermophilic bacterium *Thermotoga maritima* MSB8." Res Microbiol **154**(10): 681–7.

Lin F.H, et al. (2012). ”Thermolabile antifreeze protein produced in *Escherichia coli* for structure analysis.” Protein Expres Purif **82**: 75–82

Liu Y., F. Lu, et al. (2010). "High level expression, purification and characterization of a recombinant medium-temperature α-amylase from *Bacillus subtilis*." Biotechnol Lett **32**(1): 119–24.

Maarel M.J., B. van der Veen, et al. (2002). "Properties and applications of starch-converting enzymes of the α-amylase family." J Biotechnol **94**(2): 137–55.

MacGregor E.A. (2005). "An overview of clan GH-H and distantly - related families." Biologia (suppl.16) **60**: 5–12.

Magot M., P. Caumette, et al. (1992). "*Desulfovibrio longus* sp. nov., a sulfate-reducing bacterium isolated from an oil-producing well." Int J Syst Bacteriol **42**(3): 398–403.

Magot M., B. Ollivier, et al. (2000). "Microbiology of petroleum reservoirs." Antonie Van Leeuwenhoek **77**(2): 103–16.

Makrides S.C. (1996). "Strategies for achieving high-level expression of genes in *Escherichia coli*." Microbiol Rev **60**(3): 512–38.

Martinez-Alonso M., E. Garcia-Fruitos, et al. (2010). "Side effects of chaperone gene co-expression in recombinant protein production." Microb Cell Fact **9**: 64.

Matsubara T., Y. Ben Ammar, et al. (2004). "Degradation of raw starch granules by α-amylase purified from culture of *Aspergillus awamori* KT-11." J Biochem Mol Biol **37**(4): 422–8.

McCarter J.D. and S.G. Withers (1994). "Mechanisms of enzymatic glycoside hydrolysis." Curr Opin Struct Biol **4**(6): 885–92.

McLaughlin J.R., C.L. Murray, et al. (1981). "Unique features in the ribosome binding site sequence of the gram-positive *Staphylococcus aureus* β-lactamase gene." J Biol Chem **256**(21): 11283–91.

Mesbah M., U. Premachandran, et al. (1989). "Precice measurement of the G + C content of deoxyribonucleic acid by high performance liquid chromatography." Int J Syst Bacteriol **39**: 159–167.

Miller G. L. (1959). "Use of dinitrosalicylic acid reagent for determination of reducing sugar." Anal Biochem. **31**: 426–428.

Minton, A.P. (2000). "Implications of macromolecular crowding for protein assembly." Curr Opin Struct Biol **10**(1): 34–9.

Miranda-Tello E., M.L. Fardeau, et al. (2007). "*Petrotoga halophila* sp. nov., a thermophilic, moderately halophilic, fermentative bacterium isolated from an offshore oil well in Congo." Int J Syst Evol Microbiol **57**(Pt 1): 40–4.

Miranda-Tello E., M.L. Fardeau, et al. (2004). "*Petrotoga mexicana* sp. nov., a novel thermophilic, anaerobic and xylanolytic bacterium isolated from an oil-producing well in the Gulf of Mexico." Int J Syst Evol Microbiol **54**(Pt 1): 169–74.

Miroshnichenko M.L., N.A. Kostrikina, et al. (2003). "*Caldithrix abyssi* gen. nov., sp. nov., a nitrate-reducing, thermophilic, anaerobic bacterium isolated from a mid-Atlantic Ridge hydrothermal vent, represents a novel bacterial lineage." Int J Syst Evol Microbiol **53**(Pt 1): 323–9.

Mitidieri S., A.H. Souza Martinelli, et al. (2006). "Enzymatic detergent formulation containing amylase from *Aspergillus niger*: a comparative study with commercial detergent formulations." Bioresour Technol **97**(10): 1217–24.

Miyake R., J. Kawamoto, et al. (2007). "Construction of a low-temperature protein expression system using a cold-adapted bacterium, *Shewanella* sp. strain Ac10, as the host." Appl Environ Microbiol **73**(15): 4849–56.

Mogk A., M.P. Mayer, et al. (2002). "Mechanisms of protein folding: molecular chaperones and their application in biotechnology." Chembiochem **3**(9): 807–14.

Nakamura T., M. Tanaka, et al. (2004). "A nonconserved carboxy-terminal segment of GroEL contributes to reaction temperature." Biosci Biotechnol Biochem **68**(12): 2498–504.

Nakashima N. and T. Tamura (2004). "A novel system for expressing recombinant proteins over a wide temperature range from 4 to 35 degrees C." Biotechnol Bioeng **86**(2): 136–48.

Neidhardt F.C., R.A. VanBogelen, et al. (1984). "The genetics and regulation of heat-shock proteins." Annu Rev Genet **18**: 295–329.

Neugebauer B.H. and R. Rudolph. (1991).“Reconstitution of a heat shock effect in vitro: influence of GroE on the thermal aggregation of α-glucosidase from yeast”. Biochemistry **30**(50): 11659–11614.

Nga D., D. Cam Ha, et al. (1996). "*Desulfovibrio vietnamensis* sp. nov., a halophilic sulfate reducing bacterium from vietnamese oil field." Anaerobe **2**: 385–392.

Nielsen H., J. Engelbrecht, S. Brunak, and G. Heijne (1997) “Identification of prokaryotic and eukaryotic signal peptides and prediction of their cleavage sites”. Protein Eng **10**: 1–6.

Nurminen M., S. Butcher, et al. (1992). "The class 1 outer membrane protein of Neisseria meningitidis produced in *Bacillus subtilis* can give rise to protective immunity." Mol Microbiol **6**(17): 2499–506.

Orphan V.J., L.T. Taylor, et al. (2000). "Culture-dependent and culture-independent characterization of microbial assemblages associated with high-temperature petroleum reservoirs." Appl Environ Microbiol **66**(2): 700–11.

Orphan V.J., S.K. Goffredi, et al. (2003). “Geochemical influence on diversity and microbial processes in high temperature oil reservoirs”. Geomicrobiol J **20**: 295–311.

Palomo M., T. Pijning, et al. (2011). “*Thermus thermophilus* glycoside hydrolase family 57 branching enzyme.” J Biol Chemis. **286**(5): 3520–30.

Osmolovskaya E.A.B., M.L. Miroshnichenko, et al. (2003). “Radioisotopic, culture-based, and oligonucleotide microchip analyses of thermophilic microbial communities in a continental high-temperature petroleum reservoir”. Appl Environ Microbiol. **69**(10): 6143-51.

Pandey A., P. Nigam, et al. (2000). "Advances in microbial amylases." Biotechnol Appl Biochem **31 (Pt 2)**: 135–52.

Papa R., V. Rippa, et al. (2007). "An effective cold inducible expression system developed in *Pseudoalteromonas haloplanktis* TAC125." J Biotechnol **127**(2): 199–210.

Parente D., F. de Ferra, et al. (1991). "Prochymosin expression in *Bacillus subtilis*." FEMS Microbiol Lett **61**(2-3): 243–9.

Park K.M., S.Y. Jun, et al. (2010). "Characterization of an exo-acting intracellular α-amylase from the hyperthermophilic bacterium *Thermotoga neapolitana*." Appl Microbiol Biotechnol **86**(2): 555–66.

Pauling L. and R.B. Corey (1951). "The structure of fibrous proteins of the collagen-gelatin group." Proc Natl Acad Sci U S A **37**(5): 272–81.

Philippi G. (1977). "On the depth, time, and mechanism of origin of the heavy to medium gravity naphtenic crude oil." Geochim Cosmochim Acta **41**: 33–52.

Proudfoot A.E., L. Goffin, et al. (1996). "In vivo and in vitro folding of a recombinant metalloenzyme, phosphomannose isomerase." Biochem J **318 (Pt 2)**: 437–42.

Roseman A.M., S. Chen, et al. (1996). "The chaperonin ATPase cycle: mechanism of allosteric switching and movements of substrate-binding domains in GroEL." Cell **87**(2): 241–51.

Ruwisch R.C., Kleinitz W. et al. (1987).“ Sulfate reducing bacteria and their activities in oil production”. J Petrol Technol: 122–31.

Salin M., E.G. Kapetaniou, M. Vaismaa, et al. (2010). “Crystallographic binding studies with an engineered monomeric variant of triosephosphate isomerase.” Acta Cryst. D**66**: 934–944.

Sauza P.M. and Magalhaes P.O. (2010). “Application of microbial amylase in industry – A review.” Braz J Microbiol **41**: 850–61.

Scheraga H.A., Y. Konishi, et al. (1984). "Multiple pathways for regenerating ribonuclease A." Adv Biophys **18**: 21–41.

Schultz C. P. (2000). "Illuminating folding intermediates." Nat Struct Biol **7**(1): 7–10.

Shortle D. (1996). "The denatured state (the other half of the folding equation) and its role in protein stability." FASEB J **10**(1): 27–34.

Sivaramakrishnan S., D. Gangadharan, et al. (2006). "α Amylase from microbial sources - an overview on recent developments." Food Technol Biotechnol **42**: 173–184.

Strocchi M., M. Ferrer, et al. (2006). "Low temperature-induced systems failure in *Escherichia coli*: insights from rescue by cold-adapted chaperones." Proteomics **6**(1): 193–206.

Sung M.S., H.N. Im and K.H. Lee (2011). "Molecular cloning and chaperone activity of DnaK from cold adapted bacteria, KOPRI22215.” Bull Korean Chem Soc **32**(6): 1925–1930.

Takata H., T. Kuriki et al. (1992). “Action of neopullulanase.” J Biol Chemis **267**: 18447–52.

Takkinen K., R.F. Pettersson, et al. (1983). "Amino acid sequence of α-amylase from *Bacillus amyloliquefaciens* deduced from the nucleotide sequence of the cloned gene." J Biol Chem **258**(2): 1007–13.

Takuji O., M. Miho, et al. (1996). "Property of taka-amylase A with Glu or Asp of the catalytic residue replaced by the corresponding amine " Biosci Biotechnol Biochem **60**: 1351–52.

Tang K., R.S. Kobayashi, et al. (2008). "Isolation and characterization of a novel thermostable neopullulanase-like enzyme from a hot spring in Thailand." Biosci Biotechnol Biochem **72**(6): 1448–56.

Tang Y.C., H.C. Chang, et al. (2007). "SnapShot: molecular chaperones, Part II." Cell **128**(2): 412.

Tester R.F., J. Karkalas, et al. (2004). "Starch structure and digestibility enzyme-substrate relationship." Worlds Poult Sci J **60**: 186–195.

Thirumalai D. and G.H. Lorimer (2001). "Chaperonin-mediated protein folding." Annu Rev Biophys Biomol Struct **30**: 245–69.

Thomas J.G. and F. Baneyx (1996). "Protein misfolding and inclusion body formation in recombinant *Escherichia coli* cells overexpressing heat-shock proteins." J Biol Chem **271**(19): 11141–7.

Thuy Le A.T. and W. Schumann (2007). "A novel cold-inducible expression system for *Bacillus subtilis*." Protein Expr Purif **53**(2): 264–9.

Tsong T.Y., R.L. Baldwin, et al. (1971). "The sequential unfolding of ribonuclease A: detection of a fast initial phase in the kinetics ofunfolding. " Proc Natl Acad Sci U S A **68**(11): 2712–2715.

Turner P., A. Labes, et al. (2005). "Two novel cyclodextrin-degrading enzymes isolated from thermophilic bacteria have similar domain structures but differ in oligomeric state and activity profile." J Biosci Bioeng **100**(4): 380–90.

Tutino M.L., A. Duilio, et al. (2001). "A novel replication element from an Antarctic plasmid as a tool for the expression of proteins at low temperature." Extremophiles **5**(4): 257–64.

UriosL., V. Cueff-Gauchard, et al. (2004). "*Thermosipho atlanticus* sp. nov., a novel member of the thermotogales isolated from a mid-atlantic ridge hydrothermal vent." Int J Syst Evol Microbiol **54**(Pt 6): 1953–7.

Vabulas R.M., S. Raychaudhuri, et al. (2010). "Protein folding in the cytoplasm and the heat shock response." Cold Spring Harb Perspect Biol.2:a004390.

Verstraete M., M. Debarbouille, et al. (1992). "Mutagenesis of the Bacillus subtilis „-12, -24" promoter of the levanase operon and evidence for the existence of an upstream activating sequence." J Mol Biol **226**: 85–99.

Vieille C. and G. J. Zeikus (2001). "Hyperthermophilic enzymes: sources, uses, and molecular mechanisms for thermostability." Microbiol Mol Biol Rev **65**(1): 1–43.

Viitanen P.V., A.A. Gatenby, et al. (1992). "Purified chaperonin 60 (groEL) interacts with the nonnative states of a multitude of *Escherichia coli* proteins." Protein Sci **1**(3):363–9.

Watanabe K., H. Fujiwara, et al. (2002). "Oligo-1,6-glucosidase from a thermophile, *Bacillus thermoglucosidasius* KP1006, was efficiently produced by combinatorial expression of GroEL in *Escherichia coli*." Biotechnol Appl Biochem **35**(Pt 1): 35–43.

Wayne L.G., D. J. Brenner, et al. (1987). "Report of the Ad Hoc committee on reconciliation of approaches to bacterial systematics." Int J Syst Bacteriol **37**: 463–464.

Windish W.W. and N.S. Mhatre (1965). "Microbial amylases." Adv Appl Microbiol **7**: 273–304.

Willimsky G., H. Bang, et al. (1992). "Characterization of *cspB*, a *Bacillus subtilis* inducible cold shock gene affecting cell viability at low temperatures". J Bacteriol. **174**(20): 6326–6335.

Wolfenden R. (2007). "Experimental measures of amino acid hydrophobicity and the topology of transmembrane and globular proteins." J Gen Physiol **129**(5): 357–62.

Wolin E.A, M.J. Wolin and R.S. Wolfe (1963). "Formation of methane by bacterial extracts." J Biol Chem **238**: 2882-86.

Wu S.C., R. Ye, et al. (1998). "Enhanced secretory production of a single chain antibody fragment from *Bacillus subtilis* by co-production of molecular chaperones." J Bacteriol. **180**(11): 2830–2835.

Xu Y., T. Kobayashi, et al. (1996). "Molecular cloning and nucleotide sequence of the groEL gene from the alkaliphilic *Bacillus* sp. strain C-125 and reactivation of thermally inactivated α-glucosidase by recombinant GroEL." Biosci Biotechnol Biochem **60**(10): 1633–36.

Xu Z., L. Arthur, et al. (1997)."The crystal structure of the asymmetric GroEL-GroES- (ADP)7 chaperonin complex.". Nature **388**: 741–50.

Yakimov M.M., L. Giuliano, et al. (2003). "*Oleispira antarctica* gen. nov., sp. nov., a novel hydrocarbonoclastic marine bacterium isolated from Antarctic coastal sea water." Int J Syst Evol Microbiol **53**(Pt 3): 779–85.

Yamauchi S., Y. Ueda, et al. (2012). "Distinct features of protein folding by the GroEL system from a psychrophilic bacterium, *Colwellia psychrerythraea* 34H." Extremophiles **16**: 871–882.

Yang J.S., W.W. Chen, et al. (2007). "All-atom ab initio folding of a diverse set of proteins." Structure **15**(1): 53–63.

Yang S.J., H.S. Lee, et al. (2006). "Enzymatic preparation of maltohexaose, maltoheptaose, and maltooctaose by the preferential cyclomaltooligosaccharide (cyclodextrin) ring-opening reaction of *Pyrococcus furiosus* thermostable amylase." Carbohydr Res **341**(3): 420–4.

Yasukawa T., C. Kanei-Ishii, et al. (1995). "Increase of solubility of foreign proteins in *Escherichia coli* by coproduction of the bacterial thioredoxin." J Biol Chem **270**(43): 25328–31.

Yernool D.A., J.K. McCarthy, et al. (2000). "Cloning and characterization of the glucooligosaccharide catabolic pathway β-glucan glucohydrolase and cellobiose

phosphorylase in the marine hyperthermophile *Thermotoga neapolitana*." J Bacteriol **182**(18): 5172–79.

Zimmerman S.B. and S.O. Trach (1991). "Estimation of macromolecule concentrations and excluded volume effects for the cytoplasm of *Escherichia coli*." J Mol Biol **222**(3): 599–620.

Zuker M. (2003). "Mfold web server for nucleic acid folding and hybridization prediction." Nucleic Acids Res **31**: 3406–15.

ADDENDUM

LIST OF FIGURES AND TABLES

List of Figures **Page**

Figure 1.1. Structures of amylose and amylopectin with α-1,4 and α-1,6 glucosidic linkages…… 2
Figure 1.2. Schematic demonstration of the action of amylolytic and pullulytic enzymes…….. 3
Figure 1.3. Parallel $(\beta/\alpha)_8$ barrel of triosephosphate isomerase (TIM)……. 7
Figure 1.4. Stereo structure of the GH13 α amylases…… 9
Figure 1.5.The α-retaining double displacement bond mechanism possessed by α- amylase of GH13. …… 10
Figure 1.6. The folding funnel. ……. 16
Figure 1.7. Models for the chaperone-assisted folding of newly synthesized polypeptides in the cytosol. ……. 19
Figure 1.8. Structure of *E. coli* GroEL/GroES complex. …….. 21
Figure 1.9. Cycle of protein folding by chaperonin system. …… 23
Figure 3.1. PCR amplification of partial 16S rDNA. ……... 29
Figure 3.2. Cellular morphology of strain 64G3. …… 30
Figure 3.3. Effect of temperatures on cell growth. ……... 31
Figure 3.4. Effect of temperatures on the starch degrading activity of cellular extract of strain 64G3. …… 32
Figure 3.5. PCR amplification of a partial *amyA*. ……. 32
Figure 3.6. Incomplete ORF of *amyA* gene. ……. 33
Figure 3.7. Digesion of 20 selected plasmids with *Hind*III. …… 34
Figure 3.8. Screening of the genomic library using Southern hybridization technique. …….. 35
Figure 3.9. The complete nucleotide sequence of *P. mexicana* 64G3 α-amylase gene and its deduced amino acid residues. ……... 37
Figure 3.10. PCR amplification of *amyA* gene and restriction analysis of pET/*amyA*..…….. 38
Figure 3.11. Amylase activity of cell lysate at different temperatures (on starch agar)….. ……. 39
Figure 3.12. SDS-PAGE of the protein samples obtained during the expression and after purification steps (A) and active staining of purified rAmyA (B)……. …….. 39
Figure 3.13. Effect of IPTG concentration on production of rAmyA. …… 41
Figure 3.14. Effect of the induction periods on the production of rAmyA. …… 42
Figure 3.15. Effect of growth- temperatures on the rAmyA production . …… 43
Figure 3.16. Effect of temperature .on rAmyA activity. …….. 44
Figure 3.17. Thermostability of rAmyA. …….. 45
Figure 3.18. Effect of pHs on the enzyme activity…….. ……. 45

Figure 3.19. Hydrolysis patterns of rAmyA analyzed by TLC……. 47
Figure 3.20. Schematic representation of both cpn operons amplified and cloned in pJET1. ……. 48
Figure 3.21. PCR amplification of *cpn10, cpn60* genes and nativeRBS operon…….. 49
Figure 3.22. Analysis of pJET1 carrying *cpn10/60* operons…… 50
Figure 3.23. Schematic map of pKTH290 and the replacement of *porA* with the *cpn* operon…… 50
Figure 3.24. Enzymatic digestion of pKTH/nativeRBS and pKTH/changedRBS…… 51
Figure 3.25. SDS PAGE of soluble cellular fraction of cells carrying *cpn* operon……... 52
Figure 3.26. Growths of *B. subtilis* strains at 10°C (A) and 15°C (B)……. …… 53
Figure 3.27. Cell growth on LB–agar at 4°C for 5 days after 2 day pre-incubation at 15°C. …….. 54
Figure 3.28. Production of Cpn60 protein in *B. subtilis* grown at 10°C. ……. 55
Figure 3.29. Map of the integration vector pAC5.. …….. 56
Figure 3.30. Amylase activity of *B. subtilis*…….. 56
Figure 3.31. PCR amplification of the PamyQ/cpn using chromosomal DNA as template. …… 57
Figure 3.32. Expression of *cpn* operon in *B. subtilis* Cpn+……... 57
Figure 3.33. SDS PAGE of cellular fractions of the *B. subtilis* YPI…… 58
Figure 3.34. Activity of PI upon incubation with p-nitrophenol 59
Figure 3.35. Pattern of PI activities during cell growth of *B. subtilis* YPI at various temperatures.. 60
Figure 3.36. Distribution of PI produced by *B. subtilis* YPI at various growth temperatures. ……. 61
Figure 3.37. Cell growth and specific PI activities of in *B. subtilis* Cpn+PI and YPI at 15^{o}C……. 62
Figure 3.38. SDS PAGE of PI distribution in soluble (A) and insoluble (B) fractions. …….. 62
Figure 4.1. Native PAGE of cellular extract of strain 64G3…….. 66
Figure 4.2. Cell viability of parental and engineered *E. coli* strains at different temperatures……. 70

List of Tables

Page

Table 1.1. Reaction specificities of starch degrading α-amylases of GH13 family ……... 6
Table 1.2. Uses of amylases in various sectors of industry……. 11
Table 1.3. Reprentative folding chaperones……. 18
Table 3.1. Effect of metal ions on rAmyA activity …… 46
Table 3.2. Substrate specificity of rAmyA…….. 47
Table 4. Characteristics useful for differentiating between strain 64G3 and phylogenetically related *Petrotoga* species …… 65
Table 5.1. Bacterial strains used in this study …… 75
Table 5.2. Plasmids used in this study……. 75
Table 5.3. Primers used for PCR reactions ……..... 76

APPENDIX

Appendix A

A) Partial sequence of pKTH290 containing the cloning site and α-amylase promoter (P_{amyQ}) from *B. amyloliquefaciens*

tgagcgaacacgtgaaaattatgatttgaaaaatgataaaaatattgattacaacgaacg
tgtcaaagaaattattgaatcacaaaaaacaggtacaagaaaaacgaggaaagatgctgt
tcttgtaaatgagttgctagtaacatctgaccgagatttttttgagcaactggatcatcc
gcaaagggcgcattcaagtatcagtatcaacaagcggggcaagccccgcacatacgaaaa
gactggctgaaaacattgagcctttgatgactgatgatttggctgaagaagtgg***atcgat***
tgtttgagaaaagaagaagaccataaaaataccttgtctgtcatcagacagggtattttt
tatgctgtccagactgtccgctgtgtaaaaaatagga**ataaaggggggttgttattatttt**
tactgatatg**taaaatataat**ttgtataagaaaat**gagagggagagga**aac**atg**attcaa
– – – – – – – – – – – – – – – – – – M I Q

aaacgaaagcg***gaattc***g***aagctt***gatgtcagcctgtacggcgaaatcaaagccggcgtg
K R K R N S K L D

*EcoR*I *Hind*III

gaaggcaggaactaccagctgcaattgactgaagcacaagccgctaacggtggagcgagc
ggtcaggtaaaagttactaaagttactaaggccaaaagccgcatcaggacgaaaatcagt
gatttcggctcgtttatcggcttaaggggga

PamyQ: shaded sequence
ClaI site

Pribnow and RBS sequence

EcoRI and ***HindIII*** site

partial *PorA* gene of *Neisseria meningitidis* (AAZ91310.1)

B) Map of pKTH290

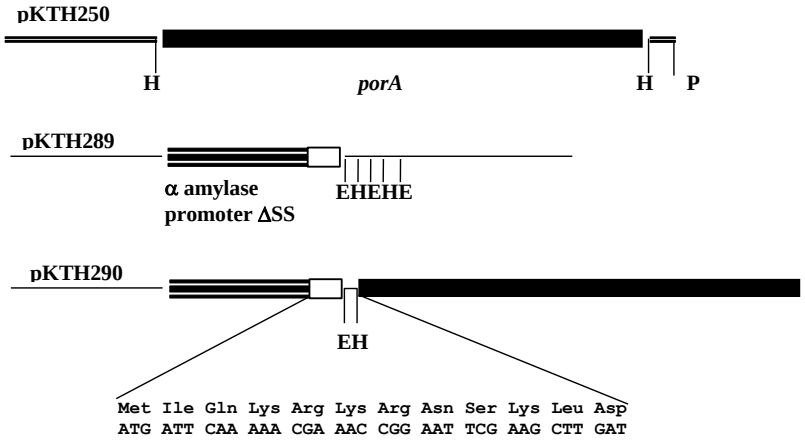

The construction of pKTH290 (Nurminen et al. 1992)

pKTH250 (a pUC 18 derived plasmid) contains the *porA* gene (black box) flanked by *Hind*III sites. pKTH289 is a derivative of the bacillary expression vector, containing the α-amylase promoter and a truncated signal sequence (ss, open box) from *B. amyloliquefaciens*. pKTH290 was constructed by *Hind*III digestion of pKTH250 and pKTH289 and ligation of the mixture.

Appendix B

Oleispira antarctica cpn10/60 operon and the deduced sequences (accession number AJ505131)

```
  1 atgaaaatccgtccattacatgatcgtattgttgttcgccgtaaagaagaagagaccgca
    M  K  I  R  P  L  H  D  R  I  V  V  R  R  K  E  E  E  T  A
 61 actgcgggtggtattatttttaccgggcgctgcggcagaaaaaccaaatcaaggtgttgtt
    T  A  G  G  I  I  L  P  G  A  A  A  E  K  P  N  Q  G  V  V
121 atctctgtgggtactggccgtattcttgataatggttcagtgcaagcgctggcggttaac
    I  S  V  G  T  G  R  I  L  D  N  G  S  V  Q  A  L  A  V  N
181 gaaggcgatgttgtcgtttttggtaaatactcaggtcaaaatactatcgatatcgatggt
    E  G  D  V  V  V  F  G  K  Y  S  G  Q  N  T  I  D  I  D  G
241 gaagaattattgattttgaatgaaagtgatatctacggcgttttagaagcttaattatta
    E  E  L  L  I  L  N  E  S  D  I  Y  G  V  L  E  A  *  -  -

301 cactcacttttttatttaacctacaaaatttaaggaaagatcatggctgctaaagacgta
    -  -  -  -  -  -  -  -  -  -  -  -  -  -  -  -  M  A  A  K  D  V
361 ttatttggtgatagcgcacgcgcaaaaatgttggtaggtgtaaacattttagccgacgca
    L  F  G  D  S  A  R  A  K  M  L  V  G  V  N  I  L  A  D  A
421 gtaagagttaccttaggacctaaaggtcgtaacgttgttatagaaaaatcatttggtgca
    V  R  V  T  L  G  P  K  G  R  N  V  V  I  E  K  S  F  G  A
481 ccgatcatcaccaaagatggtgtttctgttgcgcgtgaaatcgaattgaaagacaaattc
    P  I  I  T  K  D  G  V  S  V  A  R  E  I  E  L  K  D  K  F
541 gaaaacatgggcgcacagatggttaaggaagttgcttctcaagccaacgaccaagccggt
    E  N  M  G  A  Q  M  V  K  E  V  A  S  Q  A  N  D  Q  A  G
601 gacggcacaacgacagcgactgtactagcacaggcgattatcagcgaaggcttgaaatct
    D  G  T  T  T  A  T  V  L  A  Q  A  I  I  S  E  G  L  K  S
661 gttgcggctggcatgaatccaatggatcttaaacgtggtattgataaagctacggctgct
    V  A  A  G  M  N  P  M  D  L  K  R  G  I  D  K  A  T  A  A
721 gttgttgccgccattaaagaacaagctcagccttgcttggatacaaaagcaatcgctcag
    V  V  A  A  I  K  E  Q  A  Q  P  C  L  D  T  K  A  I  A  Q
781 gtagggacaatctctgccaatgccgatgaaacggttggtcgtttaattgctgaagcgatg
    V  G  T  I  S  A  N  A  D  E  T  V  G  R  L  I  A  E  A  M
841 gaaaaagtcggtaaagaaggtgtgattaccgttgaagaaggcaaaggccttgaagacgag
    E  K  V  G  K  E  G  V  I  T  V  E  E  G  K  G  L  E  D  E
901 cttgatgttgtagaaggcatgcagttcgatcgcggttacttgtctccgtacttcatcaac
    L  D  V  V  E  G  M  Q  F  D  R  G  Y  L  S  P  Y  F  I  N
961 aaccaagaaaaaatgaccgtagaaatggaaaatccattaattctattggttgataagaaa
    N  Q  E  K  M  T  V  E  M  E  N  P  L  I  L  L  V  D  K  K
1021 attgataaccttcaagagctgttgccaattcttgaaaacgtcgctaaatcaggtcgtcca
     I  D  N  L  Q  E  L  L  P  I  L  E  N  V  A  K  S  G  R  P
1081 ttattgatcgttgctgaagatgttgaaggccaagcactagcaacattggtagtaaacaac
     L  L  I  V  A  E  D  V  E  G  Q  A  L  A  T  L  V  V  N  N
1141 ttgcgcggcacattcaaggttgcagcggttaaagcccctggttttggcgatcgtcgtaaa
     L  R  G  T  F  K  V  A  A  V  K  A  P  G  F  G  D  R  R  K
1201 gcgatgttgcaagatcttgccatcttgacgggtggtcaggttatttctgaagagctaggg
     A  M  L  Q  D  L  A  I  L  T  G  G  Q  V  I  S  E  E  L  G
1261 atgtctttagaaactgcggatccttcttctttgggtacggcaagcaaggttgttatcgat
     M  S  L  E  T  A  D  P  S  S  L  G  T  A  S  K  V  V  I  D
1321 aaagaaaacaccgtgattgttgatggcgcaggtactgaagcaagcgttaatactcgtgtt
     K  E  N  T  V  I  V  D  G  A  G  T  E  A  S  V  N  T  R  V
1381 gaccagatccgtgctgaaatcgaaagctcgacttctgattacgacatcgaaaagttacaa
     D  Q  I  R  A  E  I  E  S  S  T  S  D  Y  D  I  E  K  L  Q
1441 gaacgcgttgctaagcttgcgggcggcgttgccgtgattaaggttggtgcgggttctgaa
     E  R  V  A  K  L  A  G  G  V  A  V  I  K  V  G  A  G  S  E
1501 atggaaatgaaagagaagaaagaccgtgttgacgatgcacttcatgcaactcgcgcagcg
     M  E  M  K  E  K  K  D  R  V  D  D  A  L  H  A  T  R  A  A
1561 gttgaagaaggtgttgttgcgggtggtggtgttgctttgattcgcgcactctcttcagta
     V  E  E  G  V  V  A  G  G  G  V  A  L  I  R  A  L  S  S  V
1621 accgttgttggtgataacgaagatcaaaacgtcggtattgcattggcacttcgtgcgatg
     T  V  V  G  D  N  E  D  Q  N  V  G  I  A  L  A  L  R  A  M
1681 gaagctcctatccgtcaaatcgcgggtaacgcaggtgctgaagggtcagtggttgttgat
     E  A  P  I  R  Q  I  A  G  N  A  G  A  E  G  S  V  V  V  D
1741 aaagtgaaatctggcacaggtagctttggttttaacgccagcacaggtgagtatggcgat
     K  V  K  S  G  T  G  S  F  G  F  N  A  S  T  G  E  Y  G  D
1801 atgattgcgatgggtattttagaccctgcaaaagtcacgcgttcatctctacaagccgcg
     M  I  A  M  G  I  L  D  P  A  K  V  T  R  S  S  L  Q  A  A
1861 gcgtctatcgcaggtttgatgatcacaaccgaagccatggttgcggatgcgcctgttgaa
     A  S  I  A  G  L  M  I  T  T  E  A  M  V  A  D  A  P  V  E
1921 gaaggcgctggtggtatgcctgatatgggcggcatgggtggaatgggcggtatgcctggc
     E  G  A  G  G  M  P  D  M  G  G  M  G  G  M  G  G  M  P  G
1981 atgatgtaa
     M  M  *
```

Shaded area (nu1-nu294): ***cpn10*** gene and its deduced sequence

2 ClaI sites (nu225-240)

\- - - - non-coding region

RBS sequence

Unshaded area (nu343-nu1989):

cpn60 gene and the deduced sequence

ClaI site: (nu1316)

*: Stop codon

Appendix C

Yeast α-glucosidase coding gene and its deduded sequence (Nu 265-2016 in pkk177GlucC)

```
   1 atgactatttctgatcatccagaaacagaaccaaagtggtggaaagaggccacaatctat
     M  T  I  S  D  H  P  E  T  E  P  K  W  W  K  E  A  T  I  Y
  61 caaatttacccagcaagttttaaagactccaataacgatggctggggtgatttaaaaggt
     Q  I  Y  P  A  S  F  K  D  S  N  N  D  G  W  G  D  L  K  G
 121 atcacttccaagttgcagtatattaaagatcttggcgttgatgctatttgggtttgtccg
     I  T  S  K  L  Q  Y  I  K  D  L  G  V  D  A  I  W  V  C  P
 181 ttttatgactctcctcaacaagatatggggtatgatatatctaactacgaaaaggtctgg
     F  Y  D  S  P  Q  Q  D  M  G  Y  D  I  S  N  Y  E  K  V  W
 241 cccacatacggtaccaacgaggactgttttgagctaattgacaagactcataagctgggt
     P  T  Y  G  T  N  E  D  C  F  E  L  I  D  K  T  H  K  L  G
 301 atgaaattcatcaccgatttggttatcaaccactgttctacagaacacgaatggttcaaa
     M  K  F  I  T  D  L  V  I  N  H  C  S  T  E  H  E  W  F  K
 361 gagagcagatcctcgaagaccaatccgaagcgtgactggttcttctggagacctcctaag
     E  S  R  S  S  K  T  N  P  K  R  D  W  F  F  W  R  P  P  K
 421 ggttatgacgccgaaggcaagccaattcctccaaacaattggaaatctttctttggtggt
     G  Y  D  A  E  G  K  P  I  P  P  N  N  W  K  S  F  F  G  G
 481 tcagcttggacttttgatgaaactacaaatgaattttacctccgtttgtttgcgagtcgt
     S  A  W  T  F  D  E  T  T  N  E  F  Y  L  R  L  F  A  S  R
 541 caagttgacttgaattgggagaatgaagactgcagaagggcaatctttgaaagtgctgtt
     Q  V  D  L  N  W  E  N  E  D  C  R  R  A  I  F  E  S  A  V
 601 ggattttggctggaccatggtgtagatggttttagaatcgataccgctggtttgtattcg
     G  F  W  L  D  H  G  V  D  G  F  R  I  D  T  A  G  L  Y  S
 661 aaacgtcctggtttaccagattccccaatttttgacaaaacctcgaaattacaacatcca
     K  R  P  G  L  P  D  S  P  I  F  D  K  T  S  K  L  Q  H  P
 721 aattgggggtctcacaatggtcctaggattcatgaatatcatcaagaactacacagattt
     N  W  G  S  H  N  G  P  R  I  H  E  Y  H  Q  E  L  H  R  F
 781 atgaaaaacagggtgaaagatggtagagaaataatgacagtcggtgaagttgcccatgga
     M  K  N  R  V  K  D  G  R  E  I  M  T  V  G  E  V  A  H  G
 841 agtgataatgctttatacaccagtgcagctagatacgaagtcagcgaagttttctccttc
     S  D  N  A  L  Y  T  S  A  A  R  Y  E  V  S  E  V  F  S  F
 901 acgcacgttgaagttggtacctcgccatttttccgttataacatagtgcccttcaccttg
     T  H  V  E  V  G  T  S  P  F  F  R  Y  N  I  V  P  F  T  L
 961 aaacaatggaaagaagccattgcatcgaacttttgttcattaacggtactgatagttgg
     K  Q  W  K  E  A  I  A  S  N  F  L  F  I  N  G  T  D  S  W
1021 gctaccacctacatcgagaatcacgatcaagcccggtcaattacgagatttgctgacgat
     A  T  T  Y  I  E  N  H  D  Q  A  R  S  I  T  R  F  A  D  D
1081 tcgccaaagtaccgtaaaatatctggtaagctgttaacattgctagaatgttcattgaca
     S  P  K  Y  R  K  I  S  G  K  L  L  T  L  L  E  C  S  L  T
1141 ggtacgttgtatgtctatcaaggtcaggagataggccagatcaatttcaaggaatggcct
     G  T  L  Y  V  Y  Q  G  Q  E  I  G  Q  I  N  F  K  E  W  P
1201 attgaaaagtatgaggacgttgatgtgaaaaacaactacgagattatcaaaaaaagtttt
     I  E  K  Y  E  D  V  D  V  K  N  N  Y  E  I  I  K  K  S  F
1261 ggtaaaaactcgaaggaaatgaaggatttttttaaaggaatcgccctactttctagagat
     G  K  N  S  K  E  M  K  D  F  F  K  G  I  A  L  L  S  R  D
1321 cattcgagaactcccatgccatggacgaaagataagcccaatgctggatttactggccca
     H  S  R  T  P  M  P  W  T  K  D  K  P  N  A  G  F  T  G  P
1381 gatgttaaaccttggtttttcttgaatgaatcttttgagcaaggaatcaatgttgagcag
     D  V  K  P  W  F  F  L  N  E  S  F  E  Q  G  I  N  V  E  Q
1441 gaatccagagatgatgactcagttctcaatttttggaaaagggccttgcaagccagaaag
     E  S  R  D  D  D  S  V  L  N  F  W  K  R  A  L  Q  A  R  K
1501 aaatataaggaacttatgatttatggttacgatttccaattcattgatttagacagtgac
     K  Y  K  E  L  M  I  Y  G  Y  D  F  Q  F  I  D  L  D  S  D
1561 cagatctttagcttcactaaagagtacggagacaagacgctgtttgctgctttgaatttc
     Q  I  F  S  F  T  K  E  Y  G  D  K  T  L  F  A  A  L  N  F
1621 agtggcgaagaaattgaattcagcctcccaagagaaggtgcttctttatcttttattctt
     S  G  E  E  I  E  F  S  L  P  R  E  G  A  S  L  S  F  I  L
1681 ggaaattatgatgatactgacgtttcctccagagttttgaaaccatgggaaggtagaatc
     G  N  Y  D  D  T  D  V  S  S  R  V  L  K  P  W  E  G  R  I
1741 tacctcgtcaaa--- 1752
     Y  L  V  K  *
```

Start codon

*: stop codon

Appendix D

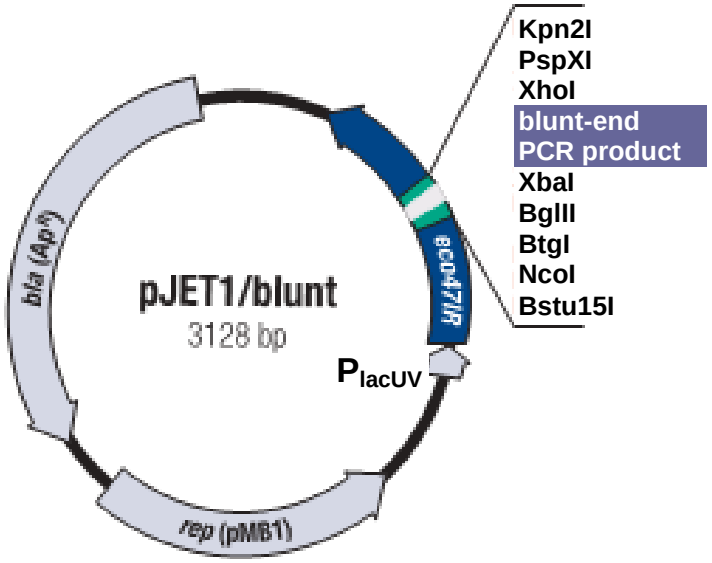

pJET1/blunt vector map (Fermentas)

pJET1/blunt vector is a pre-digested pJET1 vector (GenBank/EMBL accession number DQ317600).

Restriction enzymes that do not cut pJET1/blunt are listed below.

AarI, Acc65I, AjiI, AjuI, AlfI, BaeI, BclI, BcuI, BoxI, BplI, Bpu1102I, BseJI, BseRI, BsgI, BshTI, Bsp68I, Bsp1407I, Bst1107I, BstAPI, BtgZI, Cfr42I, CpoI, CspCI, Eco81I, Eco91I, Eco105I, Eco147I, EheI, FalI, FseI, FspAI, KpnI, KspAI, MlsI, MluI, Mph1103I, NdeI, OliI, PacI, PasI, PauI, PdiI, Pfl23II, PsiI, Psp5II, PsrI, PsyI, SanDI, SdaI, SexAI, SfiI, SgfI, SgrAI, SgsI, SrfI, TstI, Van91I, XagI, XcmI, XmaJI.

Restriction enzymes that cut pJET1/blunt once

AdeI	291	BspTI	141	Eco52I	155	PaeI	150
AloI*	455	BstXI*	466	Eco72I	173	PdmI	2736
ApaI	1030	Bsu15I*	543	EcoRI	178	PfoI	46
BamHI	I843	BtgI*	534	FaqI	274	Ppu21I	173
BbvCI	843	BveI	390	GsuI	2226	PspXI*	477
BceAI	1734	CaiI	1659	HincII	168	PstI	1036
BcgI	2657	Cfr10I	2221	HindIII	750	PvuI	2508
BfiI	2186	Cfr9I	1027	Kpn2I*	469	RsaI	2620
BglI	2255	Csp6I	2620	LguI	1125	SacI	162
BglII*	509	Eam1105I	2136	MssI	887	SalI	168
BpiI	229	Ecl136II	162	NcoI*	1018	TatI	2619
Bpu10	1101	Eco31I	534	Mva1269I	848	SmaI	1027
BsaXI	1552	Eco130I*	2208	MunI	534	ScaI	2619
BseYI	I181	Eco32I*	495	NheI	146	XbaI*	503
Bsp119	1030	Eco47III	1040	NsbI	154	XmiI	478
Bsp120I	1023			NotI	2361	XhoI*	168

Appendix E

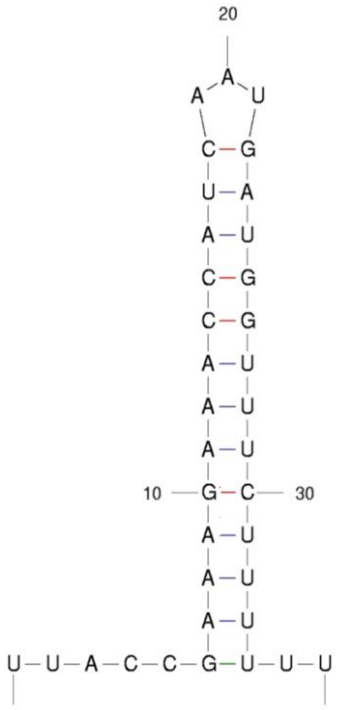

Transcriptional terminator of *B. subtilis* amylase gene (dG= -14.4)

ABBREVIATIONS

ABC	ATPase Binding Cassette
ATP	Adenosine triphosphate
bp	Base pairs
BSA	Bovin serum albumin
B. subtilis	*Bacillus subtilis*
ddH_20	distiled water
dH_20	deionized water
cpn	Chaperonin
DIG	Dioxygenin
DNA	Deoxyribonucleic acid
DNS	Dinitrosalicylic acid
EDTA	Ethylendiaminetetraacetate
EC	Enzyme commision
E. coli	*Escherichia coli*
et al.	et alia
Fig	Figure
g	Gram
h	Hour
IPTG	Isopropyl β-D-1-thiogalactopyranoside
kb	Kilobase pairs
kDa	Kilo dalton
kV	kilovolt
L	Litre
LB	Luria Bertani
Min	minute
mM	Millimolar
mL	Millilitre
Mw	Molecular weight

Nm	Nano meter
nu	nucleotide
dNTP	deoxyribonucleotide triphosphate
PAGE	Polyacrylamide gel electrophoresis
PCR	Polymerase chain reaction
PEG	Polyethylene glycol
PNPG	4-Nitrophenyl-Dglucopyranosiduronic acid
ORF	Open reading frame
OD	Optical density
RBS	Ribosome binding site
U	Unit
RT	Room temperature
SDS	Sodium dodecyl sulphate
SOC	Super Optimal broth with Catabolic repressor
TIM	Triose phosphate isomerase
TLC	Thin layer chromatography
Tris	Tris-hydroxymethyl-aminomethane
μg	Microgram
μL	Microlitre
%	Percent
°C	Degree Celsius
3D	Three-dimensional

ACKNOWLEDGEMENTS

First of all, I would like to thank my first academic supervisor, Prof. Dr. Thomas Schweder for giving me the opportunity to work at the institute, for his valuable guidance, numerous exciting ideas and inspiring discussion. I greatly appreciate his help during the preparation of this thesis. I wish to express many thanks to my second supervisor, Prof. Dr Truong Nam Hai, for supporting me scientific ideas, techniques and others during my study.

I am also grateful to Dr. Le Van Truong for his direct experiment helps and for his constructive discussion on my thesis.

I am much indebted to Prof. Dr. Lai Thuy Hien, who help me in isolation of the *Petrotoga* strain 64G3.

I want to thank all my colleagure from the working group of Prof. Dr Thomas Schweder, including Dr. Britta Jürgen, Dr. Stephanie Markert, Dr. Norma Welsch, Dr. Nguyen Thanh Trung, Dr. Cao Xuan Hieu, Dr. Johannes Kabisch and others outside the institute who help me throughout my work and give me a great working atmosphere.

Many thanks to all colleagues in the Lab Genetic Engineering (Institute of Biotechnology, Vietnam) who provided me good conditions to perform a part of the study in Vietnam.

I would like to express as well my appreciation to the 322 Project – Ministry of Education and Training of Vietnam and Institute of Marine Biotechnology for providing financial supports and working facilities during my stay in Germany.

Finally, I specically thank my family including my parents, my wife and two lovely sons for their uncountable support and love which gave me power to finish this work.

PUBLICATIONS

International peer reviewed journal

H-Cuong Le, N-Hai Truong and Thomas Schweder (2012). "Characterization of the Thermophilic Starch Degrading *Petrotoga* Strain 64G3 and the Expression of its α-amylase Gene". Biotechnology **11**(4): p. 199-208. **DOI:** 10.3923/biotech.2012.199.208